Abstract

The Duality of Neurons:

Co-transmission of Serotonin and a Neuropeptide, NLP-3, in the *Caenorhabditis elegans* Egg-Laying Circuit

Allison M. Butt

2024

Neurons typically release both a neurotransmitter and one or more neuropeptides in a process known as co-transmission. While this process is a widely observed phenomenon, the logic of why a neuron releases these two or more different types of signals to accomplish its numerous functions remains largely unclear. In this dissertation, I studied how two serotonergic neurons in the *C. elegans* egg-laying circuit—known as the Hermaphrodite Specific Neurons (HSNs)—release both the neurotransmitter serotonin and the neuropeptide NLP-3 to activate egg laying. Egg laying typically occurs in a temporal pattern with two-minute active phases, during which the HSNs are highly active and eggs are laid approximately 18 seconds apart. These periods of intense egg laying are separated by approximately 22-minute inactive phases, during which the HSNs have less frequent calcium transients and no eggs are laid. I utilized a targeted RNAi screen to identify the G protein coupled receptor NPR-36 as an NLP-3 receptor and used additional genetic and molecular experiments to support this cognate pairing. NPR-36 is expressed on and promotes egg laying by activating the egg-laying muscle cells, the same cells where two serotonin receptors also promote egg laying. Although NLP-3 is likely released only when HSNs are highly active (i.e. during the active phase), NLP-3 appears to persist through the

subsequent inactive phase to switch on the next active phase along with serotonin. I conclude from this work that NLP-3 and serotonin together overcome the long-lasting inhibitory signals that maintain the egg-laying inactive phase while also regulating discrete aspects of egg-laying activity in the active phase. My work suggests a model in which multiple signals with short and long-lasting effects compete to pattern a behavior over tens of minutes.

The Duality of Neurons:

Co-transmission of Serotonin and a Neuropeptide, NLP-3, in the *Caenorhabditis elegans* Egg-Laying Circuit

A Dissertation

Presented to the Faculty of the Graduate School

of

Yale University

In Candidacy for the Degree of

Doctor of Philosophy

By

Allison M. Butt

Dissertation Director: Dr. Michael Koelle, Ph.D.

May 2024

Acknowledgements

This is a thank you note to everyone who has supported me throughout my lifetime of schooling.

There are many educators that resulted in me landing here at Yale studying biology. To thank more recent mentors—thank you to my committee members, Drs. Mark Solomon and Valerie Reinke, and my PI, Dr. Michael Koelle, for their guidance and patience when I inevitably ran over at all of our meetings. Thank you to Dr. Jennifer Garrison, my outside reader, for taking on this task of wading through a manuscript for a student that she only just met. I also must thank one educator that probably has no idea the impact that he made on me, Mr. Whitmore. He started my adoration for the molecular understanding of our world and the cells around us when I was a sophomore in high school drawing out the full electron transport pathway on a blank piece of paper as a test. Honestly it was awesome and the best tests I ever took.

To my lab who were both educators and peers, thank you for your patience in listening and also critiquing. A special thank you to Dr. Andrew Olson who started as my rotation mentor and then proceeded to be my daily mentor and friend for 6 years. Andrew, you are an incredible person who really exercised kindness and gentle guidance, but when I needed it pushed me to step up. Thank you.

I wouldn't have gotten through this experience and the pandemic without my friends both near and far. They tolerate my annoying food restrictions and weird sense of humor in ways that I never thought people would. To my roomies, Caroline, Shivali, and Sachita, I am so endlessly proud of all of you and words

cannot convey how important you all are to my sense of self and trust in humanity. To my lab girls, Nakeirah and Halie, you both are my backbone and my comfy cozy blankets. Thank you for being an outlet, a shoulder to cry on, and two people that I could see for 8 hours a day and then want to hang out with for longer. To my 102nd Culture Squadron—Jen, Sam, Maya, Olive, Kathy, Adán, Tanner, Lindsey, Tony, Nakeirah, and Archie—having a weekly cozy family gathering to yell and laugh so much we have to pause the tv has been soul healing and grounding. I am so grateful for Jen and Sam for being there for me for the past 10 years in such incredible ways that mean so much to me. To Emily, my first roommate and soul sister, thank you for sharing the suffering that is post-bachelor's degree schooling with me from afar. Our daily texts lambasting life and those in it always were a highlight especially when yours got to start including your furry patients. And to my furry partner in crime Sylvester, (not that he can read this) he is just as much of a mess as I am and saved me more times than I can count—thanks munchkin. Adopt, don't shop.

While I don't think my family understood what I was doing most of the time or why I was doing it, they were always supportive with questions and a listening ear. I often got lost in the turbulence that is doing research and having people who inadvertently would nudge me out of that mental space was a beautiful resource.

To my family, Ruthanne, Peter, and Jenna, Mum, Daddy, and J, thank you for allowing me to always be my overly independent, strong headed self. The qualities that you instilled in me percolated to create someone that I hope you all are proud of as I am very proud to say that I am a product of who you all made me. J, I can't picture what it would be without you as you have been there for every step of my

way on this journey called life—thank you for being here. To Michael and Ida, we have been there for each other through the drama of growing up and I look forward to continuing walk through life with both of you laughing at the absurdity of it all. To my grandmothers, Barbara and Jeannine, Grammy and Mémère, thank you for supplying me with laughs, encouragement, and many phone calls. Thank you for showing me how strong and resilient women can be and that curiosity and drive never dwindles. My whole family never questioned if I could, but only were thrilled that I was doing it.

And finally, to Nikita—you have brought more laughter and love into my life than I thought possible. Thank you for being an incredible partner and friend. I am so glad I get to have many, many more years with you by my side.

Table of Contents

Table of Figures

Table of Tables

Copyright Acknowledgement

Data and figures from this dissertation are currently under review in:

Butt, AM, Van Damme, S, Santiago, E, Olson, AS, Beets, I, Koelle, MR. Neuropeptide and serotonin co-transmission sets the activity pattern in the *C. elegans* egg-laying circuit. (2024). *Current Biology*.

1. Introduction

1.1. Co-transmission in neurons

Neural networks consist of a layered web of neuronal and glial cells producing interconnected axons, dendrites, and cilia. These cells communicate at synapses and across extreme distances extra-synaptically to execute complex functions and behaviors of an organism. Stereotypically, neurons release one signal that is received by its post-synaptic cell, which will be activated or inhibited depending on the receptor it expresses for that ligand. Cellular activation is an increase in the ionic content of the cell and/or the triggering of a protein signaling cascade. This activation ultimately causes a behavior such as vesicle release, cell contraction via myosin, or increase in motility via extension of the cytoskeleton. The inhibition of a cell either reverts the cell to its state of stasis or prevents the activation of the cell, such as by decreasing the cell's positive ionic content or modifying proteins to prevent their intracellular signaling capability. These two states dictate the communication in a circuit and allow for an organism to make decisions based off of internal and external stimuli.

The post-synaptic cell in a synaptic pair could contain a multitude of receptors (both metabotropic and ionotropic) for any given signal, and it is now abundantly clear that the pre-synaptic neuron can co-transmit multiple different signal types (Nusbaum et al., 2017; Ptak et al., 2009; Ren et al., 2019; Svensson et al., 2018; Yao et al., 2023). Co-transmission is a neuronal property where the cell produces and releases more than one signaling molecule. These signaling molecules could be classical monoamine-based neurotransmitters (e.g., dopamine, serotonin, gamma-aminobutyric acid, etc.),

polypeptide-chain composed neuropeptides (e.g., vasopressin, oxytocin, Substance P, etc.), or nonclassical neurotransmitters (e.g., nitric oxide, ATP, carbon monoxide). This complexity is further magnified by the interconnected dynamics of neural circuits (Figure 1.1A) where a post-synaptic cell may influence the behavior of a secondary cell that informs the activity of the original presynaptic cell. (Nusbaum et al., 2017; Svensson et al., 2018) These circuit dynamics are utilized to produce distinct behavioral states, to tune responses across a gradient, or to allow multiple behaviors to initiate simultaneously.

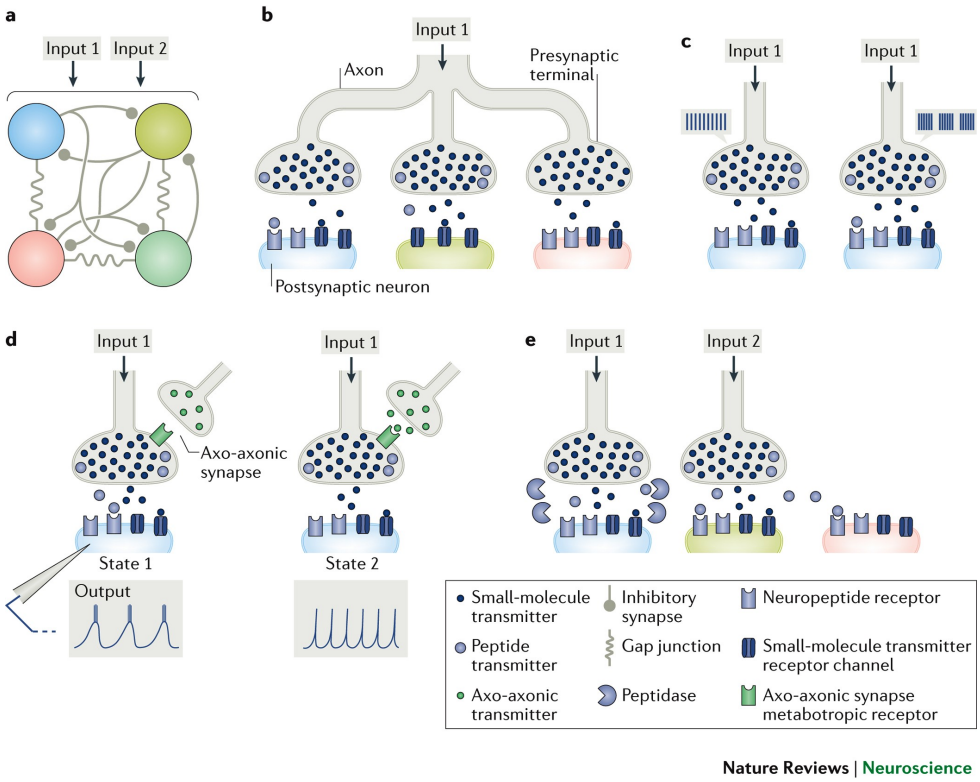

Figure 1.1: Different co-transmission models possible at the synaptic level.
The different dynamics and complexities of neuronal signaling portrayed here as multiple axons with different signals (**B**), different activation levels of the presynaptic cell (**C**), additional activation from separate locales (**D**), and further regulation of signals through degradation/reuptake after release (**E**). From Nusbaum, Blitz, and Marder (2017).

1.2. Serotonergic signaling

Serotonin is an essential molecule in the brain and throughout the body. The small-molecule amine neurotransmitter performs many functions, including influencing the sleep/wake cycle, mood regulation, and the patterning of breathing. Serotonergic neurons originate from a set of areas in the brain known as the raphe nuclei. These neurons permeate throughout the cerebral cortex and participate in numerous synaptic and, likely, extra-synaptic signaling pathways. Signaling mediated by serotonin usually occurs on the scale of milliseconds to seconds, but serotonin can also travel extra-synaptically and alter the post-signaling cell after seconds to hours in a more neuromodulatory manner. (Albert, Benkelfat, & Descarries, 2012; Filip & Bader, 2009; Okaty, Commons, & Dymecki, 2019; Ptak et al., 2009; Ren et al., 2019)

Serotonin is produced in both the enteric and nervous systems through enzymatic conversion of L-tryptophan. The rate limiting step of hydroxylation by tryptophan hydroxylase (TPH-1 and TPH-2) is followed by decarboxylation by aromatic L-amino acid decarboxylase. Serotonin is transported from the cytoplasm into small synaptic vesicles through uptake transporters and is stored in clear synaptic vesicles until release. Serotonin signaling can both activate and inhibit the post-signaling cell through a variety of G protein coupled receptors (GPCRs) and ion channels. Once released, serotonin must be taken up by reuptake transporters at the synapse or on many cell types in the blood stream and enteric system; this prevents continued signaling and eventual receptor desensitization. (Okaty et al., 2019; Terry & Margolis, 2017)

1.3. Neuropeptide signaling

Neuropeptide signaling is crucial and fairly understudied across the animal kingdom. Neuropeptides are short chain polypeptides that are stored and processed in dense core vesicles in neurons, though signaling peptides can be produced in almost any cell in the body. Neuropeptides signal in both a short or fast range and over long-distance/long-term to modulate regions of the brain and body. (Nusbaum et al., 2017) Neuropeptide receptors are predominantly GPCRs across the animal kingdom. There are debates over the classification of insulin and insulin-like signaling molecules as well as growth hormones as they could be considered neuropeptides in some animals, but their receptors are not GPCRs. Additionally, there is a family of FRMF-peptide-gated ion channels in mollusks and other small species. These contradictions to the dogma of neuropeptide signaling are crucial to identify as they may lead to additional disease treatment avenues. (Cottrell, 1997; Furukawa & Tagashira, 2023; Svensson et al., 2018)

To end neuropeptide signaling, peptidases are required to clear the neuropeptides from their signaling location, unlike neurotransmitters, which are taken up into the cell for reuse or degradation (Figure 1.1E; Nusbaum et al., 2017). Targeting the receptors of peptides and neuropeptides has become a crucial avenue for treatment of a variety of diseases such as diabetes, neurodegenerative conditions, and cancer. With a deeper understanding of neuropeptide signaling and utilization, drug targets can be more effectively designed and new diseases can be targeted by expanding our understanding of the field (Hauser, Attwood, Rask-Andersen, Schioth, & Gloriam, 2017).

1.4. Serotonin and the neuropeptide Substance P co-transmission in mammalian breathing

The first identified neuropeptide, Substance P, was initially discovered in a gut extract and observed to cause contractions of enteric muscles (Von Euler & Gaddum, 1931). It has since been observed to be crucial for many mammalian functions, such as pain response, wound healing, depression, anxiety, stress response, and nausea, along with its receptor, NK-1R (neurokinin type 1 receptor; Chen et al., 2023; Kupcova, Danisovic, Grgac, & Harsanyi, 2022; Meyer, Habib, Wagner, & Gan, 2023; Von Euler & Gaddum, 1931).

Substance P is produced in many neurons, including serotonergic neurons (Szereda-Przestaszewska & Kaczynska, 2020). The co-transmission of these two signals is required for the proper patterning of breathing in infant and adult mammals (Bright et al., 2017; Szereda-Przestaszewska & Kaczynska, 2020 and citations within). Stimulation of serotonin receptors in the rhythm-generating breathing center is able to overcome opioid-induced depression of breathing in rats (Manzke et al., 2003). In a similar manner, Substance P is able to oppose the inhibitory effects that opioid receptor agonists have on breathing rhythm when introduced to mouse brain slices (Sun et al., 2019). The promotion of breathing by either signal occurs at the intracellular level. Neurons express both receptors for opioids and for Substance P or serotonin. These receptors have opposing G protein intracellular signaling cascades where the serotonin/Substance P $G\alpha_{s/q}$ pathways directly oppose the silencing $G\alpha_{i/o}$ signaling caused by opioid receptor activation, thus preventing cellular quiescence and allowing breathing to continue.

1.5. The *Caenorhabditis elegans* egg-laying circuit as a model co-transmission serotonergic circuit

1.5.1. Egg-laying circuit dynamics

The *Caenorhabditis elegans* egg-laying circuit is composed of muscles and neurons[1] at the mid-body of the animal (as diagrammed in Figure 1.2). This circuit can be easily manipulated and observed using egg laying as a phenotypic read out. Mutations that have dampened egg laying are known as *egl* (egg-laying defective); some mutations can cause excessive egg laying, or hyperactive egg laying, as well. This quantifiable phenotypic read out is a significant asset for studying the dynamics of a circuit.

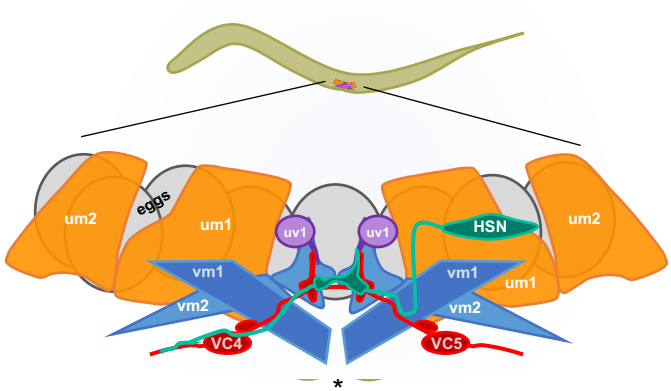

Figure 1.2: Diagram of the *Caenorhabditis elegans* egg-laying circuit.
A graphic of a *Caenorhabditis elegans* animal with a focus on the egg-laying circuit components. These are the HSNs (hermaphrodite specific neurons), vm1s and vm2s (vulval muscles), VC4 and VC5 (ventral cord), um1s and um2s (uterine muscles), and the uv1s (uterine ventral type 1 cells).

The egg laying circuit is composed of 16 muscle cells, 8 neural cells, and many epithelial cells (cells depicted in Figure 1.2 are also mirrored on the right side of the animal—excluding the VC4 and VC5 cells). The muscles of the circuit are the type 1 uterine muscles and type 2 uterine muscles (um1s and um2s, respectively; orange cells

[1] One set of these cells, the uv1s, has been classed as "neuroendocrine" cells and not neurons, but in the context of this work, I will not distinguish them from neurons.

in Figure 1.2), the type 1 vulval muscles (vm1s; dark blue in Figure 1.2), and the type 2 vulval muscles (vm2s; light blue in Figure 1.2). The neurons are the hermaphrodite specific neurons (HSNs; teal in Figure 1.2), the ventral cord neurons 4 and 5 (VC4 and VC5; red in Figure 1.2), and the type 1 uterine ventral cells (uv1s; purple in Figure 1.2). The HSNs directly synapse with the vm2s and VC4 and 5 neurons. The vm1 and vm2 muscles are connected via gap junctions. When any of these synaptic relations are disrupted through loss of signal, loss of receptor, or are physically altered, the egg laying in those mutated animals will be either decreased or increased in a manner measurable via counting the change in the eggs contained within the uterus of the animal.

To execute the behavior of egg laying, the HSNs fire, releasing serotonin and a neuropeptide called NLP-3. These two signals (discussed in further detail below in sections 1.5.2 and 1.5.3) ultimately excite the muscles of the circuit, resulting in coordinated muscle contractions and egg laying (Brewer, Olson, Collins, & Koelle, 2019). The VC neurons are activated by the HSNs and have peak activity just before egg laying, likely releasing acetylcholine onto the vm2s to further excite them to achieve egg laying (Collins et al., 2016; Kopchock, Ravi, Bode, & Collins, 2021). The uterine muscles are likely extrasynaptically activated for coordinated contraction for egg laying, however these cells are significantly understudied. The uv1s fire following egg release, releasing inhibitory neuropeptides (NLP-7 and FLP-11) and tyramine into the egg-laying circuit inhibiting the HSNs (Alkema, Hunter-Ensor, Ringstad, & Horvitz, 2005; Banerjee, Bhattacharya, Gorczyca, Collins, & Francis, 2017; Collins et al., 2016). The vm1s are being periodically activated by the VA and VB neurons (not

depicted here) as the animal executes movement, not exclusively during egg laying. The activity of these cells must all be coordinated for normal egg laying to occur throughout the adult life of the *C. elegans*.

Egg-laying behavior exists in two states: the active phase and the inactive phase. The active phase, when eggs are laid—and thus cell activity, measured via an increase in calcium ions, is high for all cells of the circuit—lasts for approximately two minutes (Waggoner, Zhou, Schafer, & Schafer, 1998). The inactive phase is an approximately 22-minute period of egg laying quiescence, although there is still HSN, VC4, VC5, and vm1 activity (Brewer et al., 2019; Collins et al., 2016; Waggoner, Hardaker, Golik, & Schafer, 2000). The lack of vm2 activity during the inactive phase is likely what prevents egg laying from occurring as the coordinated activation of the vm1 and vm2 muscles is required for an egg to successfully be laid (Brewer et al., 2019).

Egg laying is impacted by many environmental and behavioral conditions: movement, roaming/dwelling, presence of food, oxygen exposure, etc. Focusing on the first of these, the movement of the animal directly correlates to egg laying activity through positioning of the vulva during the sinusoidal body bends of the animal as seen in Figure 1.3A (Collins et al., 2016). When the vulva of the animal is at its most relaxed, the HSN neurons fire, shortly followed by the VC4 and 5 neurons (Figure 1.3B). Following this, the vm1s and vm2s contract, resulting in an egg being laid (Figure 1.3C). When cell activity occurs and the vulval slit is not in the proper phase, egg laying will not occur; however, there could still be vm1 muscle activation from the VA/VB neurons in addition to unproductive vm1 and vm2 activity. Additionally, it has been observed that animals speed up upon egg laying then ultimately slow

following egg release, and this activity has now been linked to HSN release of non-NLP-3 neuropeptides and serotonin, respectively (Gurel, Gustafson, Pepper, Horvitz, & Koelle, 2012; Huang et al., 2023). Determining how egg laying is executed at the cellular level will allow for better understanding of how decision making for essential behaviors are tied together.

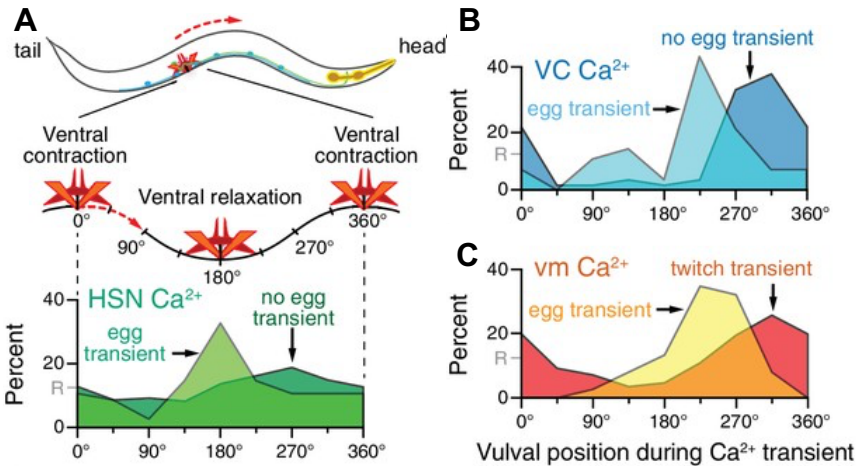

Figure 1.3: Body posture during movement affects egg laying.
A, diagram of a *C. elegans* animal and its vulval muscles as it crawls and the HSN calcium activity averaged over these body bends. **B,** calcium activity of VC neurons over the span of the body bend angles of a moving animal. **C,** vulval muscle activity over the body bend angles of a moving animal. Figure adapted from Collins et al. (2016).

1.5.2. Serotonin signaling in the egg-laying circuit

The *C. elegans* egg-laying circuit has long been known to be controlled by serotonin released into the circuit by the HSNs (Trent, Tsuing, & Horvitz, 1983; Waggoner et al., 1998). Serotonin is contained in many neurons including the HSNs, VC4s, VC5s, NSMs, and ADFs (Loer, 2022). When the *C. elegans* only tryptophan hydroxylase *tph-1* is knocked out, creating animals with functionally no serotonin production, the animals become mildly *egl*. TPH-1 expression, and thus serotonin synthesis, is in fewer neurons than those that stain for serotonin, suggesting an interesting dynamic of uptake of serotonin into neurons that do not produce it for use in signaling. However,

the HSNs are the only cells positioned to release serotonin onto the vm2s and VC4/5 neurons at the midbody, and likely are the ones to extrasynaptically signal to the vm1s, um1s, and um2s as well.

Of the serotonin receptors that *C. elegans* has evolved, almost all of those receptors affect egg laying. Serotonin receptor 1 and 7 (SER-1 and SER-7) both are activating receptors. SER-1 is a $G\alpha_q$-coupled GPCR that is expressed on the vm2s, um1s, um2s, and possibly on the HSNs, while SER-7 is a $G\alpha_s$-coupled GPCR expressed on the vm1s, vm2s, um1s, um2s, VC4, VC5, and possibly on the HSNs (Fernandez et al., 2020). Both of these receptors were extensively studied in Olson, Butt, Christie, Shelar, and Koelle (2023). We determined that knockouts of these receptors do not respond to exogenous serotonin, and both are required for vulval muscle response. Additionally, we found that the downstream signaling pathways of SER-1 and SER-7, which activate $G\alpha_q$ and $G\alpha_s$, respectively, are necessary for efficient and complete vulval muscle activation at physiological levels, but over-activation of either receptor's downstream pathway allowed for egg laying to proceed.

An inhibitory serotonin GPCR, SER-4, is also expressed in the egg-laying circuit on the vm2s (Fernandez et al., 2020). The Koelle lab (unpublished data) and Hapiak et al. (2009) have observed that the *ser-4* null allele, alongside the serotonin-gated chloride ion channel, *mod-1,* causes a hyperactive egg-laying phenotype in certain conditions. Inhibition is performed through the activation of $G\alpha_o$ whose null mutation is one of the first mutations known that causes hyperactive egg laying (Mendel et al., 1995). Interestingly, all of these components of serotonin inhibition are also required

for HSN-mediated movement slowing after egg laying described above in 1.5.1 (Gurel et al., 2012).

1.5.3. NLP-3 signaling in the egg-laying circuit

NLP-3 (neuropeptide-like peptide 3) is a group of five neuropeptides post-translationally processed from the translation of the *nlp-3* gene. NLP-3 is produced in several neurons in the animal, but, notably, NLP-3 is produced in all neurons that produce TPH-1: the NSMs, ADFs, and HSNs (Brewer et al., 2019). The translated amino acid sequence is depicted in Figure 1.4. The protein product is cleaved at dibasic residues after transport into dense core vesicles and further modified through converting glycines to amine groups on the C-terminal ends of NLP-3-1, NLP-3-2, and NLP-3-3 (green peptides in Figure 1.4) before release (Van Bael et al., 2018). It is conventionally believed that neuropeptides are only the products that are modified after cleavage to ensure longevity. Previous work identified a peptide fragment containing NLP-3-3 and NLP-3-5 as responsible for an octanol avoidance response through the receptor NPR-17 (Mills et al., 2016). Additionally, NLP-3-3 has been paired via a heterologous cell assay to NPR-42 (Beets et al., 2023).

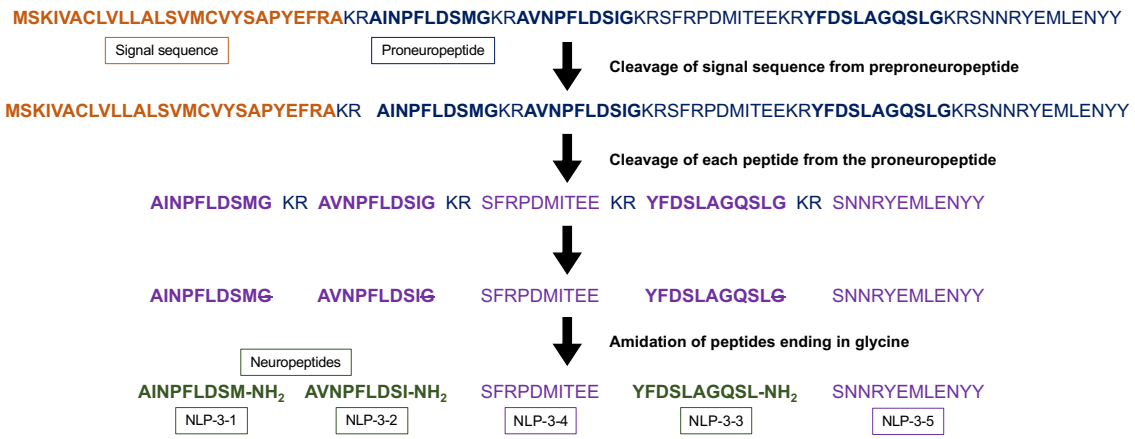

Figure 1.4: NLP-3 neuropeptide structures and processing steps.
The pre-proneuropeptide is translated and transported to the endoplasmic reticulum for packaging. After the signal sequence is cleaved, the proneuropeptide is packaged into what will become the dense core vesicles. Within the dense core vesicles, the proneuropeptide is cleaved at dibasic residues by peptidases. The produced NLP-3-1, -2, and -3 fragments are then further post-translationally modified through replacing the glycine residue with an amine group. All peptides and neuropeptides are thought to remain in the vesicle for release.

NLP-3 is necessary for normal egg laying function. In Brewer et al. (2019), a previous graduate student in the Koelle lab, Jacob Brewer, identified NLP-3 as a co-transmitted neuropeptide with serotonin from the HSN. He determined that knockout of serotonin and *nlp-3* in a double mutant strain phenocopied the severe egg-laying defect caused by genetic ablation of the HSN cells (which neither signal did on its own). NLP-3 can activate the egg-laying circuit without the presence of serotonin; however, which cells it activates was unknown as the previously paired GPCR, NPR-17, did not cause an *egl* phenotype when knocked out (unpublished data).

1.6. Thesis Overview

I aimed to answer the question of where and how NLP-3 activates the *C. elegans* egg-laying circuit. This thesis covers the discovery and characterization of an NLP-3 GPCR, which I named NPR-36, in the *C. elegans* egg-laying circuit. My collaborators determined that peptides NLP-3-1 and NLP-3-2 activate the NPR-36 receptor *in cellulo*.

I determined that NPR-36 was expressed on the vm2s, um1 and um2s, and the HSNs. I also investigated how the co-transmission of serotonin and NLP-3 affect egg laying behavior on a more holistic scale, determining that all mutants cause an increase in the duration of the inactive phase, but each signaling pathway affects the active phase in a different manner. My work is continuing the aim of revealing the complexities of co-transmission to allow for a deeper understanding of the use of neuropeptides within neural signaling.

2. Materials and Methods

2.1. *C. elegans* growth, maintenance, strain generation, and genotyping

2.1.1. C. elegans growth and maintenance

C. elegans strains were cultured at 20°C on NGM agar plates with *E. coli* strain OP50 as a food source (Stiernagle, 2006). All strains were derived from the Bristol N2 wild-type strain. Table 2.1 shows a list of strains used in this work.

Table 2.1: *C. elegans* strains used in this work.

STRAIN	FEATURE	GENOTYPE	FIGURES
N2	Bristol strain	wild type	Figure 4.1, 5.1, 5.2, 5.3, 5.4, Sup. Figure 8.2, 91., 9.2, 9.3, 9.4, 9.8, 9.9, 9.10
MT15434	Lacks serotonin	*tph-1 (mg280) II*	Figure 4.1, 5.1, 5.2, 5.3, 5.4, Sup. Figure 8.1, 8.2, 9.9
LX1978	*nlp-3* null mutant	*nlp-3 (tm3023) X*	Figure 4.1, 5.1, 5.2, 5.3, 5.4, Sup. Figure 9.9
LX2366	Double mutant lacking serotonin and *nlp-3*	*tph-1 (mg280) II; nlp-3 (tm3023) X*	Figure 4.1, Sup. Figure 8.2
MT2495	RNAi sensitive strain	*lin-15B (n744) X*	Sup. Figure 9.2, 9.3
LX2519	*nlp-3* overexpressing strain	*vsIs275 III*	Figure 4.1, Sup. Figure 8.1, 9.4
LX2593	*nlp-3* overexpression with RNAi sensitivity	*vsIs275 III; lin-15B (n744) X*	Figure 3.1
LX2598	Serotonin knockout with RNAi sensitivity	*tph-1 (mg280) II; lin-15B (n744) X*	Figure 3.2
LX2768	CRISPR knockout of *npr-36*	*npr-36 (vs195) X*	Figure 4.1, Sup. figure 8.2, 9.4
LX2769	CRISPR knockout of *npr-36*	*npr-36 (vs190) X*	Figure 4.1, 5.1, 5.2, 5.3, 5.4, Sup. Figure 8.2, 9.4, 9.8, 9.9

LX2776	Double mutant for serotonin and *npr-36*	*tph-1 (mg280) II; npr-36 (vs190) X*	Figure 4.1, Sup. Figure 8.2
LX2777	*nlp-3* overexpressor with *npr-36* knockout	*vsIs275 III; npr-36 (vs190) X*	Figure 4.1, Sup. Figure 9.4, 9.8
LX2778	Double mutant for *npr-36* and *nlp-3*	*npr-36 (vs195) X; nlp-3 (tm3023) X*	Figure 4.1
LX2779	Double mutant for *npr-36* and *nlp-3*	*npr-36 (vs190) X; nlp-3 (tm3023) X*	Figure 4.1
LX2780	Double mutant for serotonin and *npr-36*	*tph-1 (mg280) II; npr-36 (vs195) X*	Figure 4.1, Sup. Figure 8.2
LX2781	*nlp-3* overexpressor with *npr-36* knockout	*vsIs275 III; npr-36 (vs195) X*	Figure 4.1, Sup. Figure 9.4
PHX5031	*npr-36::SL2::GFP* CRISPR knock-in	*syb5031 X*	Sup. Figure 9.5
PHX5054	*npr-36::GFP* CRISPR knock-in	*syb5054 X*	
LX2866	*npr-36::SL2::GFP* with mCherry co-expression marker on egg-laying circuit neurons (*ida-1p*)	*syb5031 X; vsIs269*	Figure 4.3
LX2871	*npr-36::SL2::GFP* with mCherry co-expression marker on egg-laying circuit muscles (*unc-103ep*)	*syb5031 X; vsIs191*	Figure 4.3
LX2919	*sid-1* null mutant, preventing transport dsRNA between cells	*sid-1 (qt9) V*	Sup. Figure 9.6
LX2918	*tph-1* and *sid-1* null mutant, lacking serotonin and transport of dsRNA between cells and	*tph-1(mg280) II; sid-1 (qt9) V*	Sup. Figure 9.6
LX2924	Extrachromosomal array of myo-3p*::npr-36(fl)* and *myo-2p::mCherry* in LX2919 (*sid-1*)	*sid-1 (qt9) V; vsEx1075*	Figure 4.4
LX2925	Extrachromosomal array of myo-3p*::npr-36(fl)* and *myo-2p::mCherry* in LX2918 (*tph-1; sid-1*)	*tph-1 (mg280) II; sid-1 (qt9) V; vsEx1074*	Figure 4.4
LX2922	Extrachromosomal array of *myo-3p::gfp(fl)* and *myo-2p::mCherry* in LX2919 (*sid-1*) as a control	*sid-1 (qt9) V; vsEx1076*	Figure 4.4
LX2923	Extrachromosomal array of *myo-3p::gfp(fl)* and *myo-2p::mCherry* in LX2918 (*tph-1; sid-1*) as a control	*tph-1 (mg280) II; sid-1 (qt9) V; vsEx1077*	Figure 4.4
LX2004	Integrated array of HSN GCaMP5 and rescue of *lin-15 (vsIs183) in a lite-1 lin-15* background	*lite-1 (ce314) lin-15 (n765ts) X vsIs183*	Figure 4.5, Sup. Figure 9.7
LX2872	Integrated array of HSN GCaMP5 and rescue of *lin-15* (*vsIs183*) in a *nlp-3 lite-1 lin-15* background	*lite-1 (ce314) nlp-3 (tm3023) lin-15 (n765ts) X vsIs183*	Figure 4.5, Sup. Figure 9.7
LX2455	Double mutant of *ser-1* and *ser-7*	*ser-7 (gk414345) ser-1 (ok345) X*	Figure 5.1, 5.2, 5.3, 5.4, Sup. Figure 8.1, 8.2, 9.9

DA1814	Null mutant for serotonin GPCR *ser-1* that activates $G\alpha_q$	*ser-1 (ok345) X*	Sup. Figure 8.1
LX1984	Null mutant for serotonin GPCR *ser-7* that activates $G\alpha_s$	*ser-7(gk414345) X*	Sup. Figure 8.1, 8.2
LX2790	Double mutant lacking serotonin and overexpressing *nlp-3* with mCherry pharynx marker	*tph-1 (mg280) II; vsIs275 III*	Sup. Figure 8.1
LX2791	Double mutant lacking both activating serotonin receptors *ser-1* and *ser-7* and overexpressing *nlp-3* with mCherry pharynx marker	*vsIs275 III; ser-7 (gk414345) X ser-1 (ok345) X*	Sup. Figure 8.1
LX2792	Null *ser-7* and overexpressing *nlp-3* with mCherry pharynx marker	*vsIs275 III; ser-7 (gk414345) X*	Sup. Figure 8.1
LX2793	Null *ser-1* and overexpressing *nlp-3* with mCherry pharynx marker	*vsIs275 III; ser-1 (ok345) X*	Sup. Figure 8.1
LX2794	Double mutant of *ser-7* and *npr-36*	*ser-7 (gk414345) X F10D7.1 (vs190) X*	Sup. Figure 8.2
LX2795	Double mutant of *ser-7* and *npr-36*	*ser-7 (gk414345) X F10D7.1 (vs195) X*	Sup. Figure 8.2
FX04514	Potential null mutant of *C01F1.4*	*C01F1.4 (tm4514) II*	Sup. Figure 9.1
FX04516	Potential null mutant of *C01F1.4*	*C01F1.4 (tm4516) II*	Sup. Figure 9.1
NL2099	Hypersensitive to RNAi	*rrf-3 (pk1426) II*	Sup. Figure 9.2, 9.3
KP3948	Hypersensitive to RNAi	*eri-1 (mg366) IV; lin-15B (n744) X*	Sup. Figure 9.2, 9.3
VH624	Neuronal RNAi hypersensitive with GFP neuronal expression	*rhIs13 [unc-119::GFP + dpy-20(+)] V; nre-1 (hd20) X lin-15B (hd126) X*	Sup. Figure 9.2
GR1379	Hypersensitive to RNAi	*lin-35(n745) I; eri-1(mg366) IV*	Sup. Figure 9.2
LC108	Neuronal RNAi hypersensitive by expressing dsRNA channel *sid-1* with mCherry pharynx expression	*uIs69 [pCFJ90(myo-2p::mCherry), unc-119p::sid-1]*	Sup. Figure 9.2
TU3311	Neuronal RNAi hypersensitive with YFP neuronal expression with overexpression of the dsRNA channel *sid-1*	*uIs60 [unc-119p::yfp, unc-119p::sid-1]*	Sup. Figure 9.2
LX2145	*npr-17* null mutant	*npr-17(tm3210) III*	Sup. Figure 9.10

2.1.2. Classical C. elegans strain generation

Male N2 animals were generated through 4-hour heat shock at 30°C. Four days later, nine L4 males were picked and introduced to three young adult hermaphrodites of the desired strain (henceforth called mutation A). L4 male larvae will be heterozygous for mutation A. L4 males of mutation A are introduced to young adult hermaphrodites of

mutation A. The male progeny from this cross will be heterozygous or homozygous for mutation A. These males will be used moving forward. Any crosses performed with *tph-1* mutations must have *tph-1* as the hermaphrodite as the loss of serotonin causes a male mating defect.

Mutation A L4 males are introduced to young adult hermaphrodites with a different mutation. The following day, the adult hermaphrodites and males are moved to a new plate. This procedure is repeated two more times, where the final time the adults are discarded. If performing a cross where one component is an integrated transgenic array, ideally that integrated array is the male. This allows for a quicker crossing procedure as seen below in (B). If the transgenic array cannot be made male (i.e. it has a mating phenotype), then the protocol for crossing genetic mutants (A) is followed.

A. If the strains both possess genetic mutations, the following steps are followed:

1. Eight younger L4 hermaphrodite from a day 2 plate are moved individually to single plates.
2. Three days later, the adult hermaphrodites are lysed and genotyped according to the following procedure:
    a. For each mutation that is to be genotyped 3µl of lysing buffer (50mM KCl, 10mM Tris pH 8.2, 2.5mM $MgCl_2$, 0.45% NP-40, 0.45% Tween 20, 0.01% gelatin, 60ug/mL proteinase K) is added to a well of an 8-well PCR tube One adult is placed into each unique well. Control lyses are also performed for the mutant, wild type, and a lysis containing one mutant and one wild type animal.

b. The tubes are frozen at -80°C for 10 minutes.

c. The animals are then lysed at 60°C for 60 minutes and then heated at 90°C for 15 minutes to denature the proteinase K enzyme.

d. For each mutation, 3µl lysis buffer is moved to a new well so each mutation can be genotyped via PCR in its own tube for each animal.

e. 23µl of PCR mix is added to each tube (final concentrations of 1x Taq buffer (20mM Tris pH 8.4, 5mM KCl), 3.5mM $MgCl_2$, 0.2mM dNTPs, 1µM of each primer, 5U/µl Taq polymerase) for a final volume of 25µl.

f. PCR is performed using the following settings:

    1. 95°C for 30s
    2. 95°C for 30s
    3. Primer annealing temp for 30s
    4. 72°C for 30s
    5. Repeat steps 2-4 35 times
    6. 72°C for 10min
    7. 4°C hold

3. The PCR products are visualized on a 2% agarose gel run at 100V for 45 minutes and subsequently analyzed. The Koelle lab tries to design primers that create a smaller amplicon for the wild type and a larger amplicon for the mutant of a given gene. This is achieved through a unique three-primer design where one primer sits outside of the mutation area, and two complementary primers are designed where one is closer and within the mutation and the other lies

further outside of the mutation. This strategy produces amplicons 400-500bp in length for the mutation and 200-350bp for the wild type.

4. A plate that is homozygous or heterozygous for all mutations is selected. 16-32 hermaphrodites are singled out onto their own plates from the selected plate, preferentially selecting younger adults as mutants frequently grow slower and/or smaller.
5. Three days later, Steps A2 and A3 are repeated for the new plates.
6. If any mutation is still heterozygous, repeat Steps A4-5 to isolate a homozygous mutant for that genotype.

B. If at least one of the strains are transgenic mutants, the following steps are followed:

1. The plate from day 2 is observed for hermaphrodites that carry the co-injection marker for the integrated transgenic array. This could be fluorescent (e.g. mCherry pharynx marker) or phenotypic (e.g. multi-vulval phenotype). A hermaphrodite carrying this marker is selected and isolated to its own plate.
2. Three days later, the progeny are screened for transmitting the co-injection marker and 8-16 animals that transmit the marker are singled on to individual plates.
3. Three days following this, each plate is screened for transmission. If any percentage of progeny do not contain the marker, the parent animal is considered heterozygous for the transgenic array. Any plate with progeny that have the co-injection marker are selected for genotyping.
4. Steps A2 and A3 are followed for any genetic mutants.
5. Repeat Step B2-B4 to create a strain that is fully homozygous.

Additional specialized genotyping done for this work:

RNAi sensitive strain *lin-15B* was crossed with *tph-1* and *nlp-3ox*. *lin-15B* was followed via ARMS genotyping (Ahlawat, Sharma, Maitra, Roy, & Tantia, 2014; Medrano & de Oliveira, 2014) using the following primers: forward inner 5'-CCGAAGAGAATGAGAATTCGAATCATGGG-3', reverse inner 5'-CCATATCCGTCTGACGCATTCCCAAT-3', forward outer 5'-TGCTACTCTTTTGGATCCACGTTTTGCC-3', and reverse outer 5'-ACTTTCCAGCAAGTGCCAAGCAGTTCTC-3'. The genotyping PCR was performed with 0.7mM $MgCl_2$, 100nM of each primer, standard Taq polymerase buffer containing no $MgCl_2$, 0.2mM dNTPs, and 5U/µl Taq polymerase. Annealing was performed at 55°C and elongation was carried out for 30s for 40 cycles. The PCR products were visualized on a 3-4% agarose gel and run at 50V in the smallest gel box (this is important to use as any other size gel box is unable to be poured at the high agarose concentration) until the dye had migrated approximately half-way down the gel.

To distinguish the CRISPR-generated, *lite-1*, and *sid-1* knockout allele from the wild type, a restriction digest step is performed. A particular restriction site was either created or altered with the mutation. The PCR reaction is performed with only two primers and a restriction digestion step is performed overnight by adding 5µl of 0.6µl NEB Cutsmart Buffer, 1.4µl of NEB HF restriction enzyme, and 3µl of water to each tube and mixed thoroughly. The digest is then analyzed on a 2% agarose gel run at 100V for 45 minutes.

2.1.3. CRISPR C. elegans strain generation

The *npr-36* gene null mutations I designed for this work introduce stop codons within the first intra- or extracellular loops of the GPCR, ultimately preventing the production of any functional protein product. I generated these strains using the method described in Paix, Folkmann, Rasoloson, and Seydoux (2015). In brief, a mix of a crRNA, a tracrRNA, a repair ssODN, and Cas9 protein are injected into a wild-type adult animal. The crRNA (Synthego, no longer available) used were 5'-GUACCUUCGACGGCCGGUAU-3' and 5'-UAGCAGAAGUGACGCACAGU-3'. Repair ssODNs (Keck) with the following sequence were: 5'-CTATATTCCAGTGTGCAAGGTACCTTCGACGGCCGG**AATTC**TATCGGTGAATCTTCGATTGTGTGTGTTCCTGTTG-3' and 5'-TCTCATTAATATCTTCTTCAGTCATTTTTCCAACTG**AATTC**TGCGTCACTTCTGCTAGAAGTAAGTGGGAGGAAAC-3'. These ssODN repair templates insert 5 base pairs at the desired location (in bold) causing a frame shift and premature stop codon, as well as the creation of an EcoRI cut site upon successful cut and integration of the template. A co-CRISPR phenotypic marker, *dpy-10* (crRNA: 5'-GCUACCAUAGGCACCACGAG-3'; ssODN repair: 5'-CACTTGAACTTCAATACGGCAAGATGAGAATGACTGGAAACCGTACCGCTCGTGGTGCCTATGGTAGCGGAGCTTCACATGGCTTCAGACCAACAGCCTAT-3'), was used to identify animals containing the roller phenotype and to perform further genotyping.

Genotyping of the CRISPR strains requires an adaptation of the normal genomic mutant genotyping (2.1.2A) with the addition of a restriction digest before running on

an agarose gel. A nested PCR strategy was used to amplify the product as the highly A/T rich genetic locus caused polymerase slippage and incomplete amplification. The nest primers are: 5'-AACTGTCTGGAGAAGTCTGG-3' and 5'-CGGAAGTCTTTCAGAGCTGT-3'. The interior primers for vs190 are: 5'-AACTGTCTGGAGAAGTCTGG-3' and 5'-TTTCCGTAACTGTATCCCTGAC-3'. The interior primers for vs195 are: 5'-ATTGTGTGTGTTCCTGTTGG-3' and 5'-TTTCAGAAGCAAGAACCCACTC-3'.

CRISPR generated GFP-tagged NPR-36 strains were ordered from SUNYBiotech, LLC. Genotyping was required for these strains as the knock-in of GFP at the endogenous *npr-36* locus was too faint to follow by eye. The primers were as follows: 5'-AAGTAGTGACAAGTGTTGGCTG-3', 5'-AACGGTGCGACTCCCTAC-3', and 5'-CCTGTCTTGAACTTGATCGACG-3'. These primers are suitable for genotyping all inserts containing GFP at the 3' stop codon of *npr-36* (PHX5031, PHX5054, LX2866, LX2871). PCR reactions were carried out using Phusion (NEB) and a Phusion PCR mix scaled down for a 20µl reaction and Phusion PCR conditions.

2.2. Behavioral assays

2.2.1. Unlaid egg assay

Quantitation of unlaid eggs in adult animals was performed using adult animals 30 hours after staging as late L4 larvae as described in Chase and Koelle (2004). The staged adult animals are each placed in a 10µl drop of bleaching solution (750µl of 8.25% hypochlorite—1.25% final—in 5mL of H_2O) on the inside of the lid of a 96-well plate. The adults dissolve, and the eggs contained in each animal are manually counted

on a Leica MS5 dissecting microscope (4.0x objective). The genotype being placed in each drop should be notated before the experiment to prevent any confusion.

2.2.2. Hyperactive egg laying assay

This method allows for classification of animals into the class of "hyperactive egg-layers" defined as laying greater than 25% early-stage eggs compared to wild type. Briefly, 30-hours post-L4 adults are placed on a plate freshly seeded with OP50 food, off the food with no food transfer. After 30 minutes, egg stage is visually assessed for only eggs on the bacteria food patch until a total of 100 eggs are observed. Eggs at the 1-2, 3-4, 5-8, and 9+ cell stage are manually recorded within 5 minutes. If fewer than 100 eggs are recorded or if the counting takes more than 5 minutes, the adults should be moved to another freshly seeded plate, and the assaying should be repeated. Any eggs that are eight cells or fewer are considered early stage, whereas nine cells or more are considered normal.

2.2.3. Pattern of egg laying assay

This protocol was adapted from work published by the Schafer group (Waggoner et al., 2000) to record the long-term egg-laying behavior of different mutant genotypes.

1. 48-hours prior to the assay, NGM plates were seeded with 10µl of one week old OP50.
2. 24-hours prior to the assay, L4s were staged.
3. On the assay day, 10 minutes before recording, five 24-hour post-L4 adults were moved to the two-day old plates.
4. An OMAX camera was set up on a Leica MS5 dissecting microscope in an isolated area.

5. The plate was placed on the microscope, lid side up, with the lid on at 0.63x objective.
6. Using only the ToupViewer software, the recording was set up as follows: 10-12fps, using RAW recording setting. Each plate's gain and exposure was adjusted for the thickness of the plate. The recording is taken for 14,400 seconds.

The time of each egg-laying event is manually recorded for each animal. If more than one egg exited the animal, that was notated but marked as one "event." If the animal left and returned to the camera's field of view during the recording, this was notated. The intervals between egg-laying events were calculated in Excel. The data were analyzed in Prism and displayed using a custom script from Emerson Santiago (see Appendix C: R script to display egg-laying events for the script).

2.3. Targeted RNAi screen

2.3.1. Neuropeptide GPCR library generation

Predicted neuropeptide receptor GPCR clones (Frooninckx et al., 2012; Hobert, 2013); Table 2.2) were picked from the Ahringer (Kamath & Ahringer, 2003) or Vidal (Rual et al., 2004) bacterial RNAi feeding libraries. The dsRNA generating plasmids were generated using restriction digest cloning. SalI and SacII sites were introduced by primers used to amplify an exon rich region in the gene of interest from a *C. elegans* lysate either designed for this publication or designed by Kamath and Ahringer (2003). The primer sequences used are in Table 2.2. The L4440 plasmid and PCR fragments were digested, ligated, and sequenced before chemical transformation into HT115(DE3) cells.

Table 2.2: All RNAi feeding bacterial clones used in this this work.

Gene Name	Gene Designation	dsRNA Origin	RNAi Feeding Clone Source	Forward Primer (5'→3')	Reverse Primer (5'→3')
L4440	Empty vector	Genomic	Ahringer		
nlp-3	F48C11.3	Genomic	Ahringer		
aex-2	T14B1.2	cDNA	Vidal		
aexr-1	C25B8.5	cDNA	Vidal		
aexr-2	C25B8.7	Genomic	Ahringer		
aexr-3	C48C5.3	Genomic	Ahringer		
ckr-1	T23B3.4	Genomic	Ahringer		
ckr-2	Y39A3B.5	Genomic	Ahringer		
daf-37/frpr-20	C30B5.5	Genomic	This work	ATATGTCGACcttcactgctg atatgctgc	TTAACCGCGGagtctgtcca acttctgaacc
daf-38/gnrr-8	Y105C5A.23	Genomic	Ahringer		
dmsr-1	F57B7.1	Genomic	Ahringer		
dmsr-2	Y23H5B.4	Genomic	This work	AATTGTCGACGAGACC CGAATCCCTCAGTG	TTAACCGCGGcgtgaaacag ctttggtcc
dmsr-3	Y48C3A.11	Genomic	Ahringer		
dmsr-4	D1069.4	cDNA	Vidal		
dmsr-5	Y48A6B.1	Genomic	Ahringer		
dmsr-6	Y54G11B.1	Genomic	Ahringer		
dmsr-7	C35A11.1	Genomic	This work	atatgtcgacTCCAAATATG CTGGTCCACG	TTAACCGCGGgcaaaggga atttgtaccgag
dmsr-8	C35A5.7	Genomic	Ahringer		
dmsr-9	ZC404.13	Genomic	Ahringer		
dmsr-10	ZC404.10	Genomic	Ahringer		
dmsr-11	ZC404.11	Genomic	Ahringer		
dmsr-12	H34P18.1	Genomic	This work	AATTGTCGACcgatgaagct gggaatagtacg	AATTCCGCGGttccttcttcct cggtgc
dmsr-13	T15B7.12	cDNA	Vidal		
dmsr-14	T15B7.11	Genomic	Ahringer		
dmsr-15	T15B7.13	Genomic	Ahringer		
dmsr-16	T27B2.1	Genomic	This work	atatgtcgacCTACCACCAA CACCAAATTACC	TTATCCGCGGtgcCTTGT ATCTTTCCGAGTAG
egl-6	C46F4.1	cDNA	Vidal		
frpr-1	C02B8.5	Genomic	Ahringer		
frpr-2	C05E7.4	cDNA	Vidal		
frpr-3	C26F1.6	cDNA	Vidal		
frpr-4	C54A12.2	Genomic	Ahringer		
frpr-5	C56A3.3	cDNA	Vidal		
frpr-6	F21C10.12	Genomic	This work	ataagtcgacAGTCTGCCGA CCGTTACAGg	TTAACCGCGGGCTTCC GTTTGTTCAAGTCTG
frpr-7	F39B3.2	cDNA	Vidal		
frpr-8	F53A9.5	Genomic	Ahringer		
frpr-9	F53B7.2	Genomic	Ahringer		
frpr-10	F57H12.4	Genomic	This work	TATAGTCGACGCACAA TCATAGAAGGGCAC	ttaaCCGCGGGCTGCTG GCATTTCCATAC
frpr-11	K06C4.8	cDNA	Vidal		
frpr-12	K06C4.9	Genomic	Ahringer		
frpr-13	K06C4.17	Genomic	Ahringer		
frpr-14	K07E8.5	Genomic	Ahringer		
frpr-15	K10C8.2	Genomic	Ahringer		
frpr-16	R12C12.3	cDNA	Vidal		
frpr-17	T14C1.1	cDNA	Vidal		
frpr-18	T19F4.1	Genomic	Ahringer		
frpr-19	Y41D4A.8	Genomic	Ahringer		
frpr-21	E04D5.2	Genomic	Ahringer		
fshr-1	C50H2.1	Genomic	Ahringer		
gnrr-1	F54D7.3	cDNA	Vidal		
gnrr-2	C15H11.2	cDNA	Vidal		
gnrr-3	ZC374.1	cDNA	Vidal		
gnrr-4	C41G11.4	cDNA	Vidal		

gnrr-5	H22D07.1	Genomic	Ahringer		
gnrr-6	F13D2.2	cDNA	Vidal		
gnrr-7	F13D2.3	Genomic	Ahringer		
lat-1	B0457.1	Genomic	Ahringer		
lat-2	B0286.2	Genomic	Ahringer		
nmur-1	C48C5.1	Genomic	Ahringer		
nmur-2	K10B4.4	cDNA	Vidal		
nmur-3	F02E8.2	cDNA	Vidal		
npr-1	C39E6.6	Genomic	Ahringer		
npr-2	T05A1.1	Genomic	This work	AATTGTCGACtggctgtaag gtgatggaag	tttaccgcggATGTATGATC GGTACTGGTTGC
npr-3	C10C6.2	cDNA	Vidal		
npr-4	C16D6.2	cDNA	Vidal		
npr-5	Y58G8A.4	Genomic	Ahringer		
npr-6	F41E7.3	Genomic	Ahringer		
npr-7	F35G8.1	Genomic	Ahringer		
npr-8	C56G3.1	Genomic	Ahringer		
npr-9	ZK455.3	Genomic	Ahringer		
npr-10	C53C7.1	cDNA	Vidal		
npr-11	C25G6.5	Genomic	Ahringer		
npr-12	T22D1.12	cDNA	Vidal		
npr-13	ZC412.1	cDNA	Vidal		
npr-14	W05B5.2	Genomic	Ahringer		
npr-15	T27D1.3	Genomic	Ahringer		
npr-16	F56B6.5	Genomic	Ahringer		
npr-17	C06G4.5	Genomic	This work	AATTGTCGACTTCTCG GTTTCTGGATGTTTGG	AATTCCGCGGCTTAAA CGTCCTTGTGTGTTC
npr-18	C43C3.2	Genomic	Ahringer		
npr-19	C02H7.2	Genomic	Ahringer		
npr-20	T07D4.1	Genomic	Ahringer		
npr-21	T23C6.5	cDNA	Vidal		
npr-22	Y59H11AL.1	cDNA	Vidal		
npr-23	Y34D9A.2	Genomic	Ahringer		
npr-24	R106.2	cDNA	Vidal		
npr-25	T02E9.1	Genomic	Ahringer		
npr-26	T02D1.6	Genomic	Ahringer		
npr-27	F42C5.2	Genomic	This work	AATTGTCGACTATTGA CACTCCCTGCCACG	aataccgcggACTTTCTCCA CCACTTTCTTCC
npr-28	F55E10.7	cDNA	Vidal		
npr-29	ZC84.4	Genomic	This work	AATTGTCGACtttcagGGA TACCGAACGTATG	TATTCCGCGGttacCTTG AGGCGACCAGTG
npr-30	H10E21.2	Genomic	Ahringer		
npr-31	T07F8.2	Genomic	Ahringer		
npr-32	Y116A8B.5	Genomic	Ahringer		
npr-33	F31B9.1	cDNA	Vidal		
npr-34	Y54E2A.1	Genomic	Ahringer		
npr-35	C50F7.1	cDNA	Vidal		
npr-36	F10D7.1	Genomic	Ahringer		
npr-37	M04G7.3	cDNA	Vidal		
npr-38	T10E10.3	Genomic	Ahringer		
npr-39	F57A8.4	cDNA	Vidal		
npr-40	Y70D2A.1	cDNA	Vidal		
npr-41	B0334.6	Genomic	Ahringer		
npr-42	C01F1.4	cDNA	Vidal		
npr-43	F56A12.2	cDNA	Vidal		
ntr-1	T07D10.2	cDNA	Vidal		
ntr-2	F14F4.1	cDNA	Vidal		
pcdr-1	F59D12.1	Genomic	Ahringer		
pdfr-1/seb-1	C13B9.4	Genomic	Ahringer		
seb-2	ZK643.3	Genomic	This work	AATTGTCGACccggctccaa ctcaatcag	ttatccgcggTGGAAGACTT GTGAAGAGAGTG
seb-3	C18B12.2	cDNA	Vidal		
sphr-1	C24B5.1	Genomic	Ahringer		
sprr-1	R03A10.6	Genomic	Ahringer		
sprr-2	F42D1.3	cDNA	Vidal		

sprr-3	Y69A2AR.15	Genomic	Ahringer		
tag-89	H02I12.3	cDNA	Vidal		
tkr-1	C38C10.1	Genomic	Ahringer		
tkr-2	C49A9.7	cDNA	Vidal		
tkr-3	AC7.1	cDNA	Vidal		
trhr-1/nmur-4	C30F12.6	Genomic	Ahringer		
zzz-1	F32D8.10	Genomic	This work	aattgtcgacGGAACGATTC TGGTTATGTGTC	taaaccgcggAAACGAGCA GACGAAGCCAC
	AH9.1	Genomic	Ahringer		
	AH9.4	Genomic	Ahringer		
	B0034.5	Genomic	Ahringer		
	B0563.6	Genomic	Ahringer		
	C04C3.6	cDNA	Vidal		
	C09F12.3	Genomic	Ahringer		
	C17H11.1	Genomic	Ahringer		
	C47E8.3	cDNA	Vidal		
	C50H11.13	cDNA	Vidal		
	C54D10.5	Genomic	Ahringer		
	C54E10.3	Genomic	This work	ATAAGTCGACaacaccagg gttcgagtc	AATTCCGCGGcgaccacca atcacaagacc
	D1014.2	Genomic	Ahringer		
	F13H6.5	Genomic	This work	ataagtcgacAATACGCCGT ACCACCTC	TTAACCGCGGcatacCTG AATAGCACTTGCTG
	F16C3.1	Genomic	Ahringer		
	F36D4.4	Genomic	Ahringer		
	F40A3.7	cDNA	Vidal		
	F52D10.4	cDNA	Vidal		
	F54E4.2	Genomic	Ahringer		
	F56A11.4	Genomic	This work	ATATGTCGACTGGGAC TATTTCCGAGTGGAGC	TTATCCGCGGtaagcagcag cacacagg
	F59B2.13	Genomic	Ahringer		
	H09F14.1	cDNA	Vidal		
	H23L24.4	Genomic	Ahringer		
	K03H6.1	Genomic	Ahringer		
	K03H6.5	Genomic	Ahringer		
	R11F4.2	Genomic	Ahringer		
	R13H7.2	Genomic	Ahringer		
	T01B11.1	cDNA	Vidal		
	T02D1.4	Genomic	Ahringer		
	T11F9.1	Genomic	Ahringer		
	T21H3.5	Genomic	This work	TATTGTCGACttctctctcttcc aggcattg	ATAACCGCGGccgatttgca gagtttcctatg
	W10C4.1	Genomic	Ahringer		
	Y37E11AL.1	cDNA	Vidal		
	Y40C5A.4	Genomic	Ahringer		
	Y41D4B.24	Genomic	This work	AATAGTCGACACTGTG CCACGCTAAACTCTCC	ttaaccgcggAGTCTGCTCC AGCGATGTC
	ZK1307.7	cDNA	Vidal		
	ZK721.4	Genomic	Ahringer		
	ZK813.5	Genomic	Ahringer		
	ZK863.1	Genomic	This work	taaagtcgacGAAGACTCCC ACGTAGTACC	TAATCCGCGGtcacccgaca agtgttcc

2.3.2. RNAi plate creation

The protocol from Kamath and Ahringer (2003) was adapted for a medium through-put screen. NGM agar plates with 50μM AMP and 1mM IPTG were made at most 3 weeks before the assay (from here on called RNAi plates). Strains from the RNAi neuropeptide GPCR library were picked from glycerol stocks. The empty vector

control and positive *nlp-3* control were also picked. The bacteria were cultured overnight in LB with 100µg/mL of ampicillin and 12.5µg/mL of tetracycline. The following afternoon, 150µl of the culture was plated on the RNAi plates and allowed to air dry with the lid vented but covered in a box at room temperature overnight. The following morning, L1 larvae were plated on the RNAi plates.

2.3.3. L1 larval staging

Standard NGM agar plates with OP50 food with the *C. elegans* strain of interest were grown at 20°C. Four plates were grown to adult-prevalent starvation and harvested via the following method. The plates were rinsed into a 15mL conical tube with a total of 5mL of sterilized DI water using a glass bulb pipet and spun for 30s at 1000rpm. Three milliliters of the supernatant were removed and split between 2 standard Eppendorf tubes using a glass pipette. The tubes were spun for 30s at 2500rpm and the supernatant was once more removed. To each tube, 600µl of bleach solution (120mM NaOH, 1.056% v/v sodium hypochlorite) was added and gently tipped for 2 minutes. Then, 600µl of sterile water was added to each tube, the tubes were spun for 30s at 2500rpm, and the supernatant was removed. The process was repeated an additional time. After removing the supernatant, 600µl of water was added for a final rinse, spun at 30s for 2500rpm, and the supernatant was removed. The remaining eggs in each tube were suspended in 1mL of sterile M9 and combined into a 50mL Erlenmeyer flask (for a total of 2mL), covered with aluminum foil, and shaken at low rpm at 20°C for 18 hours to hatch. After 18 hours, the number of L1 larvae in a 10µl drop of M9 was counted three times, averaged, and used to plate 75-100 L1 larvae on each RNAi plate off the bacterial food lawn.

2.3.4. Screening

After 78 hours of incubation (30 hours post-L4), the plates were visually screened for an increase in egg retention compared to the empty vector control plates. From plates that appeared to be more gravid than the control, 30 adults were randomly selected and assayed using the unlaid egg assay to determine the average egg retention for that neuropeptide receptor knockdown. All knockdowns screened were compared via a 2-way ANOVA analysis, using the empty vector and *nlp-3* knockdown controls.

2.4. Cell-specific RNAi

Cell-specific RNAi fragments were generated using the methods in Esposito, Di Schiavi, Bergamasco, and Bazzicalupo (2007). Briefly, fragments of the gene or the cDNA were PCR amplified in a sense and antisense direction. Both fragments were PCR "fused" to a cell-specific promoter fragment. The final two products were injected into strains to drive dsRNA production cell specifically.

For HSN specific knockdown, the long *tph-1* promoter was amplified out of pJM60A; for the muscle specific knockdown, the *myo-3* promoter was amplified out of pCFJ104. The two (or four for the double knockdown) fragments generated were then introduced into the following injection mix: fragments at 50ng/µl, mCherry pharynx marker (pCFJ90) 10ng/µl, and *Escherichia coli* digested genomic DNA 250ng/µl. Control RNAi was performed using *gfp* cDNA driven by either the *tph-1* or *myo-3* promoters amplified from pPD128.110. The mixture was injected into a *sid-1* only or *tph-1; sid-1* background. Five lines of F_1 that displayed strong fluorescence were randomly selected to assay.

2.5. Calcium imaging

Five L4 larvae were moved to a new plate 24-hour before the assay. On the day of the assay, a 1cm^2 square of OP50 *E. coli* was "drawn" onto an NGM plate using a pick towards the edge but not where it slopes. The square was then carefully cut using a medium spatula and the boarders were extended to the edges of the plate so the surrounding agar can be removed easily. One 24-hour post-L4 adult was moved to the cube of agar. Using the spatula, the cube was pulled out of the plate, and the side with the animal and food was placed on a large coverslip (Kemtech SUPER WHITE GLASS, 24x260mm, 0.13-0.16mm, Ref. 0340-4050). The slide was inverted so the plain slide of the NGM cube is on top and a 22 × 22–1 coverslip (Fisher Scientific Cat. No. 12-542A) was placed on the exposed side. The animals were left for one hour to adjust to the environment between the coverslips before assaying. Using a Zeiss LSM 880 microscope, a brightfield and green fluorescence was recorded on one channel to record the GCaMP5 and egg laying and the control mCherry was recorded on the other channel. The recordings were collected with a 20× air objective at approximately 16 frames per second at 256×256 pixels at 16-bit resolution for one hour. Five paired wild-type and *nlp-3* recordings were performed, with two additional *nlp-3* recordings. Ratiometric analysis was performed using Volocity (PerkinElmer) to determine when the GFP signal was significantly changed from previous frames. The data analyzed in Volocity was further processed and, using the findpeaks function in MATLAB (See Appendix A: MATLAB code to process the calcium imaging data produced in Volocity for ratiometric analysis), calcium signal peaks were called. The output from the MATLAB function was then processed for publication using an R script (see

Appendix B: R script to create publication figures from the peaks called in the MATLAB code from Appendix A). The timepoint of egg laying was manually recorded. The time between peaks was analyzed using Prism.

2.6. Confocal imaging

24-hour post-L4 animals were placed on a microscope slide (Fisher Scientific Superfrost Cat. No. 22-178-277) containing a thin pad of 2% agarose and with 10-15µl of a solution of 150mM sodium azide and 120mM Optiprep. The animals were allowed to paralyze then a 22 × 22–1 coverslip (Fisher Scientific Cat. No. 12-542A) was placed on top. Z-stacks with two-channels were taken of at least five animals for each genotype on a Zeiss LSM 880 using a 40x water-immersion objective. Images were analyzed and processed using FIJI (ImageJ).

2.7. Statistical methods

Statistical analyses were performed using GraphPad Prism v10.1.1 for Macintosh. One- or two-way ANOVAs with Tukey multiple comparisons was performed to determine statistical significance. Non-linear curves were fit with least squares regression for semi-log plots with significance determined by extra sum-of-squares F test with a p value cut off of 0.05, compared pairwise to wild type. Mann-Whitney U tests were performed pairwise with wild type data.

3. Targeted RNAi screen for neuropeptide GPCRs identified one receptor for NLP-3

3.1. Introduction – Co-opting an innate *C. elegans* cellular process of RNAi to identify cognate neuropeptide-receptor pairs

RNAi, or RNA interference, is an inherent process in development where double-stranded RNA (dsRNA) is formed, targets a ssRNA with similar sequence, and leads to degradation of the ssRNA, preventing gene expression within poles of embryos during division or disparately functioning poles of cells. This essential process was discovered in *C. elegans* and has since been utilized across biological research to knockdown RNA expression (Wightman, Ha, & Ruvkun, 1993; Wang & Barr, 2005). Within *C. elegans*, RNAi has been achieved through several mechanisms: 1) feeding the animals bacteria expressing a dsRNA against a gene of interest, 2) through soaking the animals in a solution containing the dsRNA, and 3) through microinjection of the dsRNA. For this portion of my project, I utilized feeding RNAi as it allows for a higher-throughput approach for a screen (though in section 4.2.4 I used a variation on injection-based RNAi).

To better understand the role of NLP-3 in egg-laying behavior, I had to first identify the receptor that NLP-3 was activating to cause egg-laying. Our collaborator, Dr. Isabel Beets, had previously provided us with a possible candidate (NPR-42 (*C01F1.4*)); however, upon assaying two different null mutations of this receptor, I did not find that it phenocopied NLP-3 (Supplemental Figure 9.1). Other methods of determining cognate receptor-ligand pairs have been executed through assaying genes in known

synaptic partners, genetic screens, or heterologous cell binding assays (Beets et al., 2023). As there is limited single-cell RNA sequencing data for the mature hermaphrodite—especially for the components of the egg-laying circuit that are not neurons—and a forward genetic screen is an extremely labor intensive and time-consuming process, I designed a targeted, RNAi-feeding screen employing two *C. elegans* strains to identify a receptor for NLP-3. To specify the screen towards identifying an NLP-3 receptor specifically, not simply every GPCR that affects egg laying, I used two different *C. elegans* strains: an *nlp-3* over-expressing strain (*nlp-3OX*) that I created for Brewer et al. (2019) to find a receptor that rescues its hyperactive egg-laying phenotype and a serotonin knockout (*tph-1*) strain to find a receptor that causes an additive egg-laying phenotype that phenocopies the severe *egl* phenotype of the *tph-1; nlp-3* double mutant.

3.1.1. Creation of the neuropeptide GPCR RNAi-feeding library

I compiled a list of all predicted neuropeptide GPCRs to screen for an NLP-3 receptor (Frooninckx et al., 2012; Hobert, 2013). To assemble a feeding RNAi library, I used two libraries created previously for expressing genomic fragments of exon rich regions of genes (Kamath & Ahringer, 2003) and expressing cDNA of genes (Rual et al., 2004). The genomic library contained more of the sequences I required, though I had access to both libraries at Yale. I picked a subset to sequence and discovered that many of the wells had been contaminated with other inserts; therefore, I needed to source the genes from another library. I sourced most of the genes from the genomic RNAi library owned by other labs and filled in some gaps from the cDNA library, but some of the contamination that I found appeared to have originated from the company purveyor

of the genomic library. To fully execute the screen, I had to create 20 plasmids against GPCRs that were not represented in either library or were contaminated in the genomic library. In total, I screened 155 GPCRs (see Table 2.2 for full break down of strains made and the library that each was from).

3.1.2. Creation of the C. elegans strains for screening

I created two *C. elegans* strains to run through the screen: *tph-1* and *nlp-3OX*. However, there was a concern of poor receptor knockdown within neurons as this cell type does not express the channel required for dsRNA transport, a process that is important for RNAi (Calixto, Chelur, Topalidou, Chen, & Chalfie, 2010). To accommodate this possibility, I introduced an additional mutation to the strains to sensitize the animals to RNAi. There are different mutations that have been found to enhance response to RNAi; in this work I tested five strains with different combinations of RNAi sensitive mutations to determine which was the least egg-laying defective (Supplemental Figure 9.2) and most responsive to egg-laying defective mutations (Supplemental Figure 9.3). I ultimately selected *lin-15b*, which is believed to keep the cells in an "embryonic-like state" and was a visually healthier animal compared to other mutants (Calixto et al., 2010; my own observations).

Using the library and strains I generated, I performed the targeted RNAi screen described in Section 2.3 to identify the NLP-3 receptor, screening through 155 predicted neuropeptide receptors.

3.2. Results

I first visually screened through the experimental populations for the GPCR knockdowns that were on average more egg-laying defective than the negative-control

(empty vector knockdown) or that looked similarly as defective as the positive-control (*nlp-3* knockdown). I then quantified the number of eggs in the top 20% of the receptors I screened, resulting in the data in Figure 3.1, Figure 3.2, and Table 3.1.

3.2.1. nlp-3OX screen identified one significant hit for an NLP-3 GPCR, NPR-36

nlp-3OX animals are hyperactive egg-layers, meaning that they lay their eggs more frequently than wild-type animals, resulting in a significant decrease in unlaid eggs (1.3±0.5 eggs vs 15.5±1.4 eggs, respectively). However, introducing the *lin-15b* mutation caused the *nlp-3OX* to have 6.6±0.6 eggs when fed the empty vector negative control (Figure 3.1). Knocking down *nlp-3* (the positive control) in the *nlp-3OX; lin-15b* strain resulted in an increase in eggs to 24.9±1.2 eggs—similar to the *nlp-3* single mutant (24.4±1.7 eggs). I performed the assay over eight iterations with about 20 GPCRs per iteration; this allowed me to quantify the visual hits using the unlaid egg assay (Method in 2.2.1) which, due to time constraints, would not have been possible to perform all of in one day. To ensure that the subsets behaved similarly, I repeated the positive and negative controls with each iteration.

Figure 3.1 summarizes the quantified data from the 30 top GPCRs in this assay. *npr-36* knockdown animals accumulated 18.2±3.1 eggs, the only receptor I screened that was significantly more egg-laying defective than the empty vector control ($p<0.0001$). All other knockdowns I performed are summarized in Table 3.1.

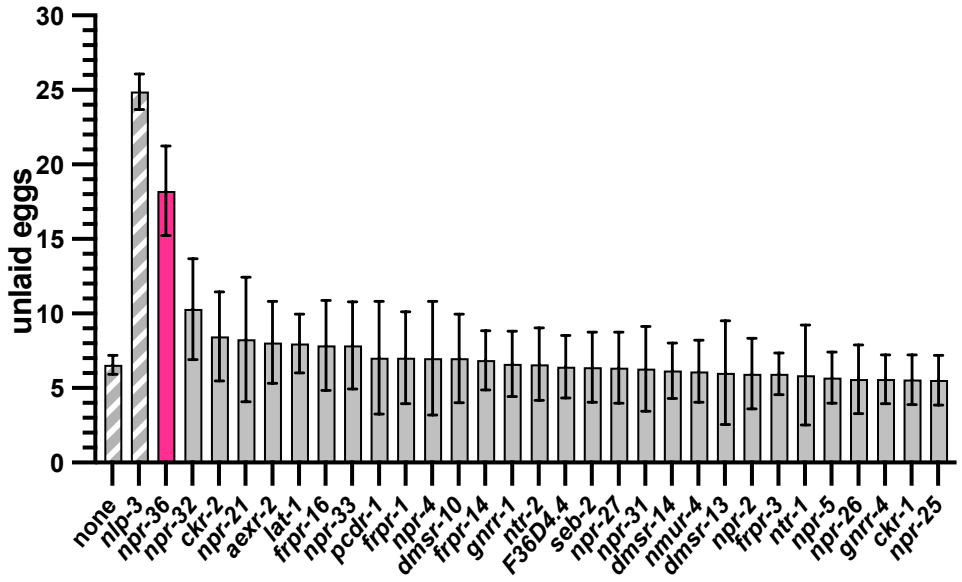

Figure 3.1: *npr-36* is the most significant GPCR screened in the *nlp-3OX* animals.

3.2.2. tph-1 screen identified several hits and corroborated NPR-36 as a potential NLP-3 GPCR

tph-1 animals are mildly *egl* with 25.7±1.6 eggs compared to wild-type animals with 15.5±1.4 eggs. The *tph-1; lin-15b* animals are also mildly *egl* with 28.6±1.1 eggs when fed the empty vector negative control. When the positive control (*nlp-3*) was knocked down in the *tph-1; lin-15b* animals, they accumulated 44.9±1.4 eggs, a severe *egl* phenotype. After I screened all 155 GPCRs against these two controls, several hits were significant compared to the empty vector control knockdown, with *npr-36* being the most severe *egl* strain with 48.2±3.5 eggs ($p<0.0001$ for empty vector compared to *npr-36, seb-2,* and *R13H7.3*; $p<0.001$ for *gnrr-4*; Figure 3.2). All other knockdowns performed are summarized in Table 3.1.

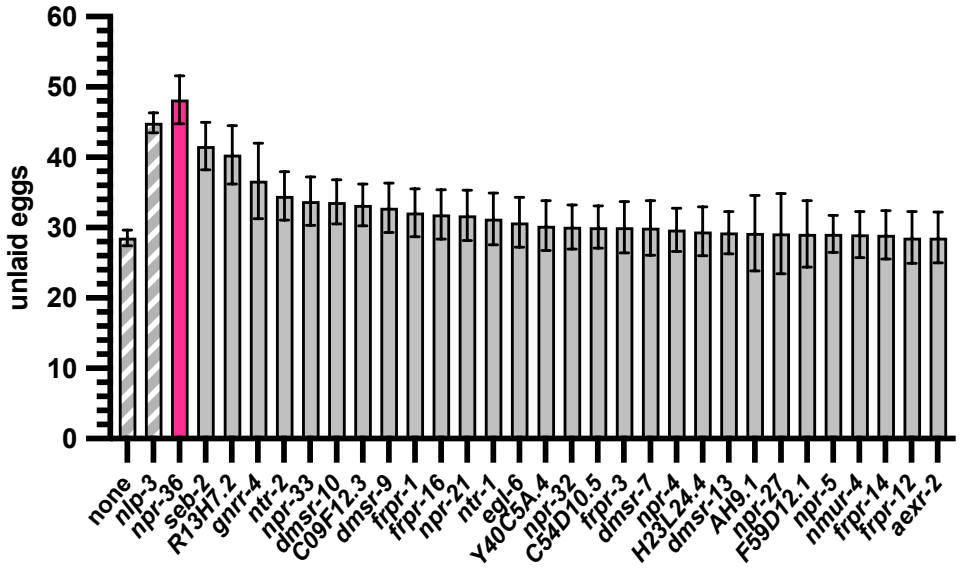

Figure 3.2: *npr-36* has the greatest egg accumulation in the *tph-1* screen.

Table 3.1: Summary of data generated through screening all predicted neuropeptide GPCRs.

Gene name	Gene designation	*nlp-3OX* number of unlaid eggs (mean ± 95% CI)	*tph-1* number of unlaid eggs (mean ± 95% CI)
Empty vector	none	6.6±0.6	28.6±1.1
nlp-3	F48C11.3	24.9±1.2	44.9±1.4
npr-36	F10D7.1	18.2±3.0	48.2±3.4
npr-32	Y116A8B.5	10.3±3.4	30.1±3.2
ckr-2	Y39A3B.5	8.5±3.0	24.8±3.0
npr-21	T23C6.5	8.3±4.2	31.8±3.6
aexr-2	C25B8.7	8.1±2.8	28.6±3.6
lat-1	B0457.1	8.0±2.0	27.3±2.8
frpr-16	R12C12.3	7.9±3.0	31.9±3.5
npr-33	F31B9.1	7.9±2.9	33.8±3.4
npr-4	C16D6.2	7.0±3.8	29.7±3.1
pcdr-1	F59D12.1	7.0±3.8	29.1±4.7
frpr-1	C02B8.5	7.0±3.1	32.1±3.4
dmsr-10	ZC404.10	7.0±3.0	33.7±3.1
frpr-14	K07E8.5	6.9±2.0	29.0±3.4
ntr-2	F14F4.1	6.6±2.4	34.5±3.5
gnrr-1	F54D7.3	6.6±2.2	28.3±3.2
	F36D4.4	6.4±5.6	23.0±3.0
npr-27	F42C5.2	6.4±2.4	29.2±1.2
seb-2	ZK643.3	6.4±2.4	41.6±3.4
npr-31	T07F8.2	6.3±2.9	25.3±2.8
dmsr-14	T15B7.11	6.2±1.9	27.4±2.7
trhr-1/nmur-4	C30F12.6	6.1±2.1	29.0±3.3
dmsr-13	T15B7.12	6.0±3.5	29.3±3.0
npr-2	T05A1.1	6.0±2.4	24.8±6.4
frpr-3	C26F1.6	6.0±1.4	30.1±3.6
ntr-1	T07D10.2	5.9±3.4	31.3±3.7
npr-5	Y58G8A.4	5.7±1.7	29.1±2.6
npr-26	T02D1.6	5.6±2.3	26.5±3.7
ckr-1	T23B3.4	5.6±1.7	24.8±3.3

gnrr-4	C41G11.4	5.6±1.6	36.7±5.4
npr-13	ZC412.1	5.5±1.7	27.1±2.8
npr-25	T02E9.1	5.5±1.7	26.8±2.6
	C04C3.6	5.4±1.6	26.2±2.6
	R11F4.2	5.4±1.5	26.2±3.4
npr-12	T22D1.12	5.4±1.1	26.7±3.6
	Y40C5A.4	5.23±1.3	30.3±3.5
dmsr-9	ZC404.13	5.1±1.3	32.8±3.5
	D1014.2	5.1±1.2	25.7±3.0
npr-42	C01F1.4	5.1±0.80	27.5±3.6
tkr-1	C38C10.1	4.9±1.0	24.8±2.3
	R13H7.2	4.9±1.0	40.4±4.2
npr-23	Y34D9A.2	4.9±1.0	27.6±3.8
frpr-12	K06C4.9	4.9±0.9	28.6±3.7
	T01B11.1	4.8±0.8	26.8±3.3
	B0034.5	4.7±1.2	22.1±2.8
	H23L24.4	4.7±0.7	29.5±3.5
	C09F12.3	4.6±1.1	33.2±3.0
	AH9.1	4.4±1.2	29.2±5.4
	C54D10.5	4.4±1.0	30.1±3.0
egl-6	C46F4.1	4.2±0.9	30.8±3.6
dmsr-7	C35A11.1	3.9±1.2	30.0±3.9
	F16C3.1	3.9±0.7	27.6±3.5
dmsr-2	Y23H5B.4	3.7±1.1	26.4±3.5
npr-17	C06G4.5	3.6±0.6	27.0±4.4
aex-2	T14B1.2		
aexr-1	C25B8.5		
aexr-3	C48C5.3		
daf-37/frpr-20	C30B5.5		
daf-38/gnrr-8	Y105C5A.23		
dmsr-1	F57B7.1		
dmsr-3	Y48C3A.11		
dmsr-4	D1069.4		
dmsr-5	Y48A6B.1		
dmsr-6	Y54G11B.1		
dmsr-8	C35A5.7		
dmsr-11	ZC404.11		
dmsr-12	H34P18.1		
dmsr-15	T15B7.13		
dmsr-16	T27B2.1		
frpr-2	C05E7.4		
frpr-4	C54A12.2		
frpr-5	C56A3.3		
frpr-6	F21C10.12		
frpr-7	F39B3.2		
frpr-8	F53A9.5		
frpr-9	F53B7.2		
frpr-10	F57H12.4		
frpr-11	K06C4.8		
frpr-13	K06C4.17		
frpr-15	K10C8.2		
frpr-17	T14C1.1		
frpr-18	T19F4.1		
frpr-19	Y41D4A.8		
frpr-21	E04D5.2		
fshr-1	C50H2.1		
gnrr-2	C15H11.2		
gnrr-3	ZC374.1		

gnrr-5	H22D07.1	
gnrr-6	F13D2.2	
gnrr-7	F13D2.3	
lat-2	B0286.2	
nmur-1	C48C5.1	
nmur-2	K10B4.4	
nmur-3	F02E8.2	
npr-1	C39E6.6	
npr-3	C10C6.2	
npr-6	F41E7.3	
npr-7	F35G8.1	
npr-8	C56G3.1	
npr-9	ZK455.3	
npr-10	C53C7.1	
npr-11	C25G6.5	
npr-14	W05B5.2	
npr-15	T27D1.3	
npr-16	F56B6.5	
npr-18	C43C3.2	
npr-19	C02H7.2	
npr-20	T07D4.1	
npr-22	Y59H11AL.1	
npr-24	R106.2	
npr-28	F55E10.7	
npr-29	ZC84.4	
npr-30	H10E21.2	
npr-34	Y54E2A.1	
npr-35	C50F7.1	
npr-37	M04G7.3	
npr-38	T10E10.3	
npr-39	F57A8.4	
npr-40	Y70D2A.1	
npr-41	B0334.6	
npr-43	F56A12.2	
pdfr-1/seb-1	C13B9.4	
seb-3	C18B12.2	
sphr-1	C24B5.1	
sprr-1	R03A10.6	
sprr-2	F42D1.3	
sprr-3	Y69A2AR.15	
tag-89	H02I12.3	
tkr-2	C49A9.7	
tkr-3	AC7.1	
zzz-1	F32D8.10	
	AH9.4	
	B0563.6	
	C17H11.1	
	C47E8.3	
	C50H11.13	
	C54E10.3	
	F13H6.5	
	F40A3.7	
	F52D10.4	
	F54E4.2	
	F56A11.4	
	F59B2.13	
	H09F14.1	
	K03H6.1	

K03H6.5	
T02D1.4	
T11F9.1	
T21H3.5	
W10C4.1	
Y37E11AL.1	
Y41D4B.24	
ZK1307.7	
ZK721.4	
ZK813.5	
ZK863.1	

3.3. Discussion

The identification of an NLP-3 receptor was crucial to understand the NLP-3 signaling dynamics in the egg-laying circuit. I identified NPR-36 as the strongest candidate, as it was the only significant hit in the *nlp-3OX* screen and resulted in the largest accumulation of eggs in the *tph-1* screen.

I named the receptor NPR-36 after the naming convention for receptors paired with NLP peptides in *C. elegans*—neuropeptide receptors. *npr-36* (*F10D7.1*) is predicted to be a member of the Rhodopsin-like GPCR family, the most abundant family of GPCRs in mammals. The gene structure of *npr-36* has been annotated to have a 5'UTR 9,161 base pairs from the start codon.[2] My correspondence with WormBase editors informed me that *npr-36* has a SL2 *trans*-splice site and thus the mRNA transcript likely has a different 5'UTR than its prediction. *npr-36* is also predicted to have two different 3'UTR splicing isoforms. The NPR-36 protein has an AlphaFold predicted structure of seven transmembrane regions and a long internal C-terminal cytoplasmic loop with a disordered region (Figure 3.3; Jumper, Evans et al. 2021, Varadi, Anyango et al. 2022). This structure is typical of a G protein coupled receptor, although the long C-

[2] This 5' UTR RNAseq annotation has been added and removed to the Wormbase sequence viewer throughout my PhD. Currently (December, 2023), *npr-36* has no annotated 5' UTR, excluding four nucleotides likely necessary as a SL2 splice acceptor site.

terminal tail is abnormal from my observations of other known GPCR structures (though this could also be due to disordered regions being unable to be crystalized or determined using cryogenic electron microscopy).

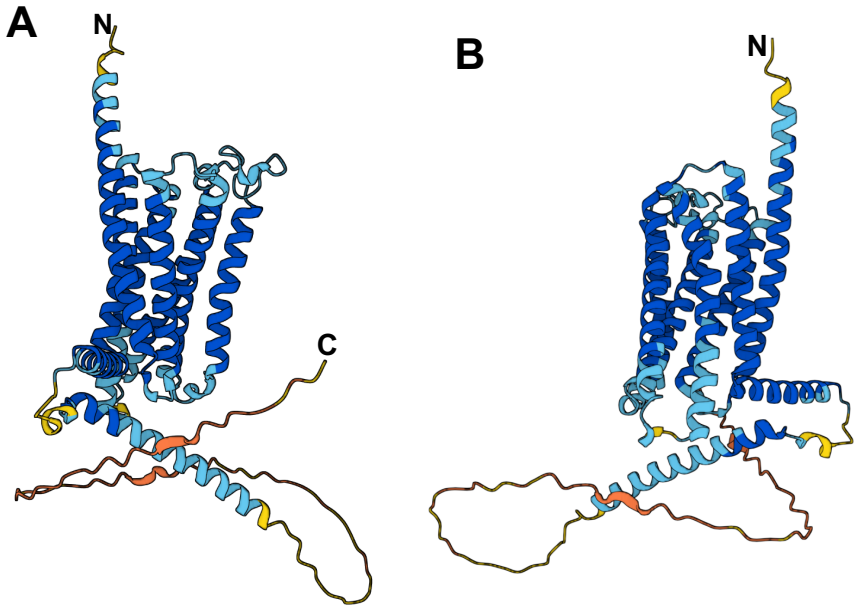

Figure 3.3: AlphaFold predicted structure of NPR-36 GPCR.
Dark blue represents high confidence of structure while orange represents low confidence, with shades in between representing confidence on that gradient. (Jumper, Evans et al. 2021, Varadi, Anyango et al. 2022)

Interestingly, *seb-2,* the second strongest hit in the *tph-1* screen, has been reported to be expressed in the vm1 cells (Lynch, Briggs, & Hope, 1995). Its recent neuropeptide pairing is weak (2.54uM EC50; Beets et al., 2023), however, and it has high orthology to a human calcitonin receptor (Davis et al., 2022). Additionally, while *seb-2* is classed as a secretin/class type-B GPCR, it has been poorly studied with most sources commenting on its inadequate coverage in *C. elegans* research. Follow up studies are needed to elucidate its effects on egg laying alongside serotonin, as it may have a stronger activation with a non-canonical neurotransmitter such as ATP.

I used the hit of NPR-36 from this chapter in the remainder of the work contained within this thesis focusing on NLP-3/NPR-36 signaling in the *C. elegans* egg-laying circuit.

4. Verifying NPR-36 as an NLP-3 receptor

4.1. Introduction – Multiple assays are needed to support NPR-36 as an NLP-3 receptor

Having identified NPR-36 as a putative NLP-3-activated GPCR, I next aimed to verify this ligand-receptor pairing. I wanted to answer three questions: do *npr-36* null mutants phenocopy *nlp-3* null mutants, do NLP-3 peptides activate NPR-36, and is NPR-36 expressed within the egg-laying circuit components?[3] This chapter is the result of these inquiries, through which answering I was able to confidently call NLP-3 and NPR-36 a cognate pair.

4.2. Results

4.2.1. CRISPR knockouts of npr-36 phenocopy nlp-3 knockouts

As RNAi is known to cause off-target effects through improper binding of the RNAi degradation components to mRNAs that are not the desired gene target, I wanted to confirm the *egl* phenotype caused by *npr-36* knockdown.[4] To do this I created two null mutants via CRISPR within the *npr-36* gene (method in Section 2.1.3). These alleles have been named *vs190* and *vs195*. I introduced five nucleotides to cause a frameshift and induce early stop codons into the first intracellular loop (*vs190*) or first extracellular

[3] As NLP-3 is a neuropeptide, which are known as modulatory molecules that can travel long distances extrasynaptically to signal, it was entirely possible that NPR-36 was expressed predominantly outside of the egg-laying circuit and still impacted vulval muscle activity. However, I thought this was unlikely as the vulval muscles are only innervated by the HSNs, VCs, and VA/VB cells which release serotonin and acetylcholine. If NLP-3/NPR-36 signaling occurred elsewhere, but then impacted egg laying through one of these neurons, knockout of serotonin or acetylcholine should have severe egg laying defects, which was not the case.

[4] RNAi, while highly effective, is variable by animal, by cell, and by transcript-target, ultimately resulting in incomplete knockdown of a gene. Additionally, transgenic array expression is also variable across the animal and between animals from the same parent.

loop (*vs195*) of NPR-36 coded for in exon two of *npr-36*, while also creating an EcoRI cut site for genotyping.

I then crossed these animals with *nlp-3* null, *nlp-3OX*, and *tph-1* null strains to evaluate the egg-laying defects caused by knockout of *npr-36*. *vs190* and *vs195* both were slightly *egl* with 22.7±2.2 and 23.3±1.9 unlaid eggs, respectively. These unlaid egg quantities were not significantly different from *nlp-3* (24.4±1.7 eggs) or *tph-1* (25.7±1.6 eggs; Figure 4.1A-C) single mutants. When crossed with *nlp-3*, both *npr-36* mutants did not cause a significant increase in *egl*-ness (26.1±1.8 and 26.5±1.9 eggs; Figure 4.1A blue genotypes 4-6, D) compared to the *nlp-3* and *npr-36* single mutants, suggesting that *nlp-3* and *npr-36* are in the same genetic pathway.

As with the RNAi screen in Chapter 3, I assayed the ability of the *npr-36* knockout to compensate for the hyperactive egg laying caused by overexpressing *nlp-3*. Both *npr-36* null mutants partially rescued the hyperactivity by returning the unlaid egg count to 17.8±1.8 and 18.2±1.6 eggs (Figure 4.1A teal genotypes 7-9, Figure 4.1E). However, these double mutants did not return to the mild egg laying defect from an *npr-36* or *nlp-3* single mutant, instead they were both not significantly different from wild type (Figure 4.1A). I believe that this could be caused by the significant overexpression of NLP-3 having off-target effects on inappropriate receptors, or it could be that there is an additional NLP-3 receptor that only has minor participation in egg laying that I did not identify. I additionally performed the early-stage egg laying assay on these mutants, confirming that the decrease in eggs in the uterus was caused by hyperactivity and not loss of embryo production (Supplemental Figure 9.4).

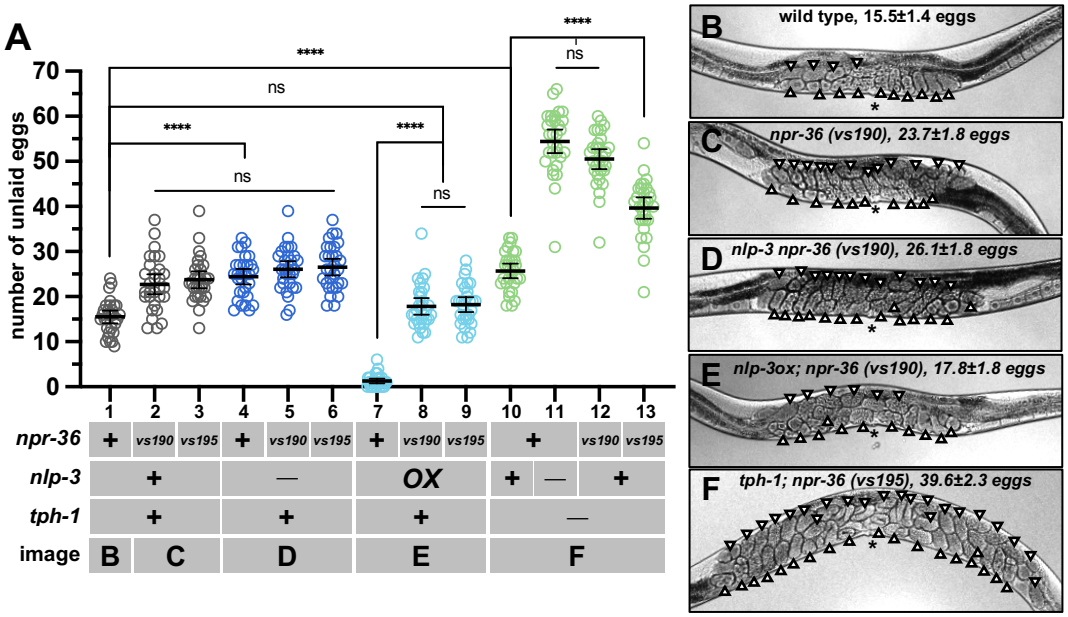

Figure 4.1: *npr-36* null mutants phenocopy *nlp-3* null mutants.
A, Number of unlaid eggs for *npr-36* mutants *vs190* and *vs195* when in a wild-type, *nlp-3*, *nlp-3OX*, and *tph-1* background. n=30. Ordinary one-way ANOVA Tukey corrected for multiple comparisons. ns = $p>0.05$; * = $p\leq0.05$; ** = $p\leq0.01$; *** = $p\leq0.001$; **** = $p\leq0.0001$. **B-F,** Representative images of unlaid eggs in animals. Genotypes with mean±95% CI. White carats indicate eggs. Asterisks are at the vulval slit at the center of the animal.

Serotonin and *nlp-3* double null mutants cause a severe *egl* phenotype (54.4±2.6 eggs; Figure 4.1A genotype 11). The *tph-1; npr-36* double mutants were also highly egg-laying defective, but *tph-1; npr-36(vs195)* (39.6±2.4 eggs) was significantly less *egl* than *tph-1; nlp-3,* while *tph-1; npr-36(vs190)* was not significantly different (50.5±2.2 eggs) from *tph-1; nlp-3* (Figure 4.1A green genotypes 10-13, Figure 4.1F). One explanation for this difference is there could be a partial protein product still produced in *vs195*; in light of this, I only used *vs190* throughout the rest of my work.

The CRISPR-induced null mutants that I produced of *npr-36* support the genetic pairing of *nlp-3* and *npr-36*.

4.2.2. NLP-3 peptides NLP-3-1 and NLP-3-2 activate NPR-36 in heterologous cells

The work in this section was performed by Sara Van Damme at KU Leuven in the lab of Dr. Isabel Beets, PhD, in an established collaboration.

C. elegans neuropeptide genes, like *nlp-3*, are post-translationally modified into multiple peptides (Husson, Mertens, Janssen, Lindemans, & Schoofs, 2007). An *in vitro* calcium mobilization assay was used to determine which of the five NLP-3 neuropeptides (Figure 4.2A, Figure 1.4) activate NPR-36 (Beets et al., 2023). We found that NPR-36 was activated by two of the NLP-3 peptides, NLP-3-1 and NLP-3-2, in the low nanomolar range (23.7nM (19.8—27.4nM) and 18.0nM (4.3—22.6nM); Figure 4.2B). NLP-3-1 and NLP-3-2 did not activate the cells when NPR-36 was not expressed (Supplemental Figure 9.5). Neuropeptide NLP-3-3 did not activate NPR-36, though it is predicted to be an active neuropeptide (Supplemental Figure 9.6). This peptide has been genetically paired with NPR-17 and biochemically with NPR-42; interestingly NPR-17 and NPR-42 did not have any egg-laying defects in my initial RNAi screen (Table 3.1; Mills et al., 2016; Beets et al., 2023).

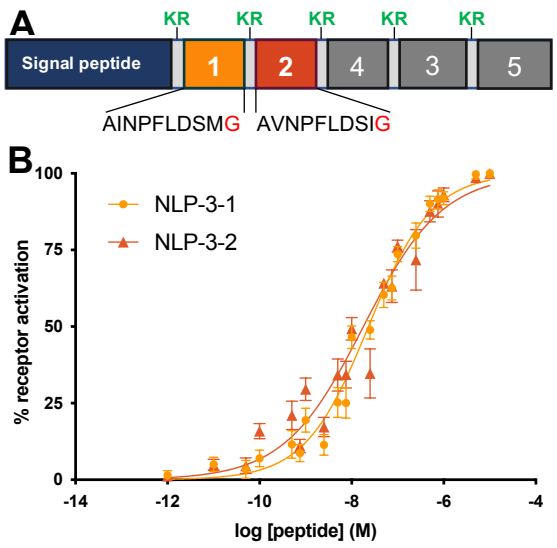

Peptide	AA sequence	EC_{50}	95% CI
NLP-3-1	AINPFLDSMamide	23.7 nM	19.8 nM to 27.4 nM
NLP-3-2	AVNPFLDSIamide	18.0 nM	14.3 nM to 22.6 nM

Figure 4.2: A calcium mobilization assay indirectly shows activation of NPR-36 via NLP-3-1 and NLP-3-2.
A, Graphic depicting the NLP-3 pre-proneuropeptide. The dibasic cut sites are in green, the glycine residues that are converted to amine groups are in red. **B,** Percent of total activation of CHO cells transiently expressing NPR-36 and aequorin by NLP-3-1 and NLP-3-2.

4.2.3. NPR-36 is expressed in the vulval and uterine muscles and the HSNs

NLP-3 is known to ultimately cause an increase in vulval muscle activity, but in what manner was unclear (Brewer et al., 2019). To determine through which cells NLP-3 signals, I identified where NPR-36 is expressed in the egg-laying circuit. After several trials, I ultimately ordered a CRISPR-knocked, *trans*-spliced GFP construct (*sl2::nls::gfp*) inserted after the C-terminal stop codon of *npr-36* at its endogenous locus.[5] SL2 is a *trans*-splicing signal that recruits a specialized splicing complex to splice the mRNA downstream to a new 5'UTR (Riddle, Meyer, and Priess (Eds.), 1997). When used for research this creates two separate mRNA sequences for translation, separating the tag from the protein of interest within the cell. In my work the SL2 sequence

[5] I also designed and ordered a GFP-fusion construct, which produced similar results, but was harder to interpret because of the subcellular localization.

separates the *gfp* mRNA from the *npr*-36 mRNA for independent translation and localization. I then crossed the *npr-36::sl2::nls::gfp* animals with mCherry marker strains for the vulval muscles (*unc-103ep::mCherry*) and the neurons (*ida-1p::mCherry*) of the egg-laying circuit.

I found that NPR-36 is strongly expressed in the vm2, um1, and um2 cells (Figure 4.3A-D), in concordance with the serotonin receptors SER-1, SER-7, and SER-4. This suggests some element of redundancy as NPR-36 must be a GPCR coupled to either $G\alpha_q$ or $G\alpha_s$ to cause muscle activation and SER-1 and SER-7 couple to these two different G proteins, respectively. This means that the NPR-36-caused internal signaling cascade must be affected through one of the already serotonin-activated G proteins in the musculature of the circuit. While we found in Olson et al. (2023) that either $G\alpha_q$ or $G\alpha_s$ alone was not enough to cause egg laying, significant increase in either pathway was able to ultimately result in egg laying. It could be that NPR-36 is used to amplify one pathway or the other to trigger egg laying more efficiently in different scenarios.

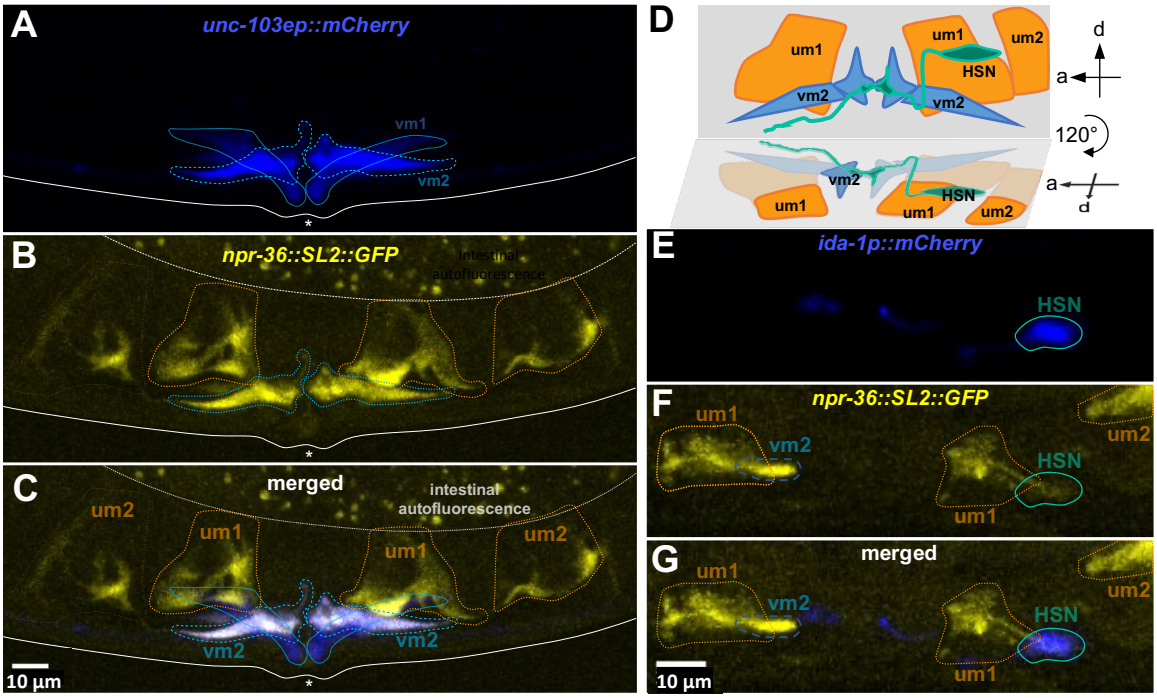

Figure 4.3: NPR-36::SL2::NLS::GFP is expressed in the vulval and uterine muscles and the HSNs.
A-C, Fluorescent images of NPR-36::SL2::NLS::GFP (**B**) with a vulval muscle mCherry colocalization marker (*unc-103ep::mCherry*; **A**). There is clear colocalization of GFP and mCherry in the vm2s (white with blue outline; **C**). There is GFP um1 and um2 expression (orange dotted line; **B** and **C**). **D,** Diagram of the *C. elegans* egg-laying circuit rotated 120° and maximally projected over a subset of *z*-stacks to better visualize the HSN cell without the um1 signal interfering. **E-G,** Fluorescent images of NPR-36::SL2::NLS::GFP (**F**) with an egg-laying circuit neuron mCherry colocalization marker (*ida-1p::mCherry*; **E**). There is colocalization of GFP and mCherry in the HSNs only (white with teal outline; **G**).

Interestingly, I saw *npr-36::sl2::nls::gfp* colocalization in the HSNs when I crossed it with the *ida-lp::mCherry* marker to label the neurons (Figure 4.3E-H). This expression data is supported by RNAseq data from the CeNGEN project where they documented *npr-36 (F10D7.1)* as expressed in the HSNs as well (Hammarlund, Hobert, Miller, & Sestan, 2018). I also saw possible head neuron expression that was too faint to identify which cells were expressing NPR-36 (Supplemental Figure 9.7). The localization pattern I found suggests that the HSNs express and release NLP-3, but also express NPR-36, the receptor for NLP-3. This could mean that NPR-36 acts as an auto-

activating receptor for the HSNs. When the HSNs release NLP-3—which as a neuropeptide is likely not released at the synapse—they are then also activating themselves via their NPR-36 receptors, resulting in an increased activity level, a.k.a. HSNs could employ a positive feedback loop. This could explain the increased HSN activity seen during egg-laying events (Collins et al., 2016).

The expression of NPR-36 on the vm2s, um1s, um2s, and HSNs means that the signaling via NLP-3 is crucial for immediate activity of the circuit, slightly against the assumptions of neuropeptide long-term neuromodulation.

4.2.4. npr-36 expression in the vulval and uterine muscles is not required for proper egg laying

To determine the necessity of NPR-36 in the musculature of the egg-laying circuit, I cell-specifically knocked down *npr-36* in the vulval muscles and uterine muscles. To do this, I followed a protocol developed by Esposito et al. (2007) and further refined in Olson et al. (2023). I expressed sense and antisense *npr-36* cDNA under the *myo-3* (pan-muscle) promoter. This will cause dsRNA against *npr-36* to form in all muscle cells, where it will be used by endogenous machinery to knockdown *npr-36* in the vm2, um1, and um2 cells. I did not see a significant effect on egg laying by knocking down *npr-36* compared to the *gfp* cDNA negative control (Figure 4.4). However, when I performed the muscle-specific knockdown of *npr-36* in a *tph-1* null background, I saw a significant increase in unlaid eggs compared to the control (32.9±2.6 eggs vs 19.7±1.2 eggs). This increase indicates significant disruption in the egg-laying circuit when both NLP-3 and serotonin are unable to activate the circuitry muscles (Figure 4.4). Unfortunately, the data gathered from HSN knockdown driven by the *tph-1* promoter was uninterpretable,

likely due to cell-toxicity frequently experienced by driving expression in the HSNs (Supplemental Figure 9.8; Brewer et al., 2019). These data indicate that NPR-36 is only necessary on the muscles when the complementary serotonin signaling is no longer present in the circuitry, indicating that the mild *egl* phenotype seen in the global knockout of *npr-36* is not solely due to its expression in the muscles of the circuit.

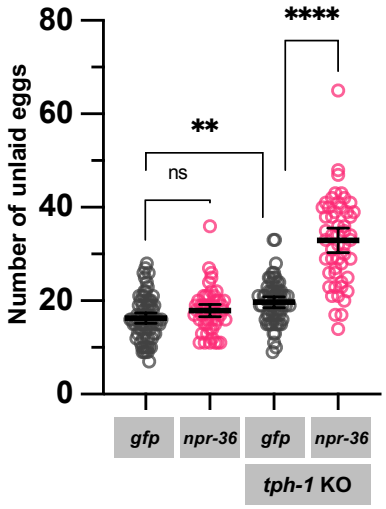

Figure 4.4: NPR-36 is not necessary in the circuit if serotonin is present.
Cell-specific RNAi knockdown of *npr-36* in the egg-laying muscles in *sid-1* and *tph-1; sid-1* strains. Five extrachromosomal strains were assayed and averaged in data shown.
gfp KD n=72; *npr-36* KD n=50; *tph-1 gfp* KD n=65; *tph-1 npr-36* KD n=52. Ordinary one-way ANOVA Tukey corrected for multiple comparisons. ns = $p>0.05$** = $p\leq0.01$; **** = $p\leq0.0001$.

4.2.5. HSN activity cannot be determined to be affected by NLP-3/NPR-36 signaling

As my muscle-specific knockdown of *npr-36* did not recapitulate the global knockout of *npr-36*, I wanted to determine if NLP-3/NPR-36 signaling had an impact on HSN activity, and, thus, circuit activity. As the HSN-specific knockdown of *npr-36* was uninterpretable, I instead performed calcium imaging on the HSNs of freely-behaving animals in wild type and *nlp-3* null animals (Figure 4.5A and B, Supplemental Figure 9.9). To determine if the frequency of HSN activity changes when *nlp-3* is knocked out, I graphed the cumulative frequency percentage of the intervals for both genotypes and

saw a slight right shift in the *nlp-3* intervals (Figure 4.5C). This shift indicates a decrease in the proportion of short intervals in the *nlp-3* animals. However, when I compared the percentage of peaks per animal that had a peak within 30 seconds to either side of it, there was no significant change between the genotypes. There is obvious animal to animal variation, but, overall, the lack of significance appears to be accurate. I was unable to conclude that NLP-3 signaling through NPR-36 on the HSNs impacts their activity.

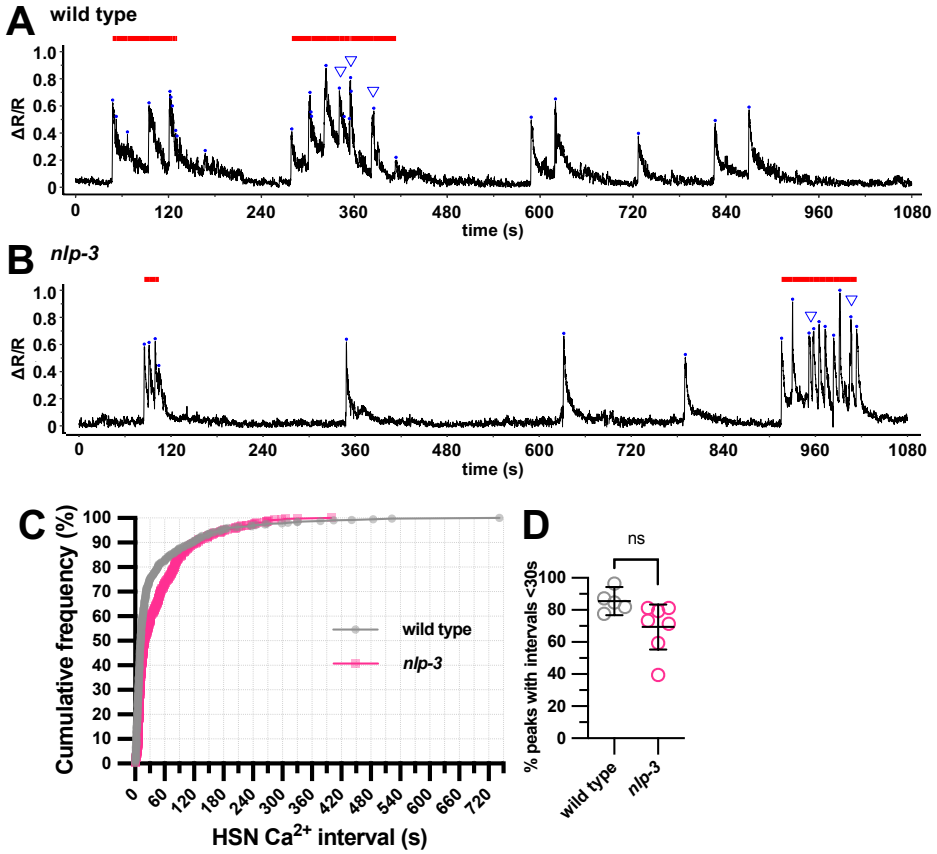

Figure 4.5: HSN calcium activity increases upon NLP-3 presence.
A and **B,** Representative HSN calcium activity traces of wild-type (**A**) or *nlp-3* null animals (**B**) in a HSN GCaMP5/mCherry background. Blue carets indicate an egg-laying event. Blue dots are called peaks. Red bars indicate bursts of HSN activity with less than 30 seconds between peaks. The full traces are in Supplemental Figure 9.9. **C,** Cumulative frequency distribution of wild-type and *nlp-3* animals. The right shift of the *nlp-3* curve indicates a decrease in rapid intervals. wild type intervals n = 423; *nlp-3* n = 529. **D,** Percentage of peaks that have less than 30-second intervals. Although the pooled intervals show a decrease in short intervals, there are two *nlp-3* animals that skew the data as seen when comparing animal-to-animal variation within the genotypes. wild type n = 5; *nlp-3* n = 7. Ordinary one-way ANOVA. ns = p>0.05.

I additionally began preliminary work to cell-specifically rescue of *npr-36* expression in the HSN cells in *npr-36* global knockouts. There were questions amongst authors as to the interpretability of rescues as there would be ectopic expression of *npr-36* from the promoters available to us as there is no "true" HSN-only or vulval muscle-only promoter. Additionally, this avenue was deemed too arduous with the number of injections. The preliminary results however are interesting, as seen in Supplemental Figure 9.10.

4.3. Discussion

This chapter covered my validation of NPR-36 as an NLP-3 GPCR. I confirmed that NLP-3 activates NPR-36 both genetically (4.2.1) and biochemically (4.2.2) and that NPR-36 was expressed in egg-laying circuit in the vm2, um1, um2, and HSN cells (4.2.3). I began to delve into the co-transmission dynamics of serotonin and NLP-3. It appears that NLP-3 signaling is needed for egg-laying muscle activity when serotonin is absent, but is not required for egg laying to proceed. Additionally, I was unable to conclude if there is NLP-3/NPR-36 autoactivation signaling utilized by the HSNs to maintain their activity.

5. Exploring how serotonin and NLP-3 pattern egg-laying

5.1. Introduction – How do neuropeptides signal differently from neurotransmitters?

As the ultimate goal of my thesis was to determine the dynamics of serotonin and NLP-3 signaling, I decided to take a more macroscopic approach to analyze egg-laying behavior. Waggoner et al. (2000) utilized a relatively straightforward assay where they recorded freely-behaving animals and manually wrote when the animals laid eggs over time. They then analyzed the intervals between those egg laying events and observed that wild-type animals had intervals that fit in two distributions, termed the active phase and the inactive phase. The active phase egg laying intervals were short (on average 18 seconds between egg-laying events), which we now know is also when cell activity for the circuit is high (see Figure 4.5 and Supplemental Figure 9.9; Brewer et al., 2019; Collins et al., 2016; Olson et al., 2023; Ravi et al., 2018). The inactive phase intervals are long spans of time between egg-laying clusters (on average 1,340 seconds or approximately 22 minutes).

I adapted the method from Waggoner et al. (2000) to suit the equipment available to me (see Section 2.2.3 for full method). I assayed wild type worms to assess reproducibility of the previous study. I also assayed *tph-1* animals and *ser-1 ser-7* animals to observe changes in the active phase and inactive phase when serotonin activation is knocked out. To test NLP-3 signaling, I used *nlp-3* and *npr-36* null animals. I performed analyses on these data sets similar to that performed in Waggoner et al. (2000).

5.2. Results

Example one hour of egg laying for each genotype I assayed is displayed in Figure 5.2 (the full data set is in Supplemental Figure 9.11).

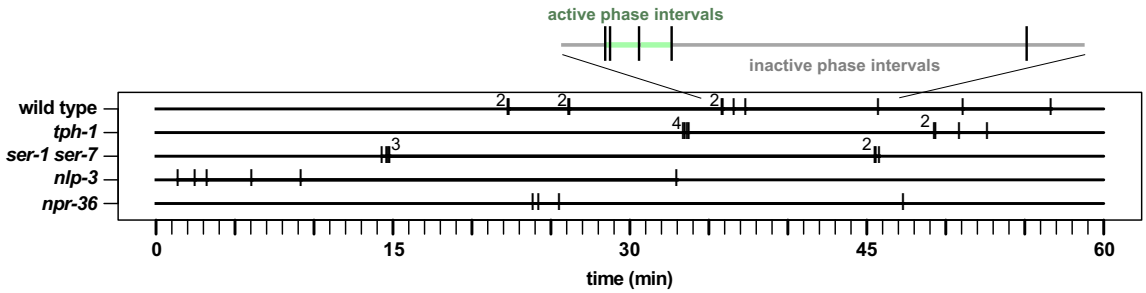

Figure 5.1: Example one hour of egg-laying events.
Hash marks indicate egg-laying events. Example graphic of active phase and inactive phase intervals depict the close grouping of egg-laying events in blue and a long interval between the final egg laid in the active phase until the next single egg laid in grey. Egg-laying events too close to visually distinguish have the number of events notated above. The full data can be found in Supplemental Figure 9.11.

5.2.1. Serotonin or NLP-3 signaling differentially effects patterning of egg laying in the inactive phase

I first analyzed if there was a change in the average inactive phase duration for the serotonin and NLP-3 signaling mutants. Waggoner et al. (2000) previously showed that animals with egg-laying defects have an increase in their inactive phase duration. To determine if the mutants that I worked with followed this trend, I first plotted the cumulative distribution of the egg-laying intervals on a logarithmic y-axis (Figure 5.2A). These distributions have a steep initial slope representing the active phase, an inflection point where there is a plateau in intervals of that duration, and a final section of the distribution that is represented by a more gradual slope at longer time spans which are the intervals of the inactive phases (Waggoner et al., 2000). I fit a semi-log line to points greater than 400 seconds (to focus on only the inactive phase intervals), and found that the slopes for the fits for all mutants have a significantly shallower slope

than wild type (Figure 5.2B-F, analysis in Table 5.1). This decrease in steepness of the slope indicates that the mutants have longer inactive phase intervals than wild type.

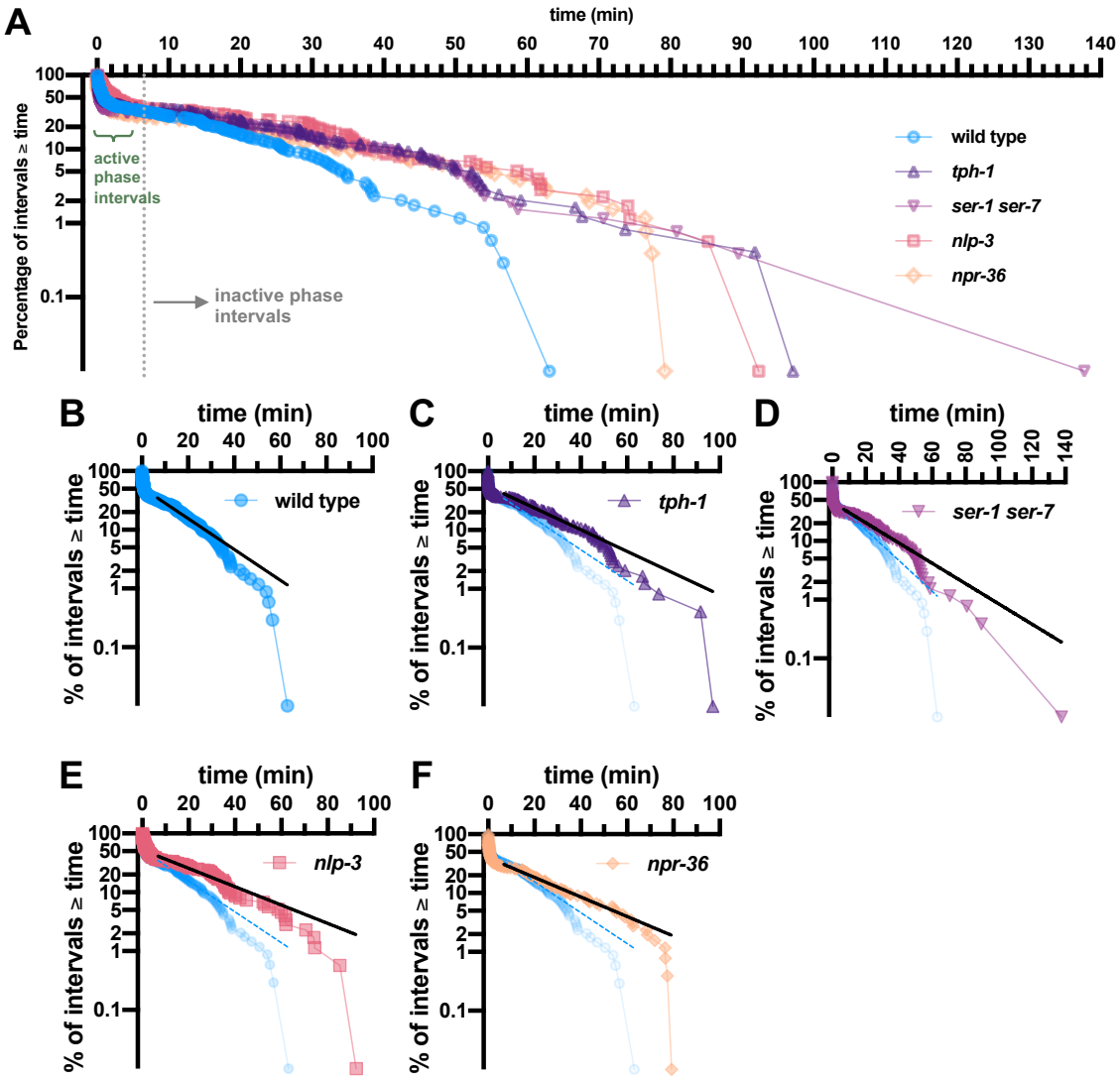

Figure 5.2: Cumulative distributions of egg-laying event intervals.
A, Cumulative distributions of wild-type, *tph-1*, *ser-1 ser-7*, *nlp-3*, and *npr-36* egg-laying intervals. **B-F,** Fitted curves to intervals greater than 400 seconds for all genotypes assayed. Mutants (**C-F**) are compared to wild type (blue points and lines). All slopes are significantly ($p \leq 0.0001$) less steep than the wild-type slope when compared pairwise. Further details in Table 5.1.

Table 5.1: Analysis of slopes of lines fitted to inactive phase intervals.
Intervals greater than 400 seconds were fitted to lines using a least squares regression (displayed in Figure 5.2B-F) and p values for comparisons to the wild-type slope were calculated using an extra sum-of-squares F test. Lines fit to each mutant had slopes significantly less steep than the wild type fit, indicating that the inactive phase intervals were more frequently longer in each mutant than the inactive phases observed in the wild type.

				Slope of lines fit on semi-log plots for >400 second intervals		
Genotype	**Number of animals recorded**	**Total hours of recording**	**Total # of intervals**	**Slope**	**95% confidence interval**	**p value for comparison to wild type**
wild type	15	60	342	-4.38×10^{-4}	-4.53×10^{-4} — -4.23×10^{-4}	———
tph-1	15	60	244	-3.08×10^{-4}	-3.17×10^{-4} — -2.98×10^{-4}	<0.0001
ser-1 ser-7	15	60	259	-2.88×10^{-4}	-3.01×10^{-4} — -2.75×10^{-4}	<0.0001
nlp-3	14	56	176	-2.60×10^{-4}	-2.80×10^{-4} — -2.40×10^{-4}	<0.0001
npr-36	15	60	256	-2.77×10^{-4}	-2.88×10^{-4} — -2.66×10^{-4}	<0.0001

After I confirmed that my mutants behaved as expected in this assay, I next determined the mean inactive phase interval length for each genotype. This involved fitting Gaussian curves to the distributions of intervals greater than 400 seconds to determine their means (Figure 5.3). The details of the Gaussian curves are in Table 5.2. Wild-type intervals had a mean value of 1201.1 (95% CI: 1049.4 — 1361.0) seconds, or approximately 20 minutes, similar to that estimated by the probability equation developed and implemented in other works (Waggoner et al., 2000; Waggoner et al., 1998). All serotonin and NLP-3 signaling mutants caused an increase in mean inactive phase duration [*tph-1:* 1581.3 (1222.9 — 2026.4) or 27.2 min; *ser-1 ser-7*: 1799.0 (1465.6 — 2171.1) or 31.8 min; *nlp-3*: 1908.4 (1586.0 — 2262.0) or 30.0 min; *npr-36*: 1632.7 (1359.7 — 1966.5) or 26.4 min]. I determined that inactive phase interval distributions were also statistically significantly different from the wild-type distribution using a Mann Whitney U test where each mutant when compared pairwise to wild type was statistically significantly different by at most $p\leq0.0006$ (Table 5.2). This work confirmed the initial conclusions from Figure 5.2 and Table 5.2 that

loss of either activating serotonin and NLP-3 signaling causes an increase in the inactive phase, which is known to lead to egg accumulation.

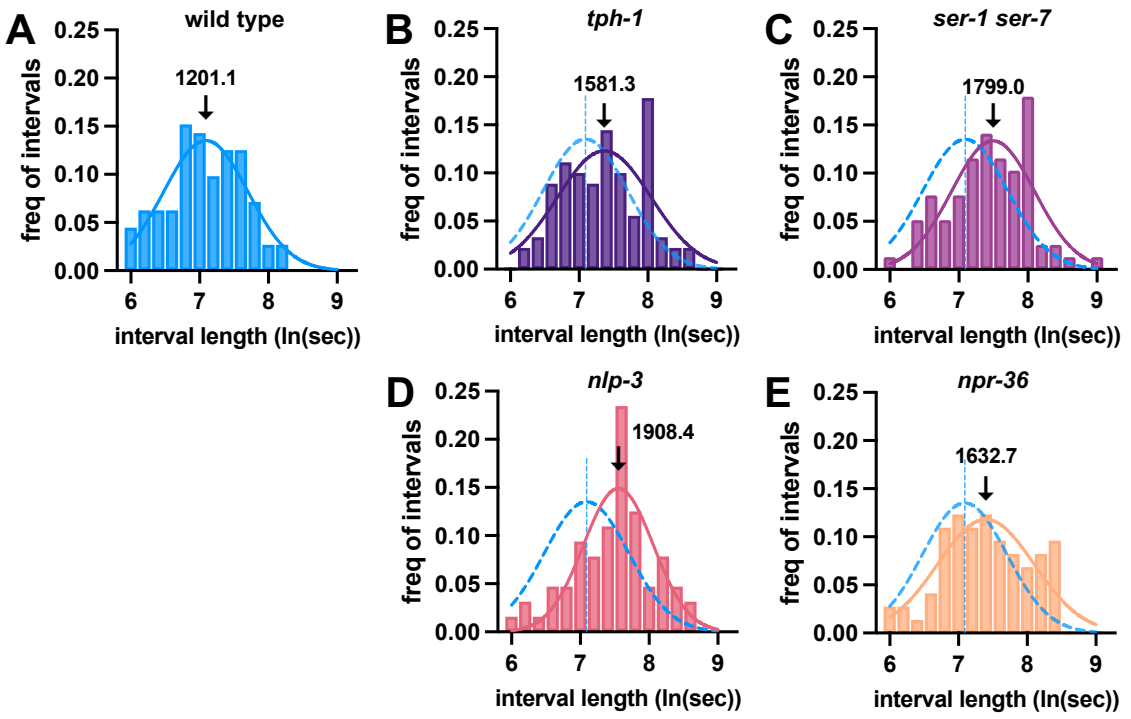

Figure 5.3: Frequency distributions of inactive phase intervals fit with Gaussian curves. Distributions of intervals greater than 400 seconds with all mutant Gaussian curves compared to wild type (dashed blue line). Means for the Gaussian curves are indicated with arrows. wild type intervals n=112; *tph-1* intervals n=90; *ser-1 ser-7* intervals n=78; *nlp-3* intervals n=64; *npr-36* intervals n=73. Further details and analysis in Table 5.2.

Table 5.2: Analysis of inactive phase intervals between egg-laying events.
All mutants were compared pairwise to wild type using a Mann-Whitney U test. Significance for >400 second intervals (inactive phase) are all exact. All mutants had significantly longer inactive phase (greater than 400 second) intervals than wild type.

				Inactive phase intervals			
Genotype	**Number of animals recorded**	**Total hours of recording**	**Total # of intervals**	**Mean length (sec)**	**95% confidence interval**	**# of intervals**	**p value for comparison to wild type**
wild type	15	60	342	1201.1	1049.4 — 1361.0	112	
tph-1	15	60	244	1581.3	1222.9 — 2026.4	90	0.0005
ser-1 ser-7	15	60	259	1799.0	1465.6 — 2171.1	78	<0.0001
nlp-3	14	56	176	1908.4	1586.0 — 2262.0	64	<0.0001
npr-36	15	60	256	1632.7	1359.7 — 1966.5	73	0.0006

5.2.2. Serotonin or NLP-3 signaling differentially effects patterning of egg laying in the active phase

I was primarily interested in differences between serotonin and NLP-3 signaling. As I did not observe any such difference within the inactive phase, I turned my focus to the active phase. If serotonin and NLP-3 mutants were to have a different phenotype from each other, one area of egg laying where this could occur (without having been previously observed) would be within this phase of egg laying. Up until this point, there had been no observable or significant difference between mutants of the two signaling molecules through observing egg accumulation or cell activation, but these assays all were observing the loss of egg laying. What if there were a difference when egg laying was occurring?

To answer this question, I created frequency distributions of intervals that were less than 400 seconds for each genotype and fit them with a Gaussian curve (Figure 5.4). Wild-type intervals had a mean of 21.5 (12.6 — 37.8) seconds (Table 5.3), similar to the 18 seconds calculated by the work from Waggoner et al. (1998). The serotonin mutant, *tph-1* and *ser-1 ser-7*, distributions were significantly different from wild type ($p \leq 0.0086$, determined pairwise using the Mann Whitney U test). Both mutants had a decrease in their mean interval duration compared to wild type [*tph-1*: 10.1 (6.3 — 19.3) sec; *ser-1 ser-7*: 5.4 (4.3 — 7.0) sec]. By abolishing activation signaling through serotonin in these mutants, NLP-3 is the only activating signaling molecule left to cause egg laying (Brewer et al., 2019; Olson et al., 2023). I conclude from these results that NLP-3 likely controls egg laying on a short, rapid time scale of 5-10 seconds during the active phase.

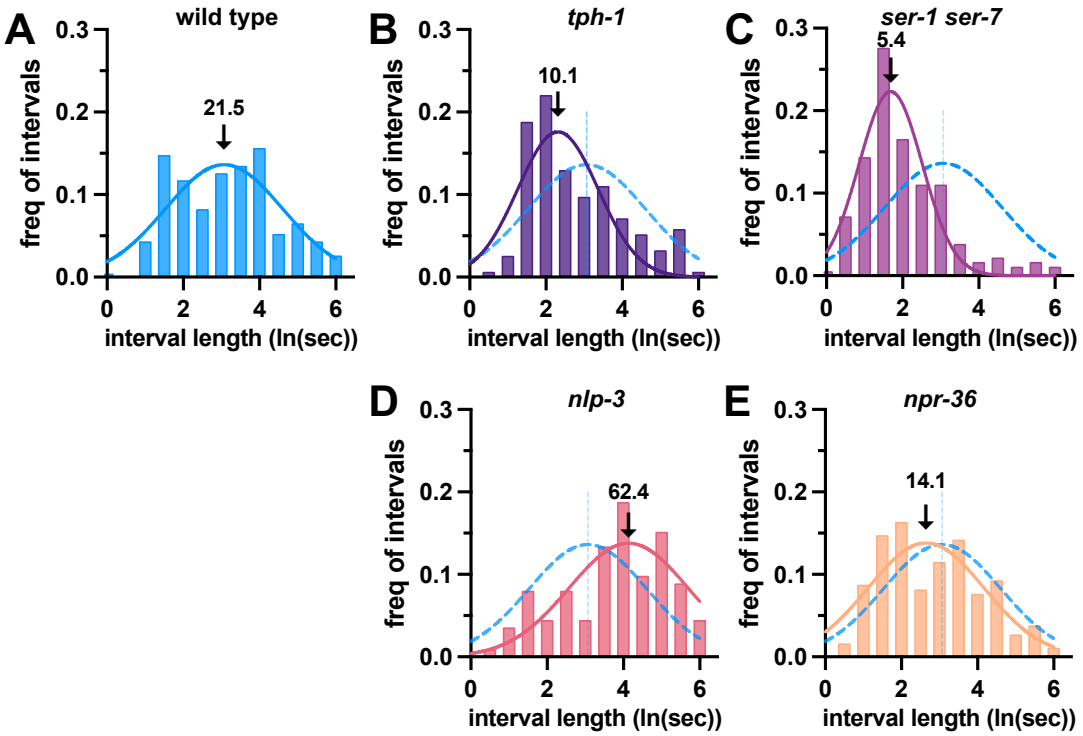

Figure 5.4: Frequency distributions for intervals less than 400 seconds fit with Gaussian distributions.
Distributions of intervals less than 400 seconds for all genotypes comparing to the wild-type Gaussian fit (dashed blue line). Means of the Gaussian curves are indicated with arrows. Wild type intervals n=230; *tph-1* intervals n=154; *ser-1 ser-7* intervals n=181; *nlp-3* intervals n=112; *npr-36* intervals n=183. Further analysis in Table 5.3.

Table 5.3: Analysis of <400 second intervals between egg-laying events.
All mutants were compared pairwise to wild type using a Mann-Whitney U test. *tph-1*, *ser-1 ser-7*, and *npr-36* all had significantly shorter active phase (<400 second intervals) when compared to wild type. *nlp-3* had significantly longer active phase when compared to wild type.

				<400 second intervals			
Genotype	**Number of animals recorded**	**Total hours of recording**	**Total # of intervals**	**Mean length (sec)**	**95% confidence interval**	**# of intervals**	**p value for comparison to wild type**
wild type	15	60	342	21.5	12.6 — 37.8	230	
tph-1	15	60	244	10.1	6.3 — 19.3	154	0.0086
ser-1 ser-7	15	60	259	5.4	4.3 — 7.0	181	<0.0001
nlp-3	14	56	176	62.4	34.6 — 161.3	112	<0.0001
npr-36	15	60	256	14.1	8.4 — 24.2	183	0.021

While the null mutation of the two serotonin receptors *ser-1* and *ser-7* caused similar shortening effects on the duration of the active phase compared to the global *tph-1* mutation, the null mutants of *nlp-3* and *npr-36* did not result in the same active phase phenotypes. When NLP-3 signaling was fully abolished, I observed a statistically significant change in the interval lengths compared to wild type ($p \leq 0.0001$ from a pairwise Mann Whitney U test). The mean active phase interval duration for *nlp-3* was 62.4 (34.6 — 161.3) seconds, a marked increase from the 21 seconds that wild type worms exhibit. However, when *npr-36* was knocked out, the active phase interval mean value decreased from 21 seconds in wild type to 14.1 (8.4 — 24.2) seconds. This decrease in interval duration during the active phase in *npr-36* animals was enough to cause a significant difference in the *npr-36* distribution compared to wild type in a pairwise Mann Whitney U test ($p \leq 0.021$). I was still able to make conclusions in regard to the effects of serotonin on egg laying through the marked changes in the *nlp-3* mutants. From these data, I hypothesize that serotonin is used to cause more spaced egg-laying events, about every 60 seconds.

Serotonin and NLP-3 signaling affect different aspects of egg laying activity during the active phase, the first instance where any egg laying phenotype differs between mutants of the two co-transmitted molecules.

5.3. Discussion

I was able to conclude from my work in this chapter that serotonin signaling through the SER-1 and SER-7 receptors causes egg laying at 60-second intervals during the active phase, while NLP-3 signaling causes rapid egg laying in 5-10 second intervals. This is the first egg-laying assay that has a difference between serotonin and NLP-3

signaling in *C. elegans*. I additionally observed that serotonin and NLP-3 are required for the active phase to begin as null mutants of *tph-1, ser-1 ser-7, nlp-3* and *npr-36* all caused longer inactive phases.

How serotonin and NLP-3 are able to regulate different active phase egg laying dynamics remains unclear. Further investigation into the circuit dynamics at the synaptic and intracellular level are required to understand how two signals released from the same cell, and likely within the same vesicle, can cause activity on two different time scales. One hypothesis is that serotonin and NLP-3 persist at the synapse for different durations of time and their GPCRs cause different signaling cascades. As NLP-3 would be initially released during high HSN activity (hypothesized to be required for NLP-3/dense-core vesicle release), NLP-3 would initially be at a high concentration near the muscles of the circuit, which could cause intense activation. NLP-3 would then, over tens of seconds, diffuse throughout the area and no longer be at high concentrations or get degraded by a peptidase at or around the receptors (Dr. Jennifer Garrison, personal communication). This would then allow for the serotonin-mediated activation to proceed. SER-1, SER-7, and SER-4 all activate different G proteins—they could create the 60-second spacing of egg laying through rapid activation of SER-1 and SER-7, then rapid inhibition of the circuit through SER-4 to temporarily turn off the receiving cells and prevent continued egg laying. Serotonin would then be taken up and released in a new spike of HSN activation.

For this hypothesis to be testable, I would need to determine how NLP-3 causes rapid egg release. I did not find that NPR-36 was activated by NLP-3 to cause the effects of NLP-3 during the active phase. The most likely explanation for this is that

there is a second NLP-3 GPCR used in egg laying that remains to be identified. As I only screened for egg accumulation, an NLP-3 receptor that primarily dictates egg-laying rate during the active phase would not have been identified in my screen, nor would it have been identified in any other egg laying assay currently employed in the field as changes to active phase egg laying is unlikely to significantly change equilibrium of eggs retained in the uterus.

A likely candidate for a second NLP-3 receptor is NPR-17, which was genetically paired with one of the NLP-3 (NLP-3-3) peptides in octanol avoidance response (Mills et al., 2016); however, from one pilot run of the assay used in this chapter, I did not observe a significant change in the distributions of intervals less than 400 seconds in an *npr-17* null mutant when compared to wild type in a Mann Whitney U test ($p=0.1023$; Supplemental Figure 9.12). The Gaussian curve mean for the one replicate of the *npr-17* null mutant that I assayed was 12.9 (1.01 — 23.5) seconds, which would require further replicates to make a strong conclusion. An additional candidate for an NLP-3 receptor could be NPR-42 which also is predicted to be weakly activated by NLP-3-3 by Beets et al. (2023). This receptor did not cause egg accumulation in my RNAi screen, but I was unable to test the pattern of egg laying in *npr-42* knockout mutants. Additional GPCRs could also be selected from databases such as that generated by Beets et al. (2023) or further work from the groups that published the neuropeptidergic connectome (Ripoll-Sanchez et al., 2023) or CeNGEN (Hammarlund et al., 2018) to screen through the assay I used here to observe changes in the active phase egg laying rate.

6. Discussion

6.1. Conclusions

In this body of work, I aimed to further dissect the role of a neuropeptide NLP-3 in the context of a serotonin-activated neural circuit. NLP-3 was shown to activate egg laying in previous work from the Koelle lab, but through what cellular pathway was unclear (Brewer et al., 2019; Olson et al., 2023). To further pursue this research question, I needed to identify what cells of the egg-laying circuit receive NLP-3 signals through an NLP-3 receptor. However, until my work, there was no known receptor for NLP-3 that affected egg laying.

I identified and validated a GPCR I named NPR-36 as an NLP-3 receptor through genetic and biochemical means. I identified that the HSNs, vm2s, and ums express NPR-36. Though cell-specific knockdown of NPR-36 in the muscles (both vulval and uterine) did not recapitulate the mild egg-laying defect seen in the *npr-36* null mutants, the *npr-36* knockdown animals did accumulate a significant number of eggs when serotonin was also absent. As my efforts to determine if the HSNs were activated by NLP-3/NPR-36 signaling was inconclusive, I was unable to determine the specific concerted signaling in the circuit executed through the release of NLP-3/activation of NPR-36.

A model illustrating the circuit dynamics of egg-laying are shown in Figure 6.1A. Serotonin, NLP-3, and acetylcholine are activating signals. Serotonin (not pictured here), tyramine, NLP-7, and FLP-11 are inhibitory signals.

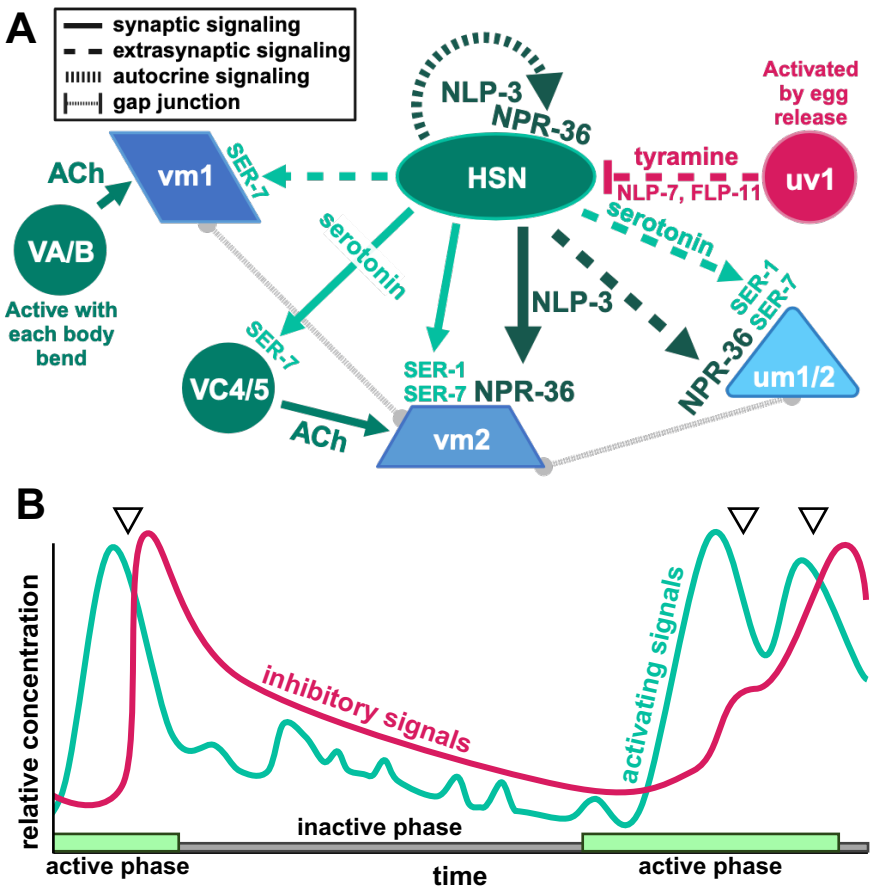

Figure 6.1: Egg-laying circuit diagram and hypothetical signaling dynamics.
A, Circuit diagram of the *C. elegans* egg-laying circuit with NPR-36 expression and NLP-3 signaling included. **B,** Graph of hypothetical signaling dynamics. After the final egg of an active phase is laid (black carets indicate egg laying events) and inhibitory signals are released (green line). During the inactive phase, both the negative and positive signals degrade/leave the synapse. I hypothesize that as the signals disperse, the spikes of HSN activity causes small releases of at least serotonin, and possibly NLP-3, into the circuit. As the negative signals continue to degrade, eventually the accumulation of eggs and a release of positive signals from the HSNs will push the activation threshold over the remaining inhibitory signals and result in activation of egg laying and entry into the active phase.

I defined the first phenotypic difference between serotonin and NLP-3 signaling. Mutants in both signaling pathways cause egg-laying defects due to a delay in activation of egg laying from loss of positive signals, lengthening the inactive phase (Figure 6.1B). I hypothesize that serotonin and NLP-3 are some of the positive signals[6]

[6] Other positive signals are things such as stretch response to eggs entering the uterus, acetylcholine release during body bends or to trigger muscle contraction, and other neuropeptides or neurotransmitters that inform the circuit that the animal is in favorable egg-laying conditions.

that accumulate in the circuit to eventually outcompete the inhibitory negative signals and trigger the next active phase. Serotonin causes egg laying every 60 seconds during the active phase. I hypothesize that this is caused by the regular (and from my anecdotal observations, less intense) activation of the HSNs that occurs throughout both the active and inactive phases (Figure 4.5 and Supplemental Figure 9.9). During the active phase when this signal reaches the HSN and serotonin is released, the further stimulation of the musculature and other neurons causes eggs to be released (Figure 6.1A). When in the inactive phase, the release of serotonin occurs without full circuit activation. NLP-3 causes rapid egg laying with a mean interval of 5 to 10 seconds. I hypothesize that this succinct egg release occurs from a rapid release of a high concentration of NLP-3 from dense core vesicles, which activates the egg-laying muscles via an unknown NLP-3 receptor. When NLP-3 has diffused and begins to be degraded, its concentration remains sufficiently high enough to activate NPR-36, which will assist in reactivating egg-laying after the inhibitory signals have been degraded and/or diffuse.

6.2. Future Directions

I was able to identify separate functions for serotonin and NLP-3 signaling during egg-laying circuit activation. To further dissect the differences in their signaling pathways, identification of the intracellular pathways being activated by each molecule would be required. While I did not identify the G protein that NPR-36 activates, further exploratory work identifying the internal secondary messengers that are activated would allow for elucidation of the dynamic activation within the receiving cells caused by serotonin and NLP-3 signaling. Could there be a signal preference with one

signaling molecule exhibiting stronger activation of the post-signaling cell? Do the secondary messenger pathways converge for serotonin and NLP-3 signing within the cell or do they activate entirely disparate pathways?

Additionally, there is likely a second NLP-3 GPCR that exclusively acts within the active phase that remains unidentified. Identification of this receptor would allow for a more robust analysis of the activation of the egg-laying circuit facilitating a more thorough understanding of the co-transmission of serotonin and a neuropeptide.

Finally, a comprehensive analysis of the dynamics involved in the inhibitory and excitatory signaling within the egg-laying circuit remains unexplored. A thorough investigation into the dynamics of the signals in the circuit, along with the activation or inhibition of the cells that perform each role would allow for the egg-laying circuit to become a manipulable model circuit. One could envision introduction of foreign receptors from complex circuits into the egg-laying circuit to determine their activation pathways or effects within a defined circuit.

7. References

Ahlawat, S., R. Sharma, A. Maitra, M. Roy and M. S. Tantia (2014). "Designing, optimization and validation of tetra-primer ARMS PCR protocol for genotyping mutations in caprine Fec genes." Meta Gene **2**: 439-449.

Albert, P. R., C. Benkelfat and L. Descarries (2012). "The neurobiology of depression--revisiting the serotonin hypothesis. I. Cellular and molecular mechanisms." Philos Trans R Soc Lond B Biol Sci **367**(1601): 2378-2381.

Alkema, M. J., M. Hunter-Ensor, N. Ringstad and H. R. Horvitz (2005). "Tyramine Functions independently of octopamine in the Caenorhabditis elegans nervous system." Neuron **46**(2): 247-260.

Banerjee, N., R. Bhattacharya, M. Gorczyca, K. M. Collins and M. M. Francis (2017). "Local neuropeptide signaling modulates serotonergic transmission to shape the temporal organization of C. elegans egg-laying behavior." PLoS Genet **13**(4): e1006697.

Beets, I., S. Zels, E. Vandewyer, J. Demeulemeester, J. Caers, E. Baytemur, A. Courtney, L. Golinelli, I. Hasakiogullari, W. R. Schafer, P. E. Vertes, O. Mirabeau and L. Schoofs (2023). "System-wide mapping of peptide-GPCR interactions in C. elegans." Cell Rep **42**(9): 113058.

Brewer, J. C., A. C. Olson, K. M. Collins and M. R. Koelle (2019). "Serotonin and neuropeptides are both released by the HSN command neuron to initiate *Caenorhabditis elegans* egg laying." PLoS Genet **15**(1): e1007896.

Bright, F. M., R. Vink, R. W. Byard, J. R. Duncan, H. F. Krous and D. S. Paterson (2017). "Abnormalities in substance P neurokinin-1 receptor binding in key brainstem nuclei in sudden infant death syndrome related to prematurity and sex." PLoS One **12**(9): e0184958.

Calixto, A., D. Chelur, I. Topalidou, X. Chen and M. Chalfie (2010). "Enhanced neuronal RNAi in *C. elegans* using SID-1." Nat Methods **7**(7): 554-559.

Chase, D. L. and M. R. Koelle (2004). "Genetic analysis of RGS protein function in *Caenorhabditis elegans*." Methods Enzymol **389**: 305-320.

Chen, J., P. Ye, R. Gu, H. Zhu, W. He, X. Mu, X. Wu, H. Pang, F. Han and X. Nie (2023). "Neuropeptide substance P: A promising regulator of wound healing in diabetic foot ulcers." Biochem Pharmacol **215**: 115736.

Collins, K. M., A. Bode, R. W. Fernandez, J. E. Tanis, J. C. Brewer, M. S. Creamer and M. R. Koelle (2016). "Activity of the *C. elegans* egg-laying behavior circuit is controlled by competing activation and feedback inhibition." Elife **5**.

Cottrell, G. A. (1997). "The first peptide-gated ion channel." J Exp Biol **200**(Pt 18): 2377-2386.

Davis, P., M. Zarowiecki, V. Arnaboldi, A. Becerra, S. Cain, J. Chan, W. J. Chen, J. Cho, E. da Veiga Beltrame, S. Diamantakis, S. Gao, D. Grigoriadis, C. A. Grove, T. W. Harris, R. Kishore, T. Le, R. Y. N. Lee, M. Luypaert, H. M. Muller, C. Nakamura, P. Nuin, M. Paulini, M. Quinton-Tulloch, D. Raciti, F. H. Rodgers, M. Russell, G. Schindelman, A. Singh, T. Stickland, K. Van Auken, Q. Wang, G. Williams, A. J. Wright, K. Yook, M. Berriman, K. L. Howe, T. Schedl, L. Stein and P. W. Sternberg (2022). "WormBase in 2022-data, processes, and tools for analyzing Caenorhabditis elegans." Genetics **220**(4).

Esposito, G., E. Di Schiavi, C. Bergamasco and P. Bazzicalupo (2007). "Efficient and cell specific knock-down of gene function in targeted *C. elegans* neurons." Gene **395**(1-2): 170-176.

Fernandez, R. W., K. Wei, E. Y. Wang, D. Mikalauskaite, A. Olson, J. Pepper, N. Christie, S. Kim, S. Weissenborn, M. Sarov and M. R. Koelle (2020). "Cellular Expression and Functional Roles of All 26 Neurotransmitter GPCRs in the *C. elegans* Egg-Laying Circuit." J Neurosci **40**(39): 7475-7488.

Filip, M. and M. Bader (2009). "Overview on 5-HT receptors and their role in physiology and pathology of the central nervous system." Pharmacol Rep **61**(5): 761-777.

Frooninckx, L., L. Van Rompay, L. Temmerman, E. Van Sinay, I. Beets, T. Janssen, S. J. Husson and L. Schoofs (2012). "Neuropeptide GPCRs in C. elegans." Front Endocrinol (Lausanne) **3**: 167.

Furukawa, Y. and I. Tagashira (2023). "Aromatic amino acids in the finger domain of the FMRFamide-gated Na[Formula: see text] channel are involved in the FMRFamide recognition and the activation." Pflugers Arch **475**(8): 975-993.

Gurel, G., M. A. Gustafson, J. S. Pepper, H. R. Horvitz and M. R. Koelle (2012). "Receptors and other signaling proteins required for serotonin control of locomotion in Caenorhabditis elegans." Genetics **192**(4): 1359-1371.

Hammarlund, M., O. Hobert, D. M. Miller, 3rd and N. Sestan (2018). "The CeNGEN Project: The Complete Gene Expression Map of an Entire Nervous System." Neuron **99**(3): 430-433.

Hapiak, V. M., R. J. Hobson, L. Hughes, K. Smith, G. Harris, C. Condon, P. Komuniecki and R. W. Komuniecki (2009). "Dual excitatory and inhibitory serotonergic inputs modulate egg laying in Caenorhabditis elegans." Genetics **181**(1): 153-163.

Hauser, A. S., M. M. Attwood, M. Rask-Andersen, H. B. Schioth and D. E. Gloriam (2017). "Trends in GPCR drug discovery: new agents, targets and indications." Nat Rev Drug Discov **16**(12): 829-842.

Hobert, O. (2013). "The neuronal genome of Caenorhabditis elegans." WormBook: 1-106.

Huang, Y. C., J. Luo, W. Huang, C. M. Baker, M. A. Gomes, B. Meng, A. B. Byrne and S. W. Flavell (2023). "A single neuron in C. elegans orchestrates multiple motor outputs through parallel modes of transmission." Curr Biol **33**(20): 4430-4445 e4436.

Husson, S. J., I. Mertens, T. Janssen, M. Lindemans and L. Schoofs (2007). "Neuropeptidergic signaling in the nematode Caenorhabditis elegans." Prog Neurobiol **82**(1): 33-55.

Kamath, R. S. and J. Ahringer (2003). "Genome-wide RNAi screening in *Caenorhabditis elegans*." Methods **30**(4): 313-321.

Jumper, J., R. Evans, A. Pritzel, T. Green, M. Figurnov, O. Ronneberger, K. Tunyasuvunakool, R. Bates, A. Zidek, A. Potapenko, A. Bridgland, C. Meyer, S. A. A. Kohl, A. J. Ballard, A. Cowie, B. Romera-Paredes, S. Nikolov, R. Jain, J. Adler, T. Back, S. Petersen, D. Reiman, E. Clancy, M. Zielinski, M. Steinegger, M. Pacholska, T. Berghammer, S. Bodenstein, D. Silver, O. Vinyals, A. W. Senior, K. Kavukcuoglu, P. Kohli and D. Hassabis (2021). "Highly accurate protein structure prediction with AlphaFold." Nature **596**(7873): 583-589.

Kopchock, R. J., 3rd, B. Ravi, A. Bode and K. M. Collins (2021). "The Sex-Specific VC Neurons Are Mechanically Activated Motor Neurons That Facilitate Serotonin-Induced Egg Laying in C. elegans." J Neurosci **41**(16): 3635-3650.

Kupcova, I., L. Danisovic, I. Grgac and S. Harsanyi (2022). "Anxiety and Depression: What Do We Know of Neuropeptides?" Behav Sci (Basel) **12**(8).

Loer, C. a. R., JB. (2022). "The Evidence for Classical Neurotransmitters in Caenorhabditis elegans." 2023, from https://www.wormatlas.org/neurotransmitterstable.htm#Serotonin.

Lynch, A. S., D. Briggs and I. A. Hope (1995). "Developmental expression pattern screen for genes predicted in the C. elegans genome sequencing project." Nat Genet **11**(3): 309-313.

Manzke, T., U. Guenther, E. G. Ponimaskin, M. Haller, M. Dutschmann, S. Schwarzacher and D. W. Richter (2003). "5-HT4(a) receptors avert opioid-induced breathing depression without loss of analgesia." Science **301**(5630): 226-229.

Medrano, R. F. and C. A. de Oliveira (2014). "Guidelines for the tetra-primer ARMS-PCR technique development." Mol Biotechnol **56**(7): 599-608.

Mendel, J. E., H. C. Korswagen, K. S. Liu, Y. M. Hajdu-Cronin, M. I. Simon, R. H. Plasterk and P. W. Sternberg (1995). "Participation of the protein Go in multiple aspects of behavior in C. elegans." Science **267**(5204): 1652-1655.

Meyer, T. A., A. S. Habib, D. Wagner and T. J. Gan (2023). "Neurokinin-1 receptor antagonists for the prevention of postoperative nausea and vomiting." Pharmacotherapy **43**(9): 922-934.

Mills, H., A. Ortega, W. Law, V. Hapiak, P. Summers, T. Clark and R. Komuniecki (2016). "Opiates Modulate Noxious Chemical Nociception through a Complex Monoaminergic/Peptidergic Cascade." J Neurosci **36**(20): 5498-5508.

Nusbaum, M. P., D. M. Blitz and E. Marder (2017). "Functional consequences of neuropeptide and small-molecule co-transmission." Nat Rev Neurosci **18**(7): 389-403.

Okaty, B. W., K. G. Commons and S. M. Dymecki (2019). "Embracing diversity in the 5-HT neuronal system." Nat Rev Neurosci **20**(7): 397-424.

Olson, A. C., A. M. Butt, N. T. M. Christie, A. Shelar and M. R. Koelle (2023). "Multiple Subthreshold GPCR Signals Combined by the G-Proteins Gα(q) and Gα(s) Activate the *Caenorhabditis elegans* Egg-Laying Muscles." J Neurosci **43**(21): 3789-3806.

Paix, A., A. Folkmann, D. Rasoloson and G. Seydoux (2015). "High Efficiency, Homology-Directed Genome Editing in *Caenorhabditis elegans* Using CRISPR-Cas9 Ribonucleoprotein Complexes." Genetics **201**(1): 47-54.

Ptak, K., T. Yamanishi, J. Aungst, L. S. Milescu, R. Zhang, G. B. Richerson and J. C. Smith (2009). "Raphe neurons stimulate respiratory circuit activity by multiple mechanisms via endogenously released serotonin and substance P." J Neurosci **29**(12): 3720-3737.

Ravi, B., L. M. Nassar, R. J. Kopchock, 3rd, P. Dhakal, M. Scheetz and K. M. Collins (2018). "Ratiometric Calcium Imaging of Individual Neurons in Behaving *Caenorhabditis Elegans*." J Vis Exp(132).

Ren, J., A. Isakova, D. Friedmann, J. Zeng, S. M. Grutzner, A. Pun, G. Q. Zhao, S. S. Kolluru, R. Wang, R. Lin, P. Li, A. Li, J. L. Raymond, Q. Luo, M. Luo, S. R. Quake and L. Luo (2019). "Single-cell transcriptomes and whole-brain projections of serotonin neurons in the mouse dorsal and median raphe nuclei." Elife **8**.

Riddle, T. B. D. L. (Ed.), Meyer, B. J. (Ed.), and Priess J. R. (Ed.) (1997). Section IV, SL2 Trans -Splicing and Operons. C. elegans II. Cold Spring Harbor (NY), Cold Spring Harbor Laboratory Press.

Ripoll-Sanchez, L., J. Watteyne, H. Sun, R. Fernandez, S. R. Taylor, A. Weinreb, B. L. Bentley, M. Hammarlund, D. M. Miller, 3rd, O. Hobert, I. Beets, P. E. Vertes and W. R. Schafer (2023). "The neuropeptidergic connectome of C. elegans." Neuron **111**(22): 3570-3589 e3575.

Rual, J. F., J. Ceron, J. Koreth, T. Hao, A. S. Nicot, T. Hirozane-Kishikawa, J. Vandenhaute, S. H. Orkin, D. E. Hill, S. van den Heuvel and M. Vidal (2004). "Toward improving *Caenorhabditis elegans* phenome mapping with an ORFeome-based RNAi library." Genome Res **14**(10b): 2162-2168.

Stiernagle, T. (2006). "Maintenance of C. elegans." WormBook: 1-11.

Sun, X., C. Thorn Perez, D. N. Halemani, X. M. Shao, M. Greenwood, S. Heath, J. L. Feldman and K. Kam (2019). "Opioids modulate an emergent rhythmogenic process to depress breathing." Elife **8**.

Svensson, E., J. Apergis-Schoute, G. Burnstock, M. P. Nusbaum, D. Parker and H. B. Schioth (2018). "General Principles of Neuronal Co-transmission: Insights From Multiple Model Systems." Front Neural Circuits **12**: 117.

Szereda-Przestaszewska, M. and K. Kaczynska (2020). "Serotonin and substance P: Synergy or competition in the control of breathing." Auton Neurosci **225**: 102658.

Terry, N. and K. G. Margolis (2017). "Serotonergic Mechanisms Regulating the GI Tract: Experimental Evidence and Therapeutic Relevance." Handb Exp Pharmacol **239**: 319-342.

Trent, C., N. Tsuing and H. R. Horvitz (1983). "Egg-laying defective mutants of the nematode *Caenorhabditis elegans*." Genetics **104**(4): 619-647.

Van Bael, S., S. Zels, K. Boonen, I. Beets, L. Schoofs and L. Temmerman (2018). "A Caenorhabditis elegans Mass Spectrometric Resource for Neuropeptidomics." J Am Soc Mass Spectrom **29**(5): 879-889.

Varadi, M., S. Anyango, M. Deshpande, S. Nair, C. Natassia, G. Yordanova, D. Yuan, O. Stroe, G. Wood, A. Laydon, A. Zidek, T. Green, K. Tunyasuvunakool, S. Petersen, J. Jumper, E. Clancy, R. Green, A. Vora, M. Lutfi, M. Figurnov, A. Cowie, N. Hobbs, P. Kohli, G. Kleywegt, E. Birney, D. Hassabis and S. Velankar (2022). "AlphaFold Protein Structure Database: massively expanding the structural coverage of protein-sequence space with high-accuracy models." Nucleic Acids Res **50**(D1): D439-D444.

Von Euler, U. S. and J. H. Gaddum (1931). "An unidentified depressor substance in certain tissue extracts." J Physiol **72**(1): 74-87.

Waggoner, L. E., L. A. Hardaker, S. Golik and W. R. Schafer (2000). "Effect of a neuropeptide gene on behavioral states in *Caenorhabditis elegans* egg-laying." Genetics **154**(3): 1181-1192.

Waggoner, L. E., G. T. Zhou, R. W. Schafer and W. R. Schafer (1998). "Control of alternative behavioral states by serotonin in *Caenorhabditis elegans*." Neuron **21**(1): 203-214.

Wang, J. and M. M. Barr (2005). "RNA interference in Caenorhabditis elegans." Methods Enzymol **392**: 36-55.

Wightman, B., I. Ha and G. Ruvkun (1993). "Posttranscriptional regulation of the heterochronic gene lin-14 by lin-4 mediates temporal pattern formation in C. elegans." Cell **75**(5): 855-862.

Yao, Z., C. T. J. van Velthoven, M. Kunst, M. Zhang, D. McMillen, C. Lee, W. Jung, J. Goldy, A. Abdelhak, P. Baker, E. Barkan, D. Bertagnolli, J. Campos, D. Carey, T. Casper, A. B. Chakka, R. Chakrabarty, S. Chavan, M. Chen, M. Clark, J. Close, K. Crichton, S. Daniel, T. Dolbeare, L. Ellingwood, J. Gee,

A. Glandon, J. Gloe, J. Gould, J. Gray, N. Guilford, J. Guzman, D. Hirschstein, W. Ho, K. Jin, M. Kroll, K. Lathia, A. Leon, B. Long, Z. Maltzer, N. Martin, R. McCue, E. Meyerdierks, T. N. Nguyen, T. Pham, C. Rimorin, A. Ruiz, N. Shapovalova, C. Slaughterbeck, J. Sulc, M. Tieu, A. Torkelson, H. Tung, N. V. Cuevas, K. Wadhwani, K. Ward, B. Levi, C. Farrell, C. L. Thompson, S. Mufti, C. M. Pagan, L. Kruse, N. Dee, S. M. Sunkin, L. Esposito, M. J. Hawrylycz, J. Waters, L. Ng, K. A. Smith, B. Tasic, X. Zhuang and H. Zeng (2023). "A high-resolution transcriptomic and spatial atlas of cell types in the whole mouse brain." bioRxiv.

8. Appendices

8.1. Appendix A: MATLAB code to process the calcium imaging data produced in Volocity for ratiometric analysis

---

This code is adapted from previous works in the Koelle lab (Brewer et al., 2019; Collins et al., 2016; Olson et al., 2023) to be used with only the "Relative Time (s)", "Area (um≤)", and "Mean (Ratio Channel)" columns exported from the Volocity software "Measure timepoints" function with the column titles deleted.

Things of note in this code—rolling average is important (in contrast to notations by past users). The larger the number at "aveSize" the more the peak values are smoothed, and the more the data are masked and manipulated. However, for HSN calcium imaging, I found it necessary to have some smoothing to reduce the background noise for the MATLAB findpeaks function to more accurately call peaks. The minimum peak prominence also helps to guide the findpeaks function to not erroneously call a background signal as a true calcium spike. Even with these modifications, I still had to manually add and remove peaks to the final data set.

I also have added in the ability to manipulate the graphs and create files that are compatible with other image viewing softwares.

```
function [tSRD, tSRDfull] = GCaMP_process(tSRDfull)

    %Function takes in an n x 3 matrix where the first column is time, second
    %column is size of object, and 3rd column is mean ratio channel. The fourth
    %column will be delta R over R once its calculated
    %if no argument is provided, will prompt user to choose a comma delineated
    %file. This file should have no words, and just be the 3 columns.

    %tSRD stands for time size ratio and delta R over R. tSRDfull(:,3) will
    %adjusted by a rolling average
    %of size aveSize. The resulting matrix is tSRD
```

```
%Function will also outpub an n by x matrix called AnalyzedPeaks that
%contains transients identified  via the findpeaks algorithm and their associated
%features (location, width, and prominance (a feature like peak height
%that uses the local features of the peak rather than absolute height).

%If there is no input, grab a file, otherwise set tSRDfull to input
if nargin == 0
   [name,path,~] = uigetfile('.csv','multiselect','on');

   if ~isequal(class(name),'cell')
      name = {name};
   end

   tSRDfull = cell(length(name),1);

   for i = 1:length(name)
      tSRDfull{i} = csvread(strcat(path,char(name{i})));
   end
end

%Create variable to hold tSRDfull and to manipulate
temptSRD = tSRDfull;
%Create the size of tSRD
tSRD = cell(length(temptSRD),1);
%Size of rolling average; we don't really see much benefit to this
%anymore, so we keep it at 1 meaning no rolling average
aveSize = 5;
%baseline in decimal. This will be used to calculate the lowest X
%percent of data points
cutOff = 0.1;
figure;

%Do the following for every file. loop through each file
for z = 1:length(temptSRD)
   %weight temptSRD by multiplying area column with ratio column
   temptSRD{z}(:,3) = temptSRD{z}(:,2).*temptSRD{z}(:,3);

   %loop through and eliminate dobuled time points by adding together the size
   %of the two objects and averaging the signal between them.
   for i = length( temptSRD{z}(:,1) ) : -1 : 2
      if temptSRD{z}(i,1) == temptSRD{z}(i-1,1)
         temptSRD{z}(i-1,2) = temptSRD{z}(i-1,2) + temptSRD{z}(i,2);
         temptSRD{z}(i-1,3) = temptSRD{z}(i-1,3) + temptSRD{z}(i,3);
         temptSRD{z}(i,:) = [];
      end
   end

   temptSRD{z}(:,3) = temptSRD{z}(:,3)./temptSRD{z}(:,2);

   %Set up tSRD as a subset of temptSRD and add an extra column of zeros
   tSRD{z} = [temptSRD{z}(1:end-aveSize+1,:) zeros(length(temptSRD{z})-aveSize+1,1)];

   %turn tSRD's ratio column to a rolling average
   for j = 1:length(tSRD{z}(:,1))
      tSRD{z}(j,3) = mean(temptSRD{z}(j:j+aveSize-1,3));
   end
```

```
        %turn tSRD's area column to a rolling average
        for k = 1:length(tSRD{z}(:,1))
           tSRD{z}(k,2) = mean(temptSRD{z}(k:k+aveSize-1,2));
        end

        %sort tSRD
        sorttSRD = sort(tSRD{z}(:,3));
        %find the index at which the cutoff would sit
        cutOffIndex = floor(cutOff*length(tSRD{z}));
        %calculate baseline as mean of the bottom cutOff of values
        baseline = mean(sorttSRD(1:cutOffIndex));

        %calculate delta R over R
        tSRD{z}(:,4) = (tSRD{z}(:,3) - baseline)/baseline;

        %write the matrix to a file
        if ~exist(strcat(path,'/analyzed'),'dir')
           mkdir(path,'analyzed')
        end
        dlmwrite(strcat(path,'/analyzed/a-',char(name(z))),tSRD{z},'precision','%6.3f')

         %Using findpeaks algorithm to find transients in column 4 (?R/R).
         %Returns the amplitude (pks), timepoint (locs), width (w), and
         %prominance (like amplitude but based on local area, not raw
         %intensity). MinPeakDistance at 0.5 is the minimum amount of time,
         %in seconds, between peaks. It elminates peaks with two or more
         %maxima with the same value, although it doesn't fix the width or
         %other calculated features of those peaks. MinPeakProminence is in
         %units of ?R/R and measure the fraction of the local baseline
         %rather than raw ratio from baseline. Writes a matrix with the prefix 'peaks'
         %using PeakFile with that information.
 %>>>can change MinPeakProminence to higher to make the background peaks
 %not called as real peaks into peaks. Change also at line 127
        [pks,locs,w,p] =
findpeaks(tSRD{z}(:,4),tSRD{z}(:,1),'Annotate','extents','WidthReference','halfheight','MinPeakDist
ance',0,'MinPeakProminence',1.85);
        PeakFile{z} = [locs,pks,w,p];

        %Create a new matrix with the PeakFile matrix and an extra column
        %of zeros.
        PeakMath = [PeakFile{z}, zeros(length(PeakFile{z}(:,1)),1)];
        %Find the difference from Time point 2 and Time point 1 and add
        %that in leau of the zero column, adding a zero to the end to keep
        %the matrix the same length.
           PeakMath(:,5) = [diff(PeakFile{z}(:,1));0];

        %write the peak matrix to a file including times, amplitudes,
        %widths and prominances.
        if ~exist(strcat(path,'/peaks'),'dir')
           mkdir(path,'peaks')
        end
        dlmwrite(strcat(path,'/peaks/peaks-',char(name(z))),PeakMath,'precision','%6.3f')

        %write the deltaR/R traces to a file
        if ~exist(strcat(path,'/traces'),'dir')
```

```
        mkdir(path,'traces')
    end

    %plot and save un-annotated deltaR/R in eps format readable by
    %Illustrator, etc.
    %subplot(length(temptSRD),1,z);
    plot(tSRD{z}(:,1),tSRD{z}(:,4));
    x0=1;
    y0=12;
    width=30;
    height=4;
    set(gcf,'units','inches','position',[x0,y0,width,height])
    grid on
    hAx=gca;  % avoid repetitive function calls
    set(hAx,'xminorgrid','on');
    set(gca,'XMinorTick','on');
    xticks(0:250:3750);
    saveas(gcf,strcat(path,'/traces/plain-',char(name(z)),'.eps'),'epsc');
    saveas(gcf,strcat(path,'/traces/plaintif-',char(name(z)),'.tif'),'tif');

    %plot and save annotated deltaR/R in eps format readable by
    %Illustrator, etc.
    subplot(length(temptSRD),1,z);
    findpeaks(tSRD{z}(:,4),tSRD{z}(:,1),'Annotate','extents','WidthReference','halfheight','MinPea
kDistance',0,'MinPeakProminence',1.85);
 %>>>can change MinPeakProminence to higher to make the background peaks
 %not called as real peaks into peaks. Change also at line 103
    x0=1;
    y0=12;
    width=20;
    height=4;
    set(gcf,'units','inches','position',[x0,y0,width,height])
    grid on
    hAx=gca;  % avoid repetitive function calls
    set(hAx,'xminorgrid','on');
    set(gca,'XMinorTick','on');
    xticks(0:250:3750);
     legend(Location="northeastoutside");
    saveas(gcf,strcat(path,'/traces/anno-',char(name(z)),'.eps'),'epsc');
    saveas(gcf,strcat(path,'/traces/annotif-',char(name(z)),'.tif'),'tif');
  end


      end
```

Appendix B: R script to create publication figures from the peaks called in the MATLAB code from Appendix A

This code was adapted by Emerson Santiago from Olson et al. (2023) for use in the publication "Neuropeptide and serotonin co-transmission sets the activity pattern in the *C. elegans* egg-laying circuit."

```
location="for pub/"

makeCalciumLongPlot <- function(calciumFile, eggFile, peakFile, name) {
   calcium <- read.csv(paste(location,calciumFile,sep=""))
   eggs <- read.csv(paste(location,eggFile,sep=""))
   peaks <- read.csv(paste(location,peakFile,sep=""))

   dev.new(file=paste(name, ".pdf",sep=""), width=11.4, height=2.75)

   print("************************************")
   print(name)

   #plot(calcium$time, calcium$amplitude, type="l")
   #points(eggs$time, rep(max(calcium$amplitude), length(eggs$time)), cex=eggs$eggs)


   # used for putting the egg-markers on the plot
   #lo <- loess(calcium$amplitude ~ calcium$time) # this is very slow
   #eggs$predictedAmplitude <- predict(lo, eggs$time)
   # because the data is very "jagged", this sticks the egg-points too low compared
   # too the perceived peaks

   calcium$amplitude <- calcium$amplitude/max(calcium$amplitude)


   # to match calcium trace
   i=1
   while (i<length(peaks$time)) {
      ind <- match(peaks$time[i], calcium$time)
      # if we get a match
      if (!is.na(ind)) {
         peaks$amplitude[i] <- calcium$amplitude[ind]
      } else {
         print("MISSING AMPLITUDE FOR TIME: ")
         print(peaks$time[i])
         peaks$amplitude[i] <- NA
      }
      i=i+1
   }

   peaks$amplitude <- peaks$amplitude/max(peaks$amplitude)
```

```
print(peaks$time)
peaks$flatline <- rep(1.1,length(peaks$time))
peaks$burstAlpha<-(getBurstingAlpha(peaks))

#m<-median(calcium$amplitude)
#calcium[calcium$amplitude<m,] <- m
#calcium <- calcium[calcium$amplitude>0.1,]

#calcium

getLocalMax <- function(data, time, range) {
   index<-match(round(time, digits=0), round(data$time, digits=0))
   print(index)
   l <- length(data$time)
   print(l)
   # TODO: boundary risk if <0 or >length, but this should be very rare
   leftInd <- index-range
   rightInd <- index+range
   print(leftInd)
   print(rightInd)
   values=double(length(leftInd))
   i=1
   while (i<=length(leftInd)) {
      values[i] <- max(data$amplitude[leftInd[i]:rightInd[i]])
      i=i+1
   }
   return(values)
}

eggs$predictedAmplitude <- getLocalMax(calcium, eggs$time, 30)

print(eggs)

library(ggplot2)
library(ggh4x) # used to add minor tick marks

plot_aesthetic = theme(panel.grid.major = element_blank(),
                       panel.grid.minor = element_blank(),
                       axis.line = element_line(colour = "black"),
                       panel.background = element_blank(),
                       panel.border = element_rect(colour = "black", fill=NA, size=1),
                       #panel.background = element_rect(fill = 'white', colour = 'black'),
                       # panel.grid.major = element_blank(),
                       #panel.grid.minor = element_line(color = 'grey80', size=0.2),
                       #axis.ticks = element_blank(),
                       axis.text = element_text(size = 10, colour='black', face = 'bold'),
                       axis.title=element_text(size=14,face="bold"),
                       plot.title = element_text(color="red", size=14, face='bold'))

p <-  ggplot(data=calcium, aes(x=time, y=amplitude)) +
  geom_line(color='black', linewidth=0.1) +
  geom_line(data=peaks, aes(x=time, y=flatline),
            color="red", alpha=peaks$burstAlpha, size=2)+
  #max(calcium$amplitude)*0.8
  geom_point(data=eggs, aes(x=time, y=predictedAmplitude+0.15),    # rep(0.95,length(time)) ),
             color="blue", x=eggs$time, size=eggs$egg*3, pch=6) +
```

```
    geom_point(data=peaks, aes(x=time, y=amplitude+0.02),    # rep(0.95,length(time)) ),
              color="blue", x=peaks$time, size=1, pch=20) +
    scale_y_continuous(
      breaks=seq(0,1,0.2),
      guide = "axis_minor" , limits=c(0,1.1)) +
    #ylim(0,1.15) + # remove this for normal plotting

    xlab('Timepoint') +
    ylab('Amplitude') +
    scale_x_continuous(
      minor_breaks = seq(0,max(calcium$time),60),
      breaks=seq(0,max(calcium$time),600),
      guide = "axis_minor" ) +
    ggtitle(name)
  print (p + plot_aesthetic)
}


ACTIVEPHASEDURATION=120 # seconds between active phases
getListPhases<-function(values)
{
  phases=list()
  cPhase=c()

  pLast=0
  i=1
  while (i<=length(values)) {
    if (values[i]-pLast > ACTIVEPHASEDURATION) {
      if (length(cPhase)>0) {
        phases[[length(phases)+1]] <- cPhase
      }
      cPhase=values[i]
    }
    else {
      cPhase=c(cPhase,values[i])
    }
    pLast=values[i]
    i=i+1
  }
  phases[[length(phases)+1]] <- cPhase

  return(phases)
}

getFirsts <- function(timeList) {
  firsts=c()
  for (p in timeList) {
    firsts=c(firsts,p[1])
  }
  return(firsts)
}

getLasts <- function(timeList) {
  lasts=c()
  for (p in timeList) {
    lasts=c(lasts,p[length(p)])
```

```
    }
    return(lasts)
}

activityAfterEggOld <- function(calciumFile, eggFile, name) {

    calcium <- read.csv(paste(location,calciumFile,sep=""))
    eggs <- read.csv(paste(location,eggFile,sep=""))

    dev.new(file=paste(name, "_AAE.pdf",sep=""), width=20, height=4)
    calcium$amplitude <- calcium$amplitude/max(calcium$amplitude)

    #print(eggs)

    listPhases<-getListPhases(eggs$time)
    #print(listPhases)

    lasts <- getLasts(listPhases)
    #print(lasts)

    FADE_FRAME=300
    sum=double(5000)
    min=4000
    for (l in lasts) {
        headSliced<-calcium[calcium$time>l[1],]
        tailSliced<-headSliced[headSliced$time<l[1]+FADE_FRAME,]
        print("##############################################")
        print(length(tailSliced$amplitude))
        print(length(tailSliced$area))
        print(length(sum))
        if (length(tailSliced$area)<min) {
            min=length(tailSliced$area)
        }
        sum=sum+(tailSliced$amplitude*tailSliced$area)
    }
    sum <- sum[1:min]
    listMean=sum/length(lasts)
    plot(listMean,type="l")

}

activityAfterEgg <- function(datasets,name) {

    FADE_FRAME=300
    sum=double(17*FADE_FRAME)
    min=4000
    totalLasts=0

    #dev.new(file=paste(name, "_AAE.pdf",sep=""), width=20, height=4)

    for (set in datasets) {
        calciumFile=set[1]
        eggFile=set[2]


        calcium <- read.csv(paste(location,calciumFile,sep=""))
```

```
        eggs <- read.csv(paste(location,eggFile,sep=""))

        calcium$amplitude <- calcium$amplitude/max(calcium$amplitude)

        print(eggs)

        listPhases<-getListPhases(eggs$time)
        #print(listPhases)

        lasts <- getLasts(listPhases)
        print(lasts)

        for (l in lasts) {
            headSliced<-calcium[calcium$time>l[1],]
            tailSliced<-headSliced[headSliced$time<l[1]+FADE_FRAME,]
            #print("##############################################")
            #print(length(tailSliced$amplitude))
            #print(length(tailSliced$area))
            #print(length(sum))
            #if (length(tailSliced$area)<min) {
            #    min=length(tailSliced$area)
            #}
            sum=sum+c((tailSliced$amplitude),rep(0,length(sum)-
length(tailSliced$amplitude)))#*tailSliced$area)
        }
        totalLasts<-totalLasts+length(lasts)
    }
    sum <- sum[1:(FADE_FRAME*15)]
    listMean=sum/totalLasts
    #plot(listMean,type="l")
    return(listMean)

}

getBurstingAlpha <- function(peaks)
{
    dT <- double(length(peaks$time))
    #dT[1]<-999999 # filler to prevent counting first peak as part of a burst
    i<-1
    while (i < length(dT))
    {
        dT[i] <- peaks$time[i+1] - peaks$time[i]
        i=i+1
    }
    print(dT)
    isBurst<-dT<30 # 30 seconds between peaks is the limit!
    useAlpha<-ifelse(isBurst, 1, 0)
    return(useAlpha)
}



cntrlOnly=list(
        c("a-1 6 cntrl matlab.csv", "eggs-1 6 cntrl matlab.csv", "1 6 23 - control"),

        c("a-11 17 control matlab.csv", "eggs-11 17 control matlab.csv", "11 17 22 - control"),
```

```
        #c("a-3323 nlp3 matlab.csv", "eggs-3323 nlp3 matlab.csv", "3 3 23 - nlp3"),
        #c("a-3323 nlp3 oops matlab.csv", "eggs-3323 nlp3 oops matlab.csv", "3 3 23 - nlp3
(oops)"),

        c("a-22823 control matlab.csv", "egg-22823 control matlab.csv", "2 28 23 - control"),

        c("a-cntrl 1017.csv", "egg-cntrl 1017.csv", "10 17 22 - control"),
        #c("a-nlp3 1017.csv", "egg-.csv", "10 17 22 - nlp3"),

        c("a-Cntrl 10 7 matlab 1 stretch.csv", "egg-Cntrl 10 7 matlab 1 copy.csv", "10 7 22 -
control")
    )
nlp3Only=list(
        c("a-1 6 nlp3 matlab.csv", "eggs-1 6 nlp3 matlab.csv", "1 6 23 - nlp3"),

        c("a-11 17 nlp3 matlab.csv", "eggs-11 17 nlp3 matlab.csv", "11 17 22 - nlp3"),

        #c("a-3323 nlp3 matlab.csv", "eggs-3323 nlp3 matlab.csv", "3 3 23 - nlp3"),
        #c("a-3323 nlp3 oops matlab.csv", "eggs-3323 nlp3 oops matlab.csv", "3 3 23 - nlp3
(oops)"),

        c("a-22823 nlp3 matlab.csv", "egg-22823 nlp3 matlab.csv", "2 28 23 - nlp3"),

        #c("a-nlp3 1017.csv", "egg-.csv", "10 17 22 - nlp3"),

        c("a-nlp3 10 7 matlab.csv", "egg-nlp3 10 7 matlab.csv", "10 7 22 - nlp3")
    )


datasets=list(
        c("a-1 6 cntrl matlab.csv", "eggs-1 6 cntrl matlab.csv", "wt_1-6_peaks.csv", "1 6 23 -
control"),
        c("a-1 6 nlp3 matlab.csv", "eggs-1 6 nlp3 matlab.csv", "nlp3_1-6_peaks.csv","1 6 23 -
nlp3"),

        c("a-11 17 control matlab.csv", "eggs-11 17 control matlab.csv", "wt-11-17_peaks.csv",
"11 17 22 - control"),
        c("a-11 17 nlp3 matlab.csv", "eggs-11 17 nlp3 matlab.csv", "nlp3_11-17_peaks.csv", "11
17 22 - nlp3"),

        c("a-3323 nlp3 matlab.csv", "noeggs-a-3323 nlp3 matlab.csv", "nlp3_3-3_peaks_1.csv", "3
3 23 - nlp3"),
        c("a-3323 nlp3 oops matlab.csv", "noeggs-a-3323 nlp3 oops matlab.csv", "nlp3_3-
3_peaks_2.csv", "3 3 23 - nlp3 (oops)"),

        c("a-22823 control matlab.csv", "egg-22823 control matlab.csv", "wt_2-28_peaks.csv", "2
28 23 - control"),
        c("a-22823 nlp3 matlab.csv", "egg-22823 nlp3 matlab.csv", "nlp3_2-28_peaks.csv", "2 28
23 - nlp3"),

        c("a-cntrl 1017.csv", "egg-cntrl 1017.csv", "wt_10-17_peaks.csv", "10 17 22 - control"),
        c("a-nlp3 1017.csv", "egg-nlp3 1017.csv", "nlp3_10-17_peaks.csv", "10 17 22 - nlp3"),

        c("a-Cntrl 10 7 matlab 1 stretch.csv", "egg-Cntrl 10 7 matlab 1 copy.csv", "wt_10-
7_peaks.csv", "10 7 22 - control"),
```

```
        c("a-nlp3 10 7 matlab.csv", "egg-nlp3 10 7 matlab.csv", "nlp3_10-7_peaks.csv", "10 7 22 -
nlp3")
      )

for (set in datasets) {makeCalciumLongPlot(set[1],set[2],set[3],set[4])}



# special plots

cntrl=c("a-cntrl 1017.csv",
      "egg-cntrl 1017.csv",
      "wt_10-17_peaks.csv",
      "10 17 22 - control")

makeSpecialCNTRLPlot <- function(calciumFile, eggFile, peakFile, name) {
   calcium <- read.csv(paste(location,calciumFile,sep=""))
   eggs <- read.csv(paste(location,eggFile,sep=""))
   peaks <- read.csv(paste(location,peakFile,sep=""))

   dev.new(file=paste(name, ".pdf",sep=""), width=11.4, height=2.75)

   print("************************************")
   print(name)

   #plot(calcium$time, calcium$amplitude, type="l")
   #points(eggs$time, rep(max(calcium$amplitude), length(eggs$time)), cex=eggs$eggs)


   # used for putting the egg-markers on the plot
   #lo <- loess(calcium$amplitude ~ calcium$time) # this is very slow
   #eggs$predictedAmplitude <- predict(lo, eggs$time)
   # because the data is very "jagged", this sticks the egg-points too low compared
   # too the perceived peaks

   calcium$amplitude <- calcium$amplitude/max(calcium$amplitude)


   # to match calcium trace
   i=1
   while (i<length(peaks$time)) {
      ind <- match(peaks$time[i], calcium$time)
      # if we get a match
      if (!is.na(ind)) {
         peaks$amplitude[i] <- calcium$amplitude[ind]
      } else {
         print("MISSING AMPLITUDE FOR TIME: ")
         print(peaks$time[i])
         peaks$amplitude[i] <- NA
      }
      i=i+1
   }
   peaks$amplitude <- peaks$amplitude/max(peaks$amplitude)

   print(peaks$time)
   peaks$flatline <- rep(1.1,length(peaks$time))
```

```
peaks$burstAlpha<-(getBurstingAlpha(peaks))

#m<-median(calcium$amplitude)
#calcium[calcium$amplitude<m,] <- m
#calcium <- calcium[calcium$amplitude>0.1,]

#calcium

getLocalMax <- function(data, time, range) {
   index<-match(round(time, digits=0), round(data$time, digits=0))
   print(index)
   l <- length(data$time)
   print(l)
   # TODO: boundary risk if <0 or >length, but this should be very rare
   leftInd <- index-range
   rightInd <- index+range
   print(leftInd)
   print(rightInd)
   values=double(length(leftInd))
   i=1
   while (i<=length(leftInd)) {
      values[i] <- max(data$amplitude[leftInd[i]:rightInd[i]])
      i=i+1
   }
   return(values)
}

eggs$predictedAmplitude <- getLocalMax(calcium, eggs$time, 30)

print(eggs)

library(ggplot2)
library(ggh4x) # used to add minor tick marks

plot_aesthetic = theme(panel.grid.major = element_blank(),
                       panel.grid.minor = element_blank(),
                       axis.line = element_line(colour = "black"),
                       panel.background = element_blank(),
                       panel.border = element_rect(colour = "black", fill=NA, size=1),
                       #panel.background = element_rect(fill = 'white', colour = 'black'),
                       # panel.grid.major = element_blank(),
                       #panel.grid.minor = element_line(color = 'grey80', size=0.2),
                       #axis.ticks = element_blank(),
                       axis.text = element_text(size = 10, colour='black', face = 'bold'),
                       axis.title=element_text(size=14,face="bold"),
                       plot.title = element_text(color="red", size=14, face='bold'))

print("======calcium=======")
print(head(calcium))
print("======eggs=======")
print(head(eggs))
print("*******peaks")
print(head(peaks))

calcium<-calcium[calcium$time>2020,]
eggs<-eggs[eggs$time>2020,]
```

```
    peaks<-peaks[peaks$time>2020,]

    calcium<-calcium[calcium$time<3100,]
    eggs<-eggs[eggs$time<3100,]
    peaks<-peaks[peaks$time<3100,]

    calcium$time<-calcium$time-2020
    eggs$time<-eggs$time-2020
    peaks$time<-peaks$time-2020

    print("======calcium=======")
    print(head(calcium))
    print("======eggs=======")
    print(head(eggs))
    print("*******peaks")
    print(head(peaks))

    p <-  ggplot(data=calcium, aes(x=time, y=amplitude)) +
      geom_line(color='black', linewidth=0.1) +
      geom_line(data=peaks, aes(x=time, y=flatline),
                color="red", alpha=peaks$burstAlpha, size=2)+
      #max(calcium$amplitude)*0.8
      geom_point(data=eggs, aes(x=time, y=predictedAmplitude+0.15),    # rep(0.95,length(time)) ),
                 color="blue", x=eggs$time, size=eggs$egg*3, pch=6) +
      geom_point(data=peaks, aes(x=time, y=amplitude+0.02),    # rep(0.95,length(time)) ),
                 color="blue", x=peaks$time, size=1, pch=20) +
      scale_y_continuous(
        breaks=seq(0,1,0.2),
        guide = "axis_minor", limits=c(0,1.1)) +
      #ylim(0,1.15) + # remove this for normal plotting

      xlab('Timepoint') +
      ylab('Amplitude') +
      scale_x_continuous(
        minor_breaks = seq(min(calcium$time),max(calcium$time),60),
        #59.99 instead of 60 so that you get a tick on the last minute
        breaks=seq(0,max(calcium$time)+1,120),
        guide = "axis_minor", limits=c(0,3100-2020) ) +
      ggtitle(name)
    print (p + plot_aesthetic)
    ggsave(filename=paste(name,".pdf"), plot=p + plot_aesthetic, height = 2.75 , width = 11.4)
}

makeSpecialCNTRLPlot(cntrl[1],cntrl[2],cntrl[3],"special plot-cntrl")

nlp3=c("a-11 17 nlp3 matlab.csv",
       "eggs-11 17 nlp3 matlab.csv",
       "nlp3_11-17_peaks.csv",
       "11 17 22 - nlp3")

makeSpecialNLP3Plot <- function(calciumFile, eggFile, peakFile, name) {
    calcium <- read.csv(paste(location,calciumFile,sep=""))
    eggs <- read.csv(paste(location,eggFile,sep=""))
    peaks <- read.csv(paste(location,peakFile,sep=""))

    dev.new(file=paste(name, ".pdf",sep=""), width=11.4, height=2.75)
```

```
print("************************************")
print(name)

#plot(calcium$time, calcium$amplitude, type="l")
#points(eggs$time, rep(max(calcium$amplitude), length(eggs$time)), cex=eggs$eggs)


# used for putting the egg-markers on the plot
#lo <- loess(calcium$amplitude ~ calcium$time) # this is very slow
#eggs$predictedAmplitude <- predict(lo, eggs$time)
# because the data is very "jagged", this sticks the egg-points too low compared
# too the perceived peaks

calcium$amplitude <- calcium$amplitude/max(calcium$amplitude)


# to match calcium trace
# to match calcium trace
i=1
while (i<length(peaks$time)) {
   ind <- match(peaks$time[i], calcium$time)
   # if we get a match
   if (!is.na(ind)) {
      peaks$amplitude[i] <- calcium$amplitude[ind]
   } else {
      print("MISSING AMPLITUDE FOR TIME: ")
      print(peaks$time[i])
      peaks$amplitude[i] <- NA
   }
   i=i+1
}
peaks$amplitude <- peaks$amplitude/max(peaks$amplitude)

print(peaks$time)
peaks$flatline <- rep(1.1,length(peaks$time))
peaks$burstAlpha<-(getBurstingAlpha(peaks))

#m<-median(calcium$amplitude)
#calcium[calcium$amplitude<m,] <- m
#calcium <- calcium[calcium$amplitude>0.1,]

#calcium

getLocalMax <- function(data, time, range) {
   index<-match(round(time, digits=0), round(data$time, digits=0))
   print(index)
   l <- length(data$time)
   print(l)
   # TODO: boundary risk if <0 or >length, but this should be very rare
   leftInd <- index-range
   rightInd <- index+range
   print(leftInd)
   print(rightInd)
   values=double(length(leftInd))
   i=1
```

```
    while (i<=length(leftInd)) {
        values[i] <- max(data$amplitude[leftInd[i]:rightInd[i]])
        i=i+1
    }
    return(values)
}

eggs$predictedAmplitude <- getLocalMax(calcium, eggs$time, 30)

print(eggs)

library(ggplot2)
library(ggh4x) # used to add minor tick marks

plot_aesthetic = theme(panel.grid.major = element_blank(),
                       panel.grid.minor = element_blank(),
                       axis.line = element_line(colour = "black"),
                       panel.background = element_blank(),
                       panel.border = element_rect(colour = "black", fill=NA, size=1),
                       #panel.background = element_rect(fill = 'white', colour = 'black'),
                       # panel.grid.major = element_blank(),
                       #panel.grid.minor = element_line(color = 'grey80', size=0.2),
                       #axis.ticks = element_blank(),
                       axis.text = element_text(size = 10, colour='black', face = 'bold'),
                       axis.title=element_text(size=14,face="bold"),
                       plot.title = element_text(color="red", size=14, face='bold'))

print("======calcium=======")
print(head(calcium))
print("======eggs=======")
print(head(eggs))
print("*******peaks")
print(head(peaks))

mini=2200
maxi=3280

calcium<-calcium[calcium$time>mini,]
eggs<-eggs[eggs$time>mini,]
peaks<-peaks[peaks$time>mini,]

calcium<-calcium[calcium$time<maxi,]
eggs<-eggs[eggs$time<maxi,]
peaks<-peaks[peaks$time<maxi,]

calcium$time<-calcium$time-mini
eggs$time<-eggs$time-mini
peaks$time<-peaks$time-mini

print("======calcium=======")
print(head(calcium))
print("======eggs=======")
print(head(eggs))
print("*******peaks")
print(head(peaks))
```

```
    p <-  ggplot(data=calcium, aes(x=time, y=amplitude)) +
      geom_line(color='black', linewidth=0.1) +
      geom_line(data=peaks, aes(x=time, y=flatline),
                color="red", alpha=peaks$burstAlpha, size=2)+
      #max(calcium$amplitude)*0.8
      geom_point(data=eggs, aes(x=time, y=predictedAmplitude+0.15),    # rep(0.95,length(time)) ),
                 color="blue", x=eggs$time, size=eggs$egg*3, pch=6) +
      geom_point(data=peaks, aes(x=time, y=amplitude+0.02),    # rep(0.95,length(time)) ),
                 color="blue", x=peaks$time, size=1, pch=20) +
      scale_y_continuous(
        breaks=seq(0,1,0.2),
        guide = "axis_minor", limits=c(0,1.1)) +
      #ylim(0,1.15) + # remove this for normal plotting

      xlab('Timepoint') +
      ylab('Amplitude') +
      scale_x_continuous(
        minor_breaks = seq(min(calcium$time),max(calcium$time),60),
        #59.99 instead of 60 so that you get a tick on the last minute
        breaks=seq(0,max(calcium$time)+1,120),
        guide = "axis_minor", limits=c(0,maxi-mini) ) +
      ggtitle(name)
    print (p + plot_aesthetic)

    ggsave(filename=paste(name,".pdf"), plot=p + plot_aesthetic, height = 2.75 , width = 11.4)
}

makeSpecialNLP3Plot(cntrl[1],cntrl[2],cntrl[3],"special plot-nlp3")


warnings()
```

8.2. Appendix C: R script to display egg-laying events

This code was written by Emerson Santiago for the publication "Neuropeptide and serotonin co-transmission sets the activity pattern in the *C. elegans* egg-laying circuit." This code creates strip charts where each hash is an egg-laying event. The code also puts in a gray bar to indicate the time that the animal spent outside of the field of view.

```
# allison time - data plot Try 1

#data <- read.csv("../pattern of egg laying data 10 9 npr17_breaks.csv")
#endpoints <- read.csv("../pattern of egg laying time 10 9 npr17_breaks.csv")

data <- read.csv("../pattern of egg laying data 12 13.csv")
endpoints <- read.csv("../pattern of egg laying time 12 13.csv")


#head(data)

#data$realworm <- paste("Worm", as.integer(substring(data$worm, 6))+((data$replicate-1)*5))
#data$UWID <- as.integer(substring(data$worm, 6))+((data$replicate-1)*5)

#endpoints$UWID <- as.integer(substring(endpoints$worm, 6))+((endpoints$replicate-1)*5)

source ( '../add_UWID.R' )
data <- addUWID(data)
data$realworm <- paste("Worm",data$UWID)
endpoints <- addUWID(endpoints)
print(data)
print(endpoints)


# convert all NAs from empty cells to FALSE
data$break.line[is.na(data$break.line)] <- FALSE

#onlyEggs <- data[!data$break.line,]

# this pattern works
#stripchart(time ~ worm, data=data[data$genotype=="N2",][data$replicate==1,])

for (geno in unique(data$genotype))
{

   print(paste("Looping over genotypes, now at: ",geno))

   if (geno=="npr-17") {
      dev.new(file=paste(geno,".pdf",sep=""),width=17.4,height=4)
   } else {
      dev.new(file=paste(geno,".pdf",sep=""),width=17.4,height=6)
   }
```

```
genoDat <- data[data$genotype == geno,]

print(head(genoDat))

#dev.new(width=10, height=3+(length(unique(genoDat$realworm))/4))
#stripchart(c(0,14400), pch="|", cex=2)
stripchart(time ~ UWID, data=genoDat[!genoDat$break.line,],
          group.names=unique(genoDat$realworm), #jitter=0.2, method='jitter',
          pch="|", cex=1, main=geno, cex.axis=0.8, cex.lab=1.5,
          las=1, add=F, xlim=c(0,14400),
          xlab="Time (seconds)", cex.main=2,
          axes=TRUE, xaxt="n"
          )

axis(side=1, # bottom
    at=seq(0,14400,1800),
    lwd.ticks=2)

axis(side=1, # bottom
    at=seq(0,14400,300),
    labels=FALSE)

print(geno)
print(unique(genoDat$UWID))

for (v in unique(genoDat$UWID))
{
   q=genoDat[genoDat$UWID==v,]

   count=1
   i=1
   while (i<length(q$time)) {
      q$stack[i]<-count
      if ( (q$time[i+1]-q$time[i]) < 60 && q$break.line[i]!=TRUE &&  q$break.line[i+1]!=TRUE ) {
         count=count+1
      } else {
         if (count>1) {
            text(q$time[i], v+0.4, labels=count, cex=0.4)
         }
         count=1
      }
      i=i+1
   }
   # for the last label
   if (count>1) {
      text(q$time[i], v+0.4, labels=count, cex=0.4)
   }



   #nb=q[is.na(q$break.line),]
   #for (egg in nb) {
   #    text(egg$time, v+0.02, "t")
   #}
```

```
        breakers=q[q$break.line,]
        breakers=breakers[!is.na(breakers$UWID),]
        if (length(breakers$UWID))  #if there are any non-NA rows
        {
           last=0
           draw=T
           for (b in breakers$time)
           {
              #stripchart(c(b), pch="|", cex=2, add=T, at=v, col="grey")
              if (draw)
              {
                 lines(c(last, b), c(v, v), lwd=2,
                    col="black", lend=2)
              }
              last=b
              draw=!draw

           }
           for (b in breakers$time)
           {
              #stripchart(c(b), pch="|", cex=2, add=T, at=v, col="grey")
              if (!draw) {
                 lines(c(last, b), c(v, v), lwd=6,
                    col="grey", lend=1)
              }

              last=b
              draw=!draw

           }
           q=endpoints[endpoints$genotype==geno,]
           q=q[q$UWID==v,]
           endpoint=q$duration[!is.na(q$worm)]
           lines(c(last, endpoint), c(v, v), lwd=2, lend=2,
                    col="black")
        }
        else
        {
        q=endpoints[endpoints$genotype==geno,]
        q=q[q$UWID==v,]
        endpoint=q$duration[!is.na(q$worm)]
        lines(c(0, endpoint), c(v, v), lwd=2,
                    col="black")
        }
     }
     # USE THIS TO PLOT DOUBLE-EGGS WITH SPECIAL MARKS (e.g. red or different point, or
  whatever)
     #q=genoDat[genoDat$egg==2,]
     #q=q[!is.na(q$worm),]
     #stripchart(time ~ UWID, data=q[q$genotype==geno,][!q$break.line,],
     #          group.names=unique(q[q$egg==2,]$realworm),
     #          pch="|", cex=1, main=geno, cex.axis=0.8, col="black",
     #          las=1, add=T) # rotation of axis labels
  }
```

```
warnings()


#for final figure plots
# allison time - data plot

data <- read.csv("../split data 8 29 repsonlysplit_v2.csv")

endpoints <- read.csv("../split pattern times 8 29 repsonlysplit_v2.csv")

#head(data)

#data <- addUWID(data)
#endpoints <- addUWID(endpoints)


data$realworm <- paste("Worm", data$UWID)

print(tail(data))
print(tail(endpoints))

#onlyEggs <- data[!data$break.line,]

# this pattern works
#stripchart(time ~ worm, data=data[data$genotype=="N2",][data$replicate==1,])



# returns a color corresponding to the duration of the interval
#   between egg-laying events
getColor <- function(duration) {
   color="black"
   # calculated from WT triple gauss fit
   # high mu = 7.04, sigma = 0.57
   # mid mu = 3.55, sigma = 1.16
   # break = mid mu +
   #    (mid sigma / (mid sigma + high sigma)) * (high mu - mid mu)
   #highmidbreak=361

   # calculated from WT triple gauss fit
   # mid mu = 3.55, sigma = 1.16
   # low mu = 1.55, sigma = 0.3
   # break = low mu +
   #    (low sigma / (low sigma + mid sigma)) * (mid mu - low mu)
   #midlowbreak=7.1

   #if (duration>highmidbreak) {color="green"}
   #else if (duration>midlowbreak) {color="blue"}
   #else {color="magenta"}
   return(color)
}


dev.new(file=paste("repsOnly.pdf",sep=""),width=17.4/2,height=5.5/2)

#bottom, left, top, right
```

```
par(mar=c(5, 5, 4, 2) +0.1)

print(head(data))

maxX=3600 # 14400
minX=0

#dev.new(width=10, height=3+(length(unique(genoDat$realworm))/4))
#stripchart(c(0,14400), pch="|", cex=2)
stripchart(time ~ UWID, data=data,
          group.names=unique(data$geno), #jitter=0.2, method='jitter',
          pch="|", cex=1, main="Representative Data", cex.axis=0.8, cex.lab=1.5,
          las=1, add=F, xlim=c(minX,maxX),
          xlab="Time (minutes)", cex.main=2,
          axes=TRUE, xaxt="n",ylim=c(0.5,5.5)
          )


axis(side=1, # bottom
    at=seq(minX,maxX,300),
    lwd.ticks=2,
    labels=seq(0,60,5))

axis(side=1, # bottom
    at=seq(minX,maxX,60),
    labels=FALSE)

v=1
for (worm in unique(data$UWID))
{
   print(data[data$UWID==worm,])
   q<-data[data$UWID==worm,]

   if (length(q$UWID))  #if there are any non-NA rows
   {
      last=0
      for (b in q$time)
      {
         if (last>0)
         #stripchart(c(b), pch="|", cex=2, add=T, at=v, col="grey")
         {
            color=getColor(b-last)
            if (color=="black")
            {
            lines(c(last, b), c(v, v), lwd=2,
               col=color, lend=2, ljoin=1)
            #points(b,v,col="black",cex=1,pch=1)
            }
         }
         else if (last==0)
         {
            color=getColor(b-last)
            lines(c(last, b), c(v, v), lwd=2,
               col="black", lend=2, ljoin=1)
         }
         last=b
```

```
        }
        last=0
        for (b in q$time)
        {
           if (last>0)
           #stripchart(c(b), pch="|", cex=2, add=T, at=v, col="grey")
           {
              color=getColor(b-last)
              if (color=="black")
              {
              lines(c(last, b), c(v, v), lwd=2,
                 col=color, lend=2, ljoin=1)
              }
           }
           last=b
        }
        last=0
        for (b in q$time)
        {
           if (last>0)
           #stripchart(c(b), pch="|", cex=2, add=T, at=v, col="grey")
           {
              color=getColor(b-last)
              if (color=="black")
              {
              lines(c(last, b), c(v, v), lwd=2,
                 col=color, lend=2, ljoin=1)
              #points(c(last+(b-last)/2), c(v), col=color, cex=1.5)
              }
           }
           last=b
        }
        #q=endpoints[endpoints$genotype==geno,]
        #q=q[q$UWID==v,]
        #endpoint=q$duration[!is.na(q$worm)]
        #lines(c(last, endpoint), c(v, v), lwd=2, lend=2,
        #           col="black")
        {
        lines(c(last, 3600), c(v, v), lwd=2,
                     col="black")
        }
     }


     v=v+1
}

warnings()
```

8.3. Appendix D*: Additional work with serotonin receptors and NLP-3*

To confirm that NLP-3/NPR-36 signaling is not within the same pathway as serotonin signaling, I crossed serotonin mutants with an *nlp-3OX* mutant and with the *npr-36* null mutants that I generated for this work. I did not observe a rescue of the *nlp-3OX* phenotype upon knocking out serotonin signaling. I observed an additive egg-laying phenotype when crossing the serotonin receptor *ser-7* with *npr-36*. Both of these findings are consistent with NLP-3 signaling occurring separate from serotonin signaling within the egg-laying circuit.

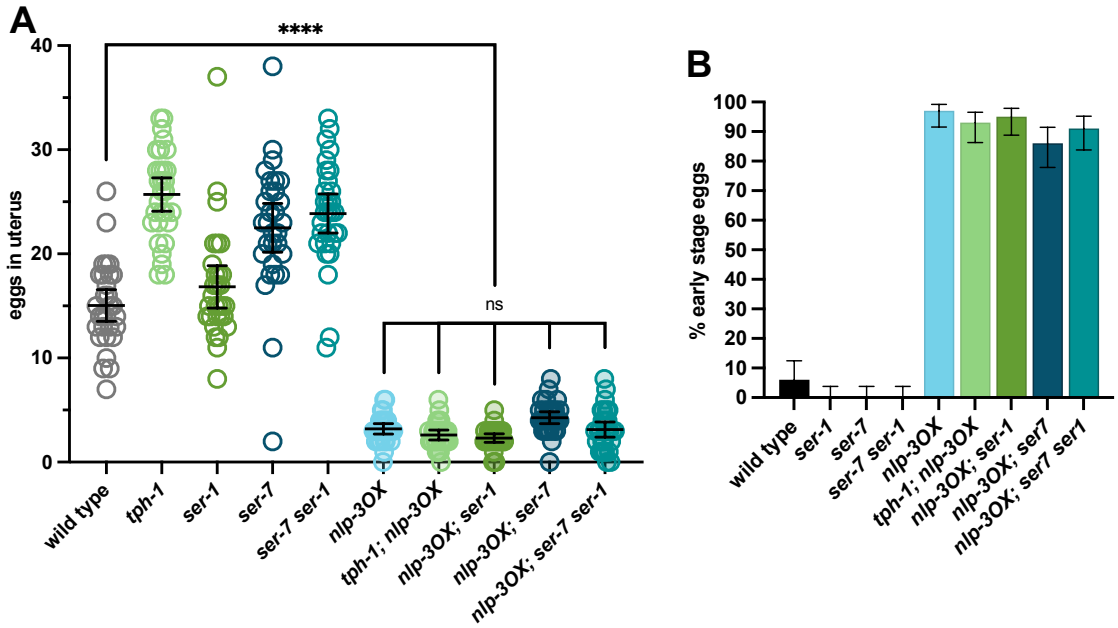

Supplemental Figure 8.1: Serotonin mutants do not compensate for the hyperactive egg-laying phenotype caused by *nlp-3OX*.
A, Eggs in uterus wild type, mutants for serotonin signaling, *nlp-3* overexpression, and *nlp-3 overexpression* crossed with each serotonin mutant. n=30. Ordinary one-way ANOVA Tukey corrected for multiple comparisons. ns = $p>0.05$; **** = $p\leq0.0001$. **B**, Early-stage egg-laying assay showing that the overexpressing *nlp-3* strains crossed with serotonin mutants maintain the hyperactive egg-laying phenotype caused by overexpressing *nlp-3.* n=30

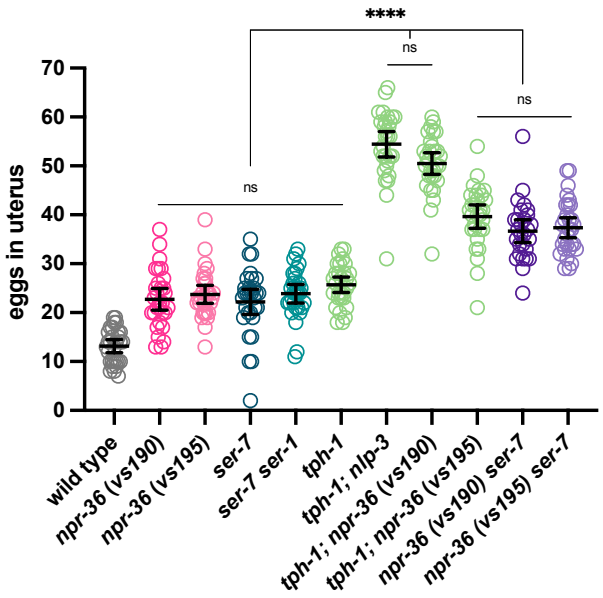

Supplemental Figure 8.2: *npr-36* and *ser-7* mutants have additive egg-laying phenotypes.
npr-36 ser-7 double mutants both are significantly more egg-laying defective than the single mutants of *npr-36* or *ser-7* alone. They do not achieve as severe in egg-laying defect as the *tph-1; nlp-3* or *tph-1; npr-36(vs190)*, but similar to *tph-1; npr-36(vs195)*. n=30. Ordinary one-way ANOVA Tukey corrected for multiple comparisons. ns = $p>0.05$; **** = $p\leq0.0001$.

9. Supplemental Figures

9.1. Chapter 3 Supplemental Figures

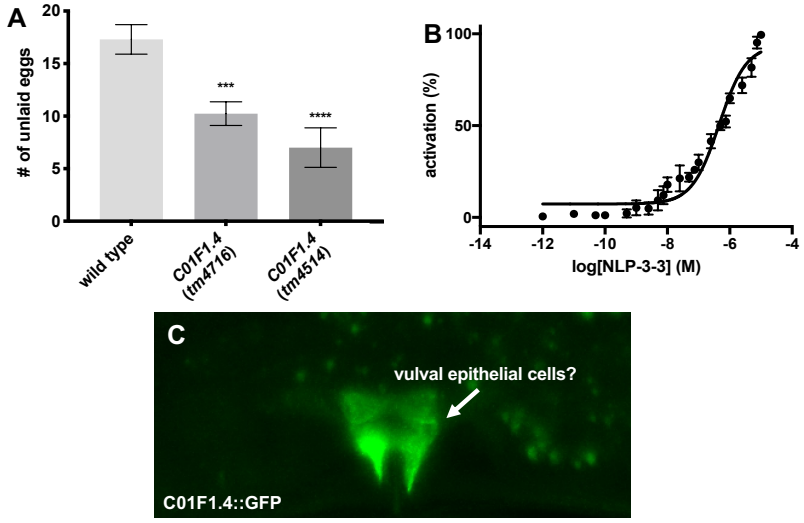

Supplemental Figure 9.1: Potential NLP-3 receptor NPR-42 (*C01F1.4*) does not phenocopy NLP-3. **A**, Unlaid egg assay of two different C01F1.4 mutants cause a loss of eggs in the uterus in contrast to *nlp-3* mutants. n=30. Ordinary one-way ANOVA Tukey corrected for multiple comparisons. *** = p≤0.001; **** = p≤0.0001. **B**, Indirect binding assay of NLP-3 peptides with NPR-42 indirectly shows activation in CHO cells at an EC_{50} of approximate 550nM, significantly outside the expected relevant physiological range. **C**, Extrachromosomally expressed, GFP-tagged NPR-42 (*C01F1.4::gfp*; from Robert Fernandez) is only expressed in what appears to be some vulval epithelial cells in the midbody of the animal.

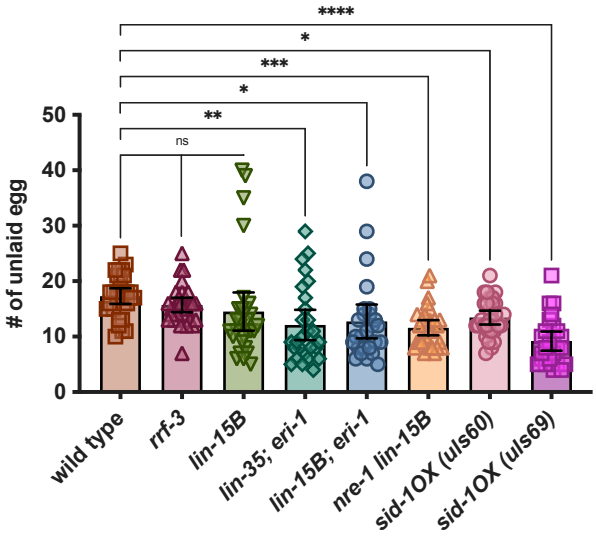

Supplemental Figure 9.2: All RNAi-hypersensitive mutants assayed for egg-laying defects. Unlaid egg assay performed on various RNAi-hypersensitive mutations on a normal bacterial lawn. Only *rrf-3* and *lin-15b* were not significantly different from wild type. n=30. Ordinary one-way ANOVA Tukey corrected for multiple comparisons. ns = p>0.05; * = p≤0.05; ** = p≤0.01; *** = p≤0.001; **** = p≤0.0001.

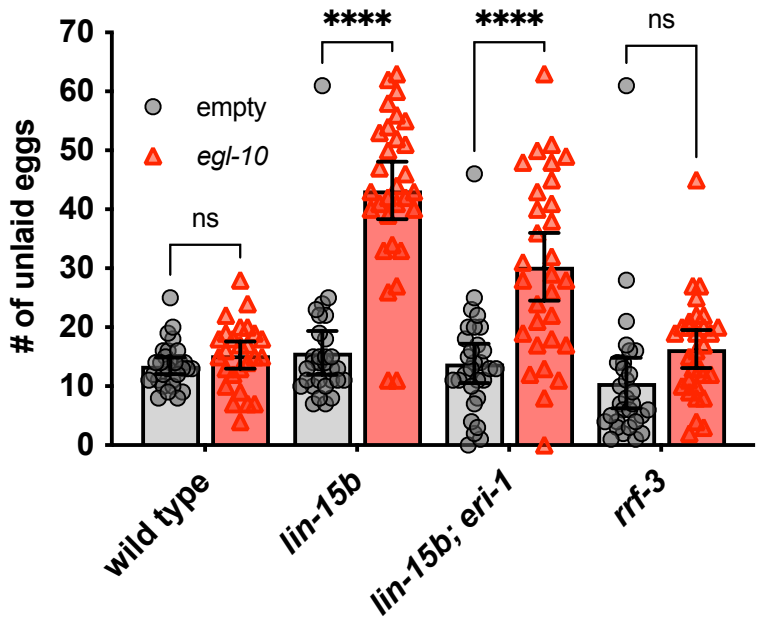

Supplemental Figure 9.3: Efficaciousness of RNAi mutations when knocking down known severe *egl*-inducing gene, *egl-10*.
lin-15b was the most successful mutant to convey effective knockdown of *egl-10. lin-15b; eri-1* animals were also significantly more *egl*, but these animals were visually poorly developed and did not look healthy enough to continue to use for further crosses or assays. n=30. Ordinary one-way ANOVA Tukey corrected for multiple comparisons. ns = $p>0.05$; *** = $p\leq0.001$.

9.2. Chapter 4 Supplemental Figures

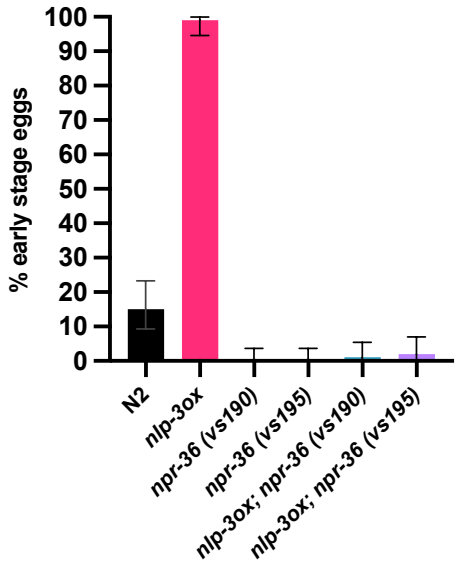

Supplemental Figure 9.4: Early-stage egg laying assay on *npr-36* null mutants.
npr-36 null mutants suppress the *nlp-3* overexpression hyperactive egg-laying phenotype. n=30. 95% CI shown.

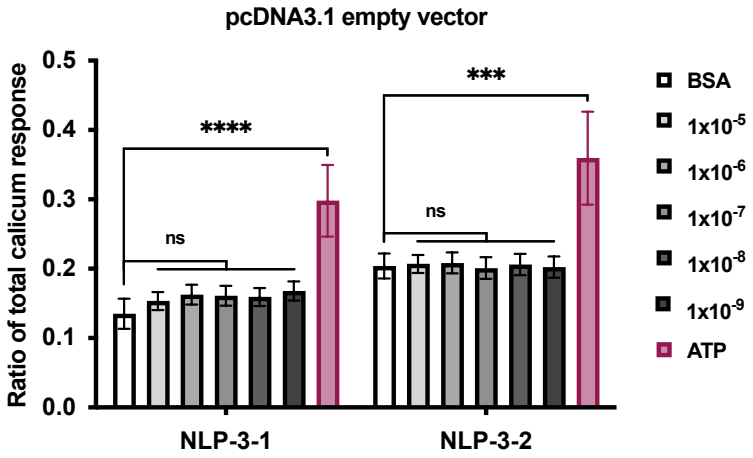

Supplemental Figure 9.5: NLP-3-1 and NLP-3-2 peptides do not activate endogenous receptors in CHO-cells.
Normalized calcium response of cells transfected with empty vector (negative control) challenged with 10 µM, 1µM, 0.1µM, 0.01µM, and 1nM of NLP-3-1 or NLP-3-2 peptides. Shown as the ratio of peptide-evoked response to the total calcium response. BSA is a negative control. ATP is a positive control activating an endogenous GPCR. Error bars represent SEM. BSA and ATP, n≥6; NLP-3 peptides, n≥12. ns, not significant (p≥0.05); ***, p≤0.001; ****, p≤0.0001; two-way ANOVA with Šidák correction for multiple comparisons.

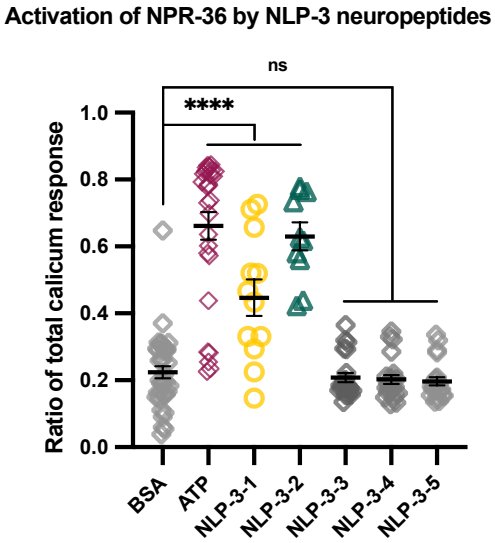

Supplemental Figure 9.6: NLP-3-1 and NLP-3-2 peptides activate NPR-36.
Normalized calcium response of CHO-cells expressing NPR-36, challenged with 10 µM of each of the five NLP-3 peptides. Shown as the ratio of peptide-evoked response to total calcium response. BSA is a negative control. ATP is a positive control for cell response, targeting an endogenous GPCR. Error bars represent SEM. BSA, n=37; ATP, n=28; NLP-3 peptides, n≥10. ns, not significant (p≥0.05); ****, p≤0.0001; ordinary one-way ANOVA with Dunnett correction for multiple comparisons.

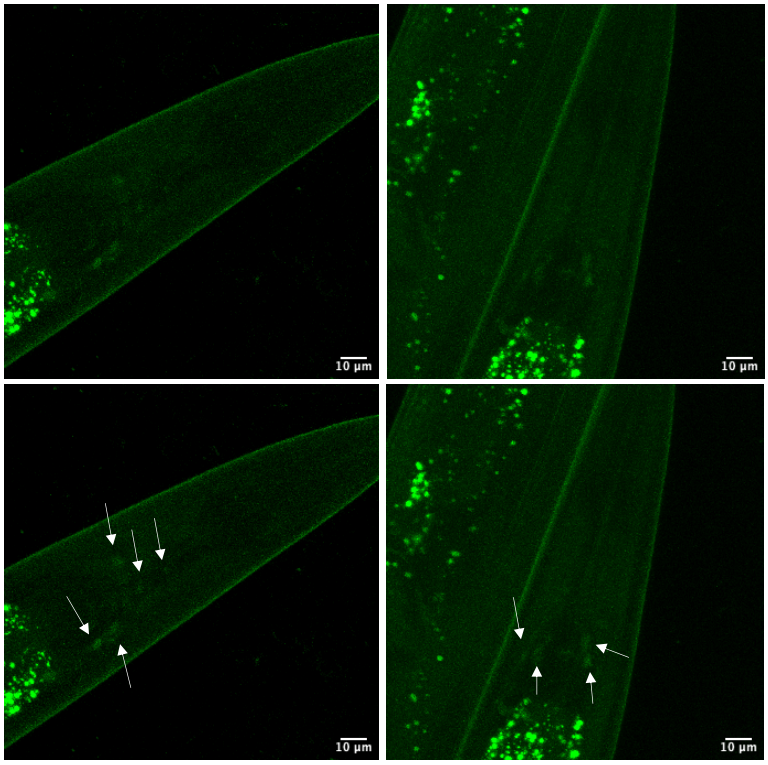

Supplemental Figure 9.7: Example head images from *npr-36::sl2::nls::gfp* animals with and without arrows identifying likely head neurons.

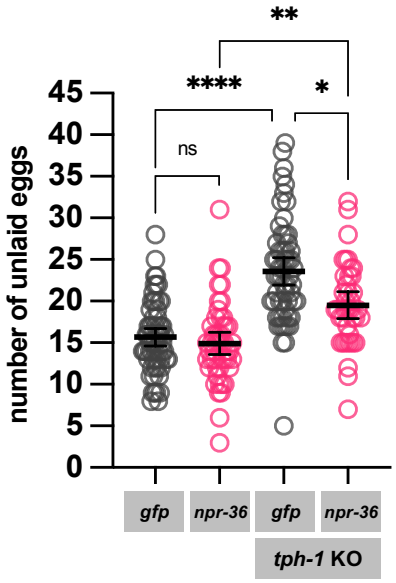

Supplemental Figure 9.8: Cell-specific knockdown of *npr-36* in the HSNs had uninterpretable controls.
gfp n = 72; *npr-36* n = 50; *tph-1 KO gfp* n = 65; *tph-1 KO npr-36* n = 52. All data are pooled from 5 injected lines with at least 10 animals assayed from each injection.
Ordinary one-way ANOVA Tukey corrected for multiple comparisons. ns = $p>0.05$; * = $p\leq0.05$; ** = $p\leq0.01$; **** = $p\leq0.0001$.

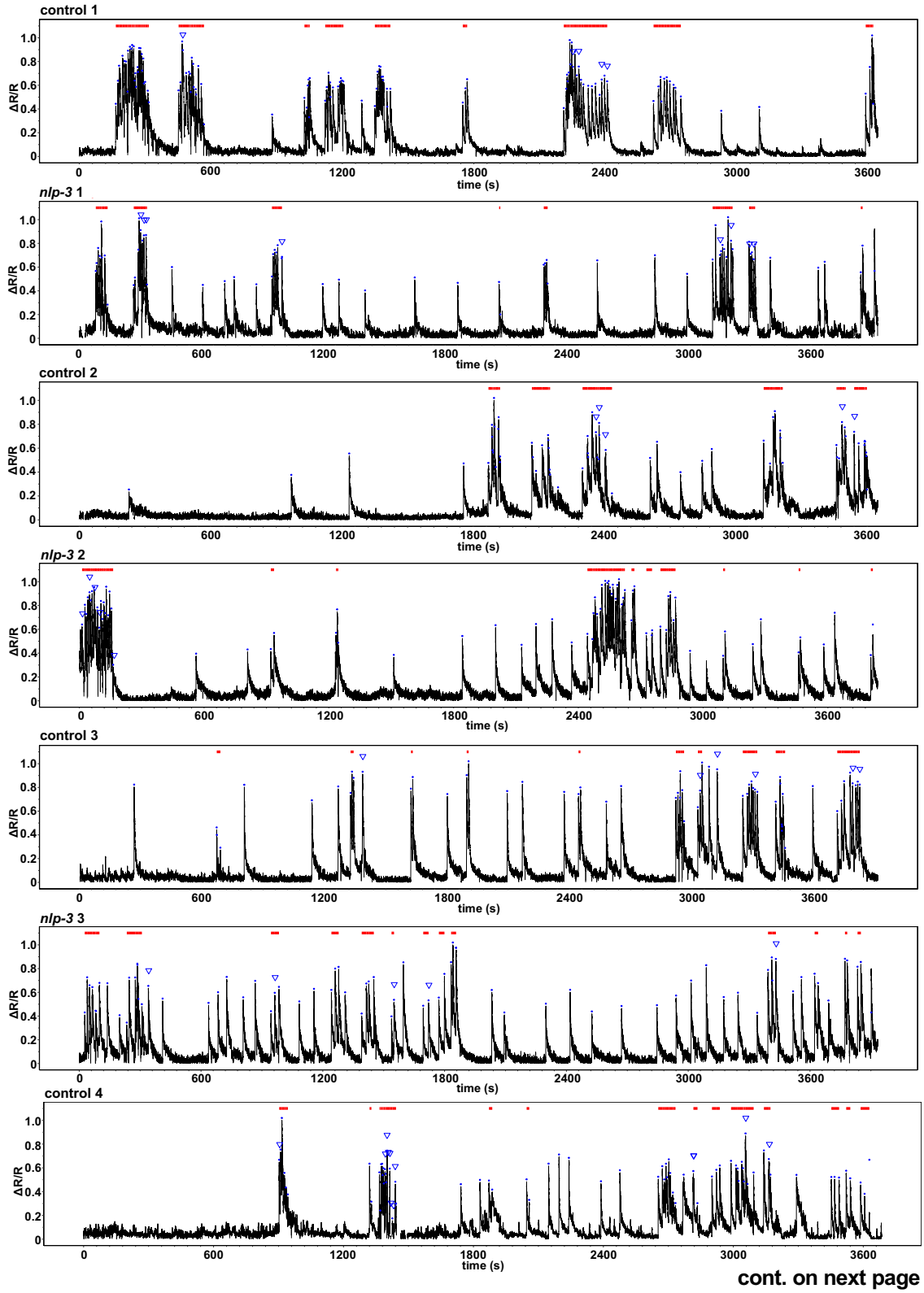

cont. on next page

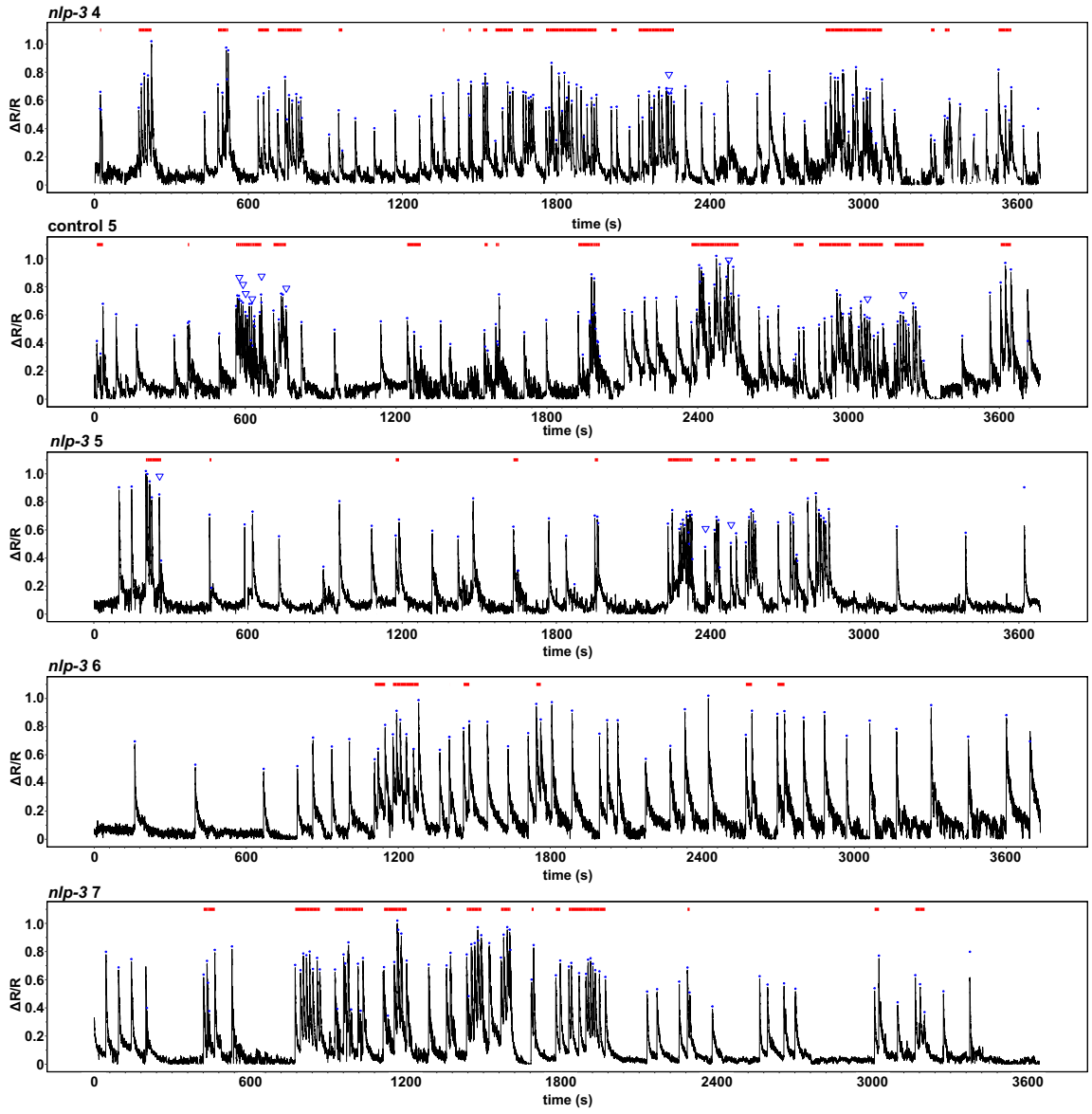

Supplemental Figure 9.9: HSN calcium traces for all animals recorded.
Five wild-type and seven *nlp-3* null animals were recorded for 1 hour each. Red bars indicate two or more peaks that have an interval(s) of less than 30 seconds between them. Blue dots indicate called peaks. Blue carets indicate egg-laying events. Control is wild-type for *nlp-3*. Traces of control and *nlp-3* animals with the same number were recorded on the same day. Data display is generated by the code in Appendix B.

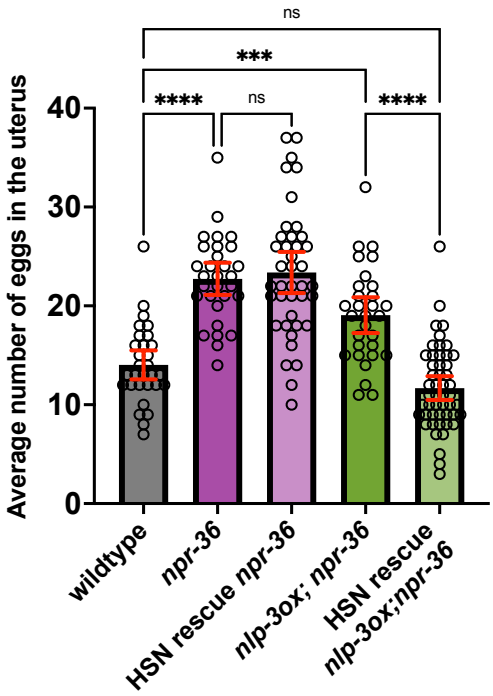

Supplemental Figure 9.10: Rescue *npr-36* expression in the HSNs preliminarily appeared to restore the hyperactive egg-laying phenotype caused by *nlp-3* overexpression.
Injection of *npr-36* cDNA and a GFP co-injection marker into *npr-36 (vs190)* animals with and without *nlp-3* overexpression. Rescue of *npr-36* in the HSNs alone did not significantly decrease the mild egg-laying defect of *npr-36* null animals. However, when *npr-36* was rescued when *nlp-3* was also overexpressed, there was a significant decrease in eggs retained compared to the control. There is a slight increase in *egl*ness of all animals in this assay compared to that seen in Figure 4.1A. This, along with concern from members of the lab in relation to the ectopic expression of *npr-36* and injection workload with this strategy, led to the decision to halt this work. Rescue data sets have 10 animals assayed from 4 (*npr-36* rescue) or 5 (*npr-36* rescue with *nlp-3* overexpression) distinct injection lines, for a total of 40 or 50 animals, respectively. n=30 for all other genotypes. Ordinary one-way ANOVA Tukey corrected for multiple comparisons. ns = $p>0.05$; *** = $p\leq0.001$; **** = $p\leq0.0001$.

9.3. Chapter 5 Supplemental Figures

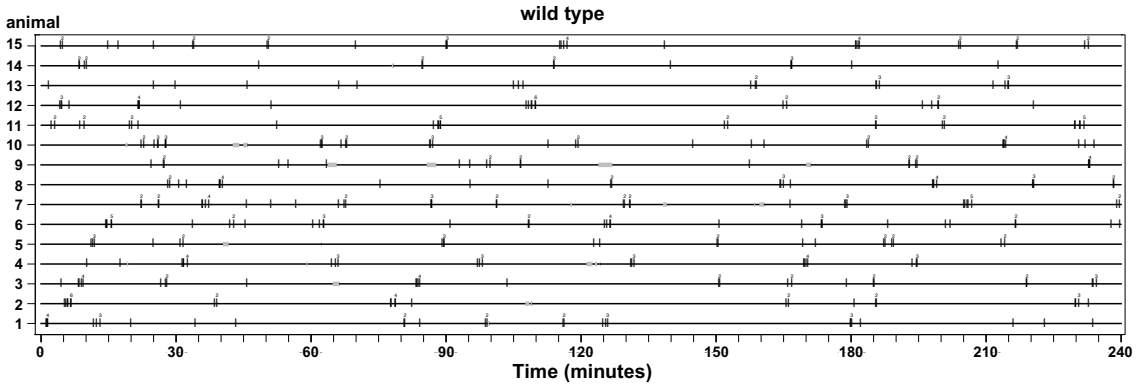

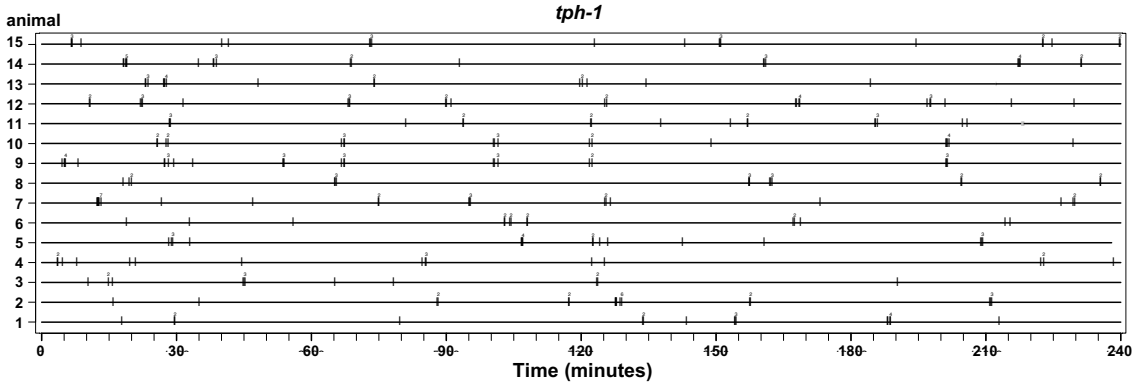

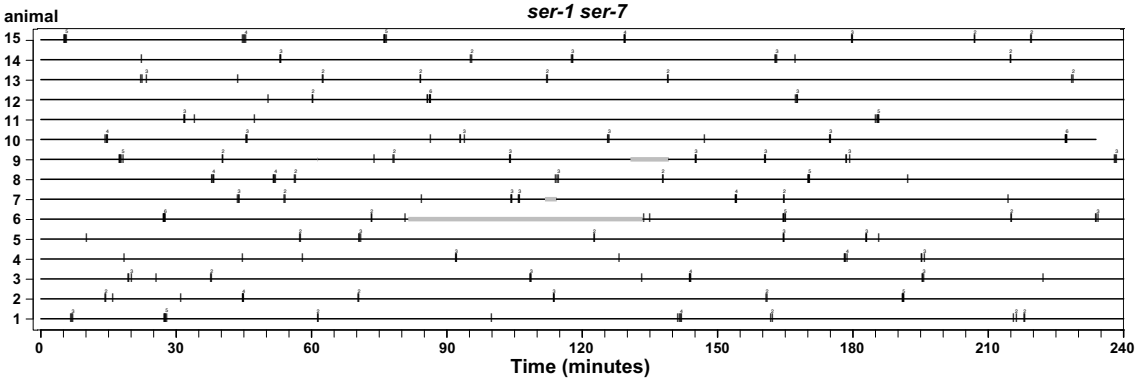

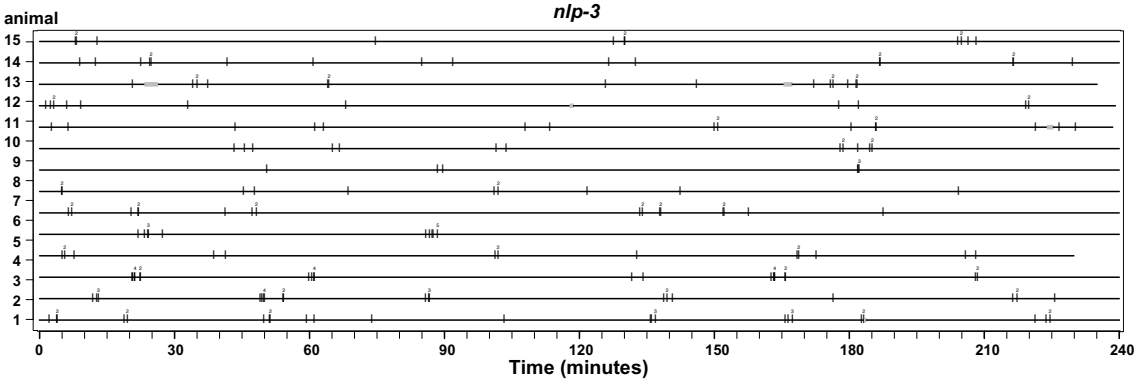

cont. on next page

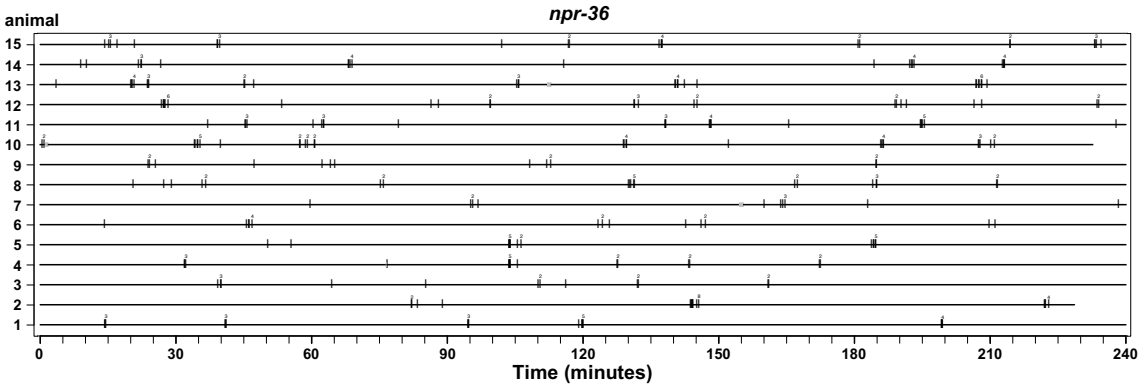

Supplemental Figure 9.11: Full data set from pattern of egg-laying assay.
Strip charts showing the results of 4-hour recordings for 15 wild-type, *tph-1*, *ser-1 ser-7*, and *npr-36*, and 14 *nlp-3* animals, representing the complete data set analyzed in Table 5.1, Table 5.2, Table 5.3, Figure 5.1, Figure 5.2, Figure 5.3, and Figure 5.4. Black hash marks indicate egg-laying events. Number of egg-laying events occurring in a short time span are denoted above the hash. Gray bars indicate time when the animal left the field of view. Assay was performed in 3 technical replicates per genotype, with five animals per technical replicate (excluding the one replicate of nlp-3 that had one animal that never entered the field of view. Data displayed generated using code from Appendix C.

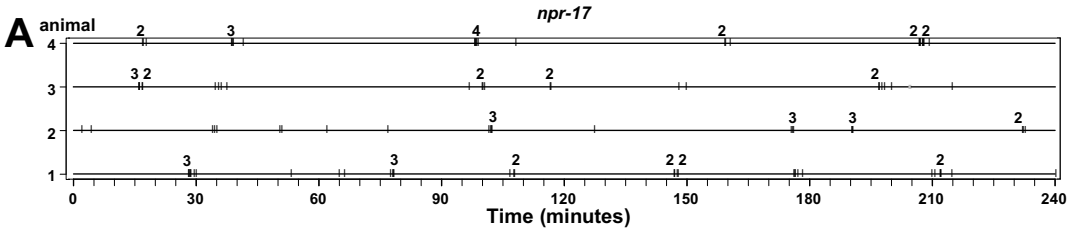

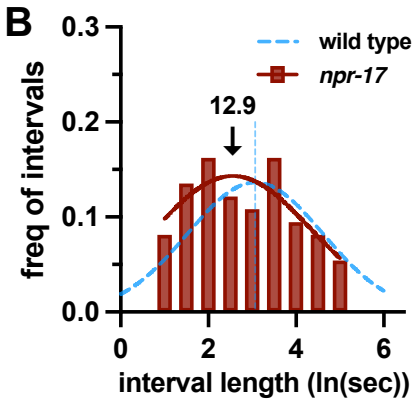

Genotype	Number of animals recorded	Total hours of recording	Total # of intervals	<400 second intervals: Mean length (sec)	<400 second intervals: 95% confidence interval	<400 second intervals: # of intervals	<400 second intervals: p value for comparison to wild type
wild type	15	60	342	21.5	12.6 — 37.8	230	
npr-36	4	16	101	12.9	1.01 — 23.5	74	0.1023

Supplemental Figure 9.12: *npr-17* mutant does not appear to operate as an NLP-3 receptor for the egg-laying active phase.
A, Preliminary pattern of egg laying experiment on *npr-17* null animals. Black hash marks indicate egg-laying events. Number of egg-laying events occurring in a short time span are denoted above the hash. Gray bars indicate time when the animal left the field of view. Hash marks too close to visually distinguish have egg-laying event counts written above. **B,** Distribution of intervals less than 400 seconds for *npr-17* comparing to the wild-type Gaussian fit (dashed blue line). Mean of the Gaussian *npr-17* curve is indicated with an arrow. Mann Whitney U test to compare wild type to *npr-17* was not statistically significantly different (p=0.1023).